Author Response to Review of Referee #2 for "Seasonal Variability of Stratospheric Methane: Implications for Constraining Tropospheric Methane Budgets Using Total Column Observations"

K. M. Saad[1], D. Wunch[1,2], N. M. Deutscher[3,4], D. W. T. Griffith[3], F. Hase[5], M. De Mazière[6], J. Notholt[4], D. F. Pollard[7], C. M. Roehl[1], M. Schneider[5], R. Sussmann[8], T. Warneke[4], and P. O. Wennberg[1]

[1]California Institute of Technology, Pasadena, California, USA
[2]University of Toronto, Toronto, Ontario, Canada
[3]University of Wollongong, Wollongong, NSW, Australia
[4]University of Bremen, Bremen, Germany
[5]Karlsruhe Institute of Technology, IMK-ASF, Karlsruhe, Germany
[6]Royal Belgian Institute for Space Aeronomy, Brussels, Belgium
[7]National Institute of Water and Atmospheric Research, Omakau, New Zealand
[8]Karlsruhe Institute of Technology, IMK-IFU, Garmisch-Partenkirchen, Germany

Correspondence to: K. M. Saad (katsaad@caltech.edu)

We thank Referee #2 for their comments.

The primary change in the updated manuscript is a reprocessing of the TCCON tropospheric methane (CH_4) column-averaged dry-air mole fractions (DMFs), which is described in detail in added supplement, "Updates to Tropospheric Methane Data" (Appendix A). Although some of the regression statistics and comparisons have changed as a result of measurement updates, the main conclusions, the mismatch in tropospheric seasonality and the dependence of the stratospheric contribution error on tropopause height, remain the same.

In our responses below, page and line numbers included refer to the previous discussion draft. Appendices are referred to based on their order in the revised manuscript, and their headings are noted to avoid ambiguity.

It lacks precision in the text in many places (see specific comments), so are legends of some figures. Several important sentences, often when synthetizing results are confusing and not clear and make the reading not fluid at all with this version (see specific comments). I find the result section, a bit too descriptive, not providing systematically explanations or hypotheses for the inferred results. This has to be improved as it is not done either in the discussion part.

When discussing values presented in figures, the text now repeats these values more consistently. We have characterized the results more systematically, with greater detail and hypothesized explanations given for each feature. In addition to changing the wording where requested in the specific comments, we have altered ambiguous phrases, removed redundancies, and partitioned long sentences to make explanations simpler and more straightforward. We have also described and removed inconsistencies in terminology for greater clarity. The discussion of the figures in Section 3 has been updated to delineate the results quantitatively and with more detail. We also have made existing explanations more evident and provide additional hypotheses for results.

About the hypotheses, for instance among several other things reported below, I wonder why the aseasonal run disable the seasonal emissions and scale up the rest instead of prescribing the annual mean of seasonally changing sources ? This is strange as it changes the spatial distribution of emissions on the top of the suppression of seasonality.

We agree that producing aseasonal emissions by changing the seasonally varying fluxes to be constant throughout each year for each grid box would be ideal. Unfortunately, the model infrastructure made such a simulation difficult to execute as it required the emissions code to be re-written, risking differences due to compiling changes. Thus the scaling technique was developed as an alternative to assess first-order impacts of emissions seasonality. We have added this explicitly as a limitation that should be improved on in the future. However, most of the notable results, especially the phase lag in the tropospheric seasonality, are consistent between the model runs despite any differences in the spatial distribution of emissions. This demonstrates the robustness of our conclusions regardless of the emissions fields used. Additionally, the analyses comparing the base and aseasonal simulations are aggregated on zonal or hemispheric scales and therefore should not vary because of the spatial differences of their emissions at smaller scales.

Abstract : “large number of highly variable sources" not all methane source are highly variable. On what scale ? And sinks ? I suggest because of a large number of uncerain sources and sinks.

The phrase, “highly variable sources” has been removed for conciseness.

Page 2 : lines 1-5 : the words "atmospheric inversion" should appear somewhere in this paragraph.

The term “atmospheric inversion” has been added for clarity.

Lines 16-17:Do they have the same bias as aircraft observations of clear-sky only measurements (aircraft do not fly in bad weather conditions)? It is worth noticing this issue somewhere.

TCCON FTS instruments do not make measurements in rainy or completely overcast weather, which is now noted.

Lines18-20 : Fraser et al : how did they do that ? did they account for observation systematic errors as well ? Please be more precise when quoting papers. Idem for Wecht et al.

Additional descriptions of the approaches of Fraser et al. (2013) and Wecht et al. (2014) are now included in the introduction, and greater detail was added for several other references elsewhere in the manuscript. While Fraser et al. (2013) performed a variety of observing system simulation experiments (OSSEs) to test measurement and sampling biases, their focus was the information content of different types of observations in relation to atmospheric inversions. We have included their sector and regional error reduction results for the reader’s reference.

Lines 33-35 : ambiguous sentence. Please rephrase. Indeed tropospheric CTM do not reproduce well stratospheric transport...

"Insofar as," has been changed to, "Provided that," to make the conditional aspect of the sentence more clear and reduce ambiguity.

Page 3 : Line 6 : "systematic model biases" : strange expression. Maybe systematic errors would be enough. What about the random part or errors? Do you address this as well ? Please reformulate.

By biases, we refer to the measurement-model mismatch due to inaccuracies inherent in the model; we agree that "systematic errors" also relays this meaning and have changed the wording. Because the focus of this work is on systematic differences between observations and the model, we do not quantify random model error except to note how the scatter and goodness of fit of the linear regression analyses compare between subsets of data (e.g. Northern vs. Southern Hemisphere and $X^t_{\mathrm{CH_4}}$ vs. $X_{\mathrm{CH_4}}$).

Line 6 : "seasonal cycle and spatial distribution of CH4" concentrations ? emoissions ? please be more precise.

This phrase now reads, "the seasonal cycle and spatial distribution of $\mathrm{CH_4}$ DMFs" for clarity.

Line 15 : it would be good to briefly recall how the TCCON total columns are inferred. In particular, what is the influence of the modelled CH4 profile used in the retrieval (as a prior) on the final product. As this profile comes from a model, it would be worth commenting on this considering the topic of the paper.

A brief description of the TCCON total column retrievals is now included at the end of the first paragraph of Section 2.1. In addition, a detailed description and references for the $\mathrm{CH_4}$ a priori profiles have been added to the text. In testing the influence of the TCCON prior profiles in their comparisons to aircraft in situ profiles, Wunch et al. (2010) found that the total column retrievals using TCCON a priori profiles produced the same calibration values as those using the aircraft profiles as priors.

The newly added Appendix A, "Updates to Tropospheric Methane Data," includes a more detailed description of how the $X^t_{\mathrm{CH_4}}$ measurements are determined, processed to address spectroscopy-related errors, and calibrated to in situ aircraft profiles. The consideration of the chosen TCCON priors on the model comparison is addressed by smoothing the GEOS-Chem profiles using the TCCON scaled priors, as described in Appendix B3, "Model Smoothing for Measurement Comparisons." The strong agreement between the integrated and smoothed GEOS-Chem column-averaged $\mathrm{CH_4}$ DMFs also supports a negligible influence of the TCCON priors the results (Fig. 12).

L16 : "precise" : please be more quantitative here or remove the word. How precise compared to surface networks for instance? how is your data uncertainty estimated ?

In addition to the details provided in response to the previous comment, Wunch et al. (2015), which describes in detail the determination of the TCCON total column uncertainty budgets and quantitative measures thereof, has been added to the references cited on p.3 l.16. A sensitivity study to assess uncertainties related to a priori profiles, spectroscopy, and instrumentation found aggregated $X_{\mathrm{CH_4}}$ errors to be below 0.5%, or about 5 ppb (Wunch et al., 2015). Appendix A, "Updates to Tropospheric

Methane Data," provides more details on the tropospheric measurement uncertainties, including $X^t_{\mathrm{CH_4}}$ precision values and the aircraft in situ calibration curve, for reference.

Page 4 : Lines 14-15 : please provide a reference for emissions and OH. Do they vary inter-annually ? For OH concentrations, what is your ratio NH/SH ? More precisions are needed here. Indeed you release emissions evey hour but their time evolution is monthly or annually probably. Please precise this not to le the reader think that we know methane emissions with an hourly time step !

References were cited for the "default" offline $\mathrm{CH_4}$ simulation, which included a description of these fluxes. We have since added details and references for each of the emissions categories have been added for the reader's convenience. The list of emissions, which were grouped by time evolution (annual, monthly, and daily), now includes references and additional details that should make the time scales of their variability more apparent to the reader.

The Northern to Southern Hemisphere ratio of 1.0 (monthly range of $0.975 - 1.02$, applying a six month lag in the Southern Hemisphere) is consistent with the ratio of 0.97 ± 0.12 found by Patra et al. (2014). The tropospheric OH are monthly-averaged output from a GEOS-Chem tropospheric chemistry simulation (Park et al., 2004). The description of tropospheric OH and stratospheric loss parameterization fields now include references.

Section 2.2 : It would be useful to position GEOS-CHEM with other transport models based on previous Transcom-like experiment (e.g. : Patra et al., 2011): is it a "fast" model (inter-hemispheric exchange time ?), what about stratosphere/troposphere exchange time ? ... It would be very useful for other modellers to use the results of the paper.

Unfortunately, Patra et al. (2011) does not disaggregate the quantitative metrics asked for by the reviewer by model in the TransCom-$\mathrm{CH_4}$ model comparison. Based on Fig. 8 therein, the interhemispheric exchange time in GEOS-Chem appears near the model median and slightly below observations over the 1996-2007 time series, which we have added to the conclusions for the reader's reference.

Page 5 : Line 1-2 : this first sentence needs precision : what is GGG2014 ? What is GEOS5 ? Acronyms have to be defined and explained

GGG is the name of the software and not an acronym. GGG2014, the current version of the TCCON retrieval software package, is described more fully in Section 2.1, where it is first introduced, to avoid confusion. The full name for the GEOS-Chem GEOS5 meteorology is now included on p.5 l.2.

Lines 10-15: the choice to disable the seasonal emissions and scale up the rest is strange as it changes the spatial distribution of emissions on the top of the suppression of seasonality. Why not prescribing the annual mean of seasonally changing sources ?

Please see the above response to the related general comment.

Line 15 . What is “TCCON daily median scaled priors" ? you need to provide more details here.

GEOS-Chem smoothed column-averaged DMFs were only calculated for days in which TCCON measurements were made and were smoothed using solar zenith angles, vertical scaling factors, and surface pressures for TCCON measurements used in the comparisons. The added discussion of the TCCON retrieval in Section 2.1 provides a description of the vertical scaling factor that clarifies subsequent references. To further lessen confusion, this sentence has been changed to, “For comparisons with column measurements, model vertical profiles were smoothed with corresponding TCCON $\mathrm{CH_4}$ averaging kernels, interpolated for the daily mean solar zenith angles, and prior profiles, scaled with daily median vertical scaling factors and interpolated to the daily mean surface pressures measured at each site, following the methodology in Rodgers and Connor (2003) and Wunch et al. (2010).”

What is the influence of these "priors" on the TCCON products and on the comparison proposed here.

As mentioned in the note above referring to the comment about p.3 l.15, Wunch et al. (2015) describes sensitivity experiments to assess the systematic errors in the TCCON retrievals that could potentially result from the a priori profiles. As Fig. 10 of that document illustrates, shifting the trace gas profiles down 1 km in altitude and increasing the temperature by 1 K and pressure by 1 hPa throughout the vertical profile each alter $X_{\mathrm{CH_4}}$ by about $0.05 - 0.1\%$. For the purposes of this work, the strong agreement between the GEOS-Chem column-averaged $\mathrm{CH_4}$ DMFs and those smoothed using the TCCON scaled a priori profiles, as described in Appendix B3, “Model Smoothing for Measurement Comparisons,” demonstrates the unlikelihood of the TCCON priors being the reason for the measurement-model disagreement (Fig. 12).

Line 20 : "While XtCH4 20 changed slightly" : how much is the change ? please provide % for instance. Why only testing above levels ? please provide explanations.

The median change in $X^t_{\mathrm{CH_4}}$ of about 1 and 5 ppb for a respective one and two-level increase in tropopause is now stated.

Accurately representing GEOS-Chem’s tropospheric column for the purpose of comparison to measurements depends on setting the tropopause so that the calculation from model output is consistent with the way the model defines the troposphere. Shifting the tropopause level allowed us to test the degree to which calculating $X^t_{\mathrm{CH_4}}$ using the daily average tropopause could bias the comparison. Furthermore, because the vertical gradient of $\mathrm{CH_4}$ is steepest across the UTLS, choosing a lower tropopause level would change the vertical integration much less than choosing a higher level. Thus, integrating to higher pressure levels would provide a better measure of sensitivity to the integration tropopause height chosen.

Line 24: ”small”. Please be more precise. Remain within ±5 ppb for instance ? Idem for larger NH changes : ‘varies from -10 to +13 ppb ?

Quantification of the seasonal cycle has been added: “within ± 4 ppb” for the Southern Hemisphere and “varies between -10 and $+13$ ppb” for the Northern Hemisphere troposphere.

Page 6 : Lines1-2 : what do you mean by " common " ? Why the age of air increases when seasonality is supressed ? Please provide more clear explanations.

Because the transport of tropospheric air to the stratosphere air is governed by vertical ascent in the tropics (Brewer, 1949; Dobson, 1956), stratospheric air has a shared source of CH_4 that lessens the interhemispheric gradient seen in the troposphere (Boering et al., 1995, 1996). The age of air does not increase with dampened seasonality; rather the signal of tropospheric seasonality in a given parcel of air dissipates as its residence time increases (Mote et al., 1996). We now discuss this in more detail in Appendix A, "Updates to Tropospheric Methane Data."

Line 3 : "relatively short" : please provide an estimate

The model's equilibrium lifetime of CH_4 in the stratosphere is about 22 months, which we now state in the text.

Page 7 : Line 9-10 : tropospheric slope does not seem lower than one for southern stations. Indeed it seems there is a little north-south gradient in the tropospheric slopes. Did you investigate it ?

The tropospheric slope did not have an interhemispheric difference prior to the $X^t_{CH_4}$ update. However, with the updated $X^t_{CH_4}$ observations, the plots show interhemispheric differences in both $X^t_{CH_4}$ and X_{CH_4}. These Northern and Southern Hemisphere comparisons between TCCON and GEOS-Chem are described fully in Section 3.

Figs 4 : this figure is not enough analysed. You do not comment : - the negative bias of GEOS-CHEM at most sites for the trospospheric & total columns (4ab) - the fact that stratospheric columns of GEOS-CHEM seems underestimated for more southern sites and overestimated for more northern sites (4c) - possible reasons for the poorer agreement in the stratosphere.

The discussion of Fig. 4 now includes a systematic description of the plots, with associated hypotheses. The underestimation of CH_4 concentrations in GEOS-Chem has been documented elsewhere. In the TransCom-CH4 model comparison, GEOS-Chem CH_4 concentrations were lower than the model median, and when using the same OH fields much lower than the range of other models (Patra et al., 2011). The negative bias was previously described as an offset when discussing the impact of the aseasonal simulations, and we have added that the direction of the offset (i.e. GEOS-Chem is systematically low) and provide a hypothesis for why the offset changes between simulations.

The stratospheric contribution of CH_4 increases from the equator to the poles due to the zonal gradient in tropopause height. We have added a discussion of the zonal gradients in the measurement-model differences in $X^t_{CH_4}$, X_{CH_4}, and the stratospheric contribution. We also directly compare the agreement (both slopes and R^2 values) across plots and hypothesize why correlations vary for different vertical levels.

You may also consider two slopes, one for the southern stations (larger thabn 1) and one for the northern stations

(smaller than 1) on fig 4a, or a non linear continuous decrease of the slope from south to north. Why only keeping a global slope ?

We had plotted regression lines across all sites in Fig. 4 and listed in the text the individual hemispheric regression results for the stratospheric contribution. However, we agree that providing regression equations for each hemisphere is more illustrative. Regression lines and equations for Northern and Southern Hemispheres now appear on the plots in Fig. 4.

Page 8 Line 3-6 : any possible explanation for the differences with ACE ?

The structure of the differences with ACE-FTS measurements illustrated in Fig. 5 demonstrate that the cause is systematic to the model. GEOS-Chem is too low above the tropical tropopause in both boreal spring and fall and too high in boreal spring directly above the Northern Hemisphere mid-latitude tropopause and in the Southern Hemisphere high altitudes. The ACE-FTS data gaps in the tropical troposphere prevent assessing whether vertical ascent into the stratosphere is too weak. Because the stratospheric loss parameterization is produced from NASA Global Modeling Initiative (GMI) model output, biases in the rate of loss could result from intra-model differences in transport schemes. A more thorough description of Fig. 5 and possible explanations for differences have been added to the paragraph on p.8 l.3.

Additionally, the ACE-FTS climatology plotted in Fig. 5 is an older version of the measurements (v. 2.2, Jones et al., 2012), which also could impact some of individual grid box differences; however, a comparison to the monthly means of the v.3.5 CH_4 DMFs (which are used in the $X^t_{CH_4}$ calculation) indicate that the data version likely would not change main features of Fig. 5.

Line 12-14 : "As the effective..pressure heights" : unclear sentence. Please rephrase.

The sentence has been rephrased: "The disagreement exhibits a large spread for relatively few tropopause pressure heights because the model's effective tropopause, that is, the pressure level at which the model divides the troposphere from the stratosphere in GEOS-Chem, is defined at discrete grid level pressure boundaries."

Page 10 line 10 : "production" or emissions ?

We infer that the referee meant p.10 l.5 and have changed "production" to "emissions." Otherwise, we do not understand the comment in the context of p.10 l.10.

Page8-9 Line 15-4 : the part about troposphere is confusing as figure 6b shows similar trend for stratosphere and troposphere but you mention in the text much lower sensitivity. Please clarify this section.

While the slope is similar between the stratospheric contribution and tropospheric column, the correlation coefficient is higher for the stratosphere than the troposphere, meaning that the tropopause height can explain a higher percentage of the variance in the measurement-model mismatch for the stratospheric contribution versus $X^t_{CH_4}$. Moreover, despite the similar slopes, the direction of the relationship with respect to $\Delta CH_4 = 0$ is opposite: Fig. 6 shows that the mismatch increases as the tropopause height decreases for the stratospheric contribution (with the model's contribution of the stratosphere becoming

larger than that of the measurements) and vice versa for the tropospheric mismatch (with the measurements and model showing better agreement when the tropopause height is lower). These points of clarification have been added to Section 3.1.

Page 10 Line 5 : "production" do you mean emissions as there is no methane 3D production in the atmosphere ?

As stated above, "production" has been changed to "emissions."

More, your statement brings more the summer large wetland emissions as an explanation for the phase of the modelled signal than the loss which should produce more a fall maximum as in surface observations (although Par falls is not the best example to discuss seasonal variations as the signal is complex). Please clarify.

We agree that the emissions are likely the main driver of the model's surface seasonality, and we have removed, "and loss," for clarity.

Park Falls was chosen because of the TCCON sites that also have surface observations, the $X^t_{\mathrm{CH_4}}$ seasonality most closely matches the Northern Hemisphere mean shown in Fig. 7; thus Fig. 8 provides a good basis to compare surface and tropospheric column measurements. While the site does have a complicated seasonality near the surface, we find it notable that GEOS-Chem is able to capture several of those features, especially the local minimum in October, but still deviates from the observations, as we note on p.10 l.8.

Page 11 : Lines 1-3 : please develop a bit why you discard OH as an hypothesis to explain the inferred changes?

The sensitivity experiments we ran tested a number of different OH (as well as emissions and meteorology) fields, which included scaling the default OH fields and using different scalings of the "Standard Chemistry + Biogenic VOCs" OH output (which is now described in more detail in Appendix B1, "Equilibrium Sensitivity Experiments"). The seasonal phase shift appeared in all simulations, regardless of OH used, although the seasonal cycle amplitude and the shape of the springtime maximum varies between simulations. A table delineating these simulations has now been added to Appendix B1. Additionally, p.11 l.2 now refers to a figure, also in Appendix B1, which illustrates the tropospheric seasonality of each of these simulations, as well as deviations from the base simulation.

Lines 7-8 : "The model sensitivity kernel implicitly includes.. " well do you mean variance matrices associated with observations ? with prior emissions ? Indeed, transport errors are generally implicitly include in atmospheric inversions by inflating observations errors but are not part formally of the variance matrix of emissions. Lines 7-8 : "which are compounded if vertical levels are subject to different errors" Confusing sentence. What do you mean ? pleas clarify.

The sensitivity kernel refers to the linear operator that maps $\mathrm{CH_4}$ emissions to $\mathrm{CH_4}$ concentrations; together with the error covariance matrices, the sensitivity kernel is used to calculate the gain matrix used in inversions to determine posterior emissions. The literature is inconsistent in how to refer to this operator; thus we use the term "sensitivity kernel" because we thought it describes the function of the operator: to provide the change in the $\mathrm{CH_4}$ concentration resulting from a perturbation to emissions for a given grid box. The response of modeled $\mathrm{CH_4}$ concentrations to changing emissions depends on the model's

transport and chemical loss, as well as assumptions about when and where fluxes occur. Therefore, uncertainties in these terms will be implicitly included in the sensitivity kernel. We have clarified what we refer to as the sensitivity kernel after the introduction of the term and have altered the wording to make the logic more linear. The subsequent sentence now states, "The model's stratospheric response to emissions perturbations differ from that of the troposphere and are subject to different transport and loss errors."

Page 12 : Line 6 'Although the stratosphere accounts for about 30% ' if you refer to top panel of figure 9, I suggest up to 35 % (JJA)

The top panel of Fig. 9 is the fraction of total emissions that are seasonally varying (that is, from wetlands, rice paddies, biomass burning events) in GEOS-Chem. The 30% value cited is the mean fraction of the total column of CH_4 (in units of molec·cm^{-2}) that exists in the stratosphere.

Fig9 : The legend of figure 9 is unclear. Top panel : fraction of what ? Bottom panel : the orange curve is a difference or the error of the aseasonal ? Unclear.

The upper panel of Fig. 9 is now labeled. As the caption reads, the orange curve is the difference between base and aseasonal simulation tropospheric columns. The label provides a qualitative description to improve on the originally submitted figure after we received feedback that the label, which explicitly stated that the curve is the tropospheric difference, was unclear.

line 10 : "The seasonality of the stratospheric error will therefore distort the inversion mechanism and thus posterior emissions estimates." : well only if these error are not included in the inversion variance matrices. I would be more confortable writing may distort or precise the conditions of influence of the seasonality in the stratospheric signals on surface emissions through inversions.

The uncertainties associated with transport are generally accounted for in inversions as a subjective percent error applied to all grid boxes, which would not capture the stratospheric errors presented here. Incorporating stratospheric uncertainties into the error covariance matrix would require a thorough characterization of those errors as a function of longitude, latitude, altitude, and month. Such efforts would be indispensable in improving the forward model, but our concern is that the error covariance matrix is not equipped to correct for these systematic biases. The conditions of influence of the stratospheric seasonality are delineated in the subsequent text.

Line 11 : "product of transport errors" : how did you evaluate the possibility of issues related to OH radicals ?

We infer that this refers to p.14 l.8. As mentioned above, we ran sensitivity experiments testing various OH fields, and these are now described in more detail in Appendix B1, "Equilibrium Sensitivity Experiments." Because the tropospheric phase shift appeared in all simulations, regardless of OH used, we believe that the tropospheric OH cannot account for the error in seasonality. We have added a table describing these simulations and a figure that plots the tropospheric seasonality of each of these simulations to Appendix B1.

Lines 10-12 : it is never mention except in caption of figure 4 that 't' in CH4t refers to troposphere

The description of the tropospheric CH_4 columns introduces the superscript t notation to indicate a tropospheric column-averaged DMF (p.4, l.1).

"their emissions are very uncertain" : you may quote a recent estimate such as in Kirschke et al. 2013 or IPCC.

The 2000-2009 range for natural wetlands given by Kirschke et al. (2013) (142-284 TgC·year^{-1}) is now included.

Page 13 : Lines 7-8 : "both the magnitude and seasonality of the difference is significant" : the unit (tons) makes it difficult to say so. There is obviously a sensitivity if transport error shift the seasonality but what does it give in terms of ppb ? or in terms of % of initial emissions ? This would be more clear for the reader.

The value plotted in Fig. 10b is a sensitivity, in units of kgCH_4 per 1 ppb, and can be thought of as the change in emissions needed to increase the DMF at the surface by 1 ppb. Because the seasonality of wetland emissions is such that many grid boxes have no wetland emissions in the winter (Fig. 10a), the emissions related to the phase lag as a percentage change from the prior would produce infinite or very large percentages. Thus, presenting the values as percentages would provide a large range of values but very little information about the absolute emissions. We have set the units of Fig. 10 a and b equal, to make the comparison more clear to the reader. Additionally, we have updated the calculation as the sensitivity to 1 ppb increase in CH_4 over the tropospheric column, not merely at the surface, as the focus on this analysis is the assimilation of column data.

Lines 8-10 : "The largest disagreements between measured and modeled Xt occur ... than annually." This sentence is unclear to me. Please rephrase.

This sentence has been expanded and clarified, "Large differences between measured and modeled $X^t_{CH_4}$ are concurrent with low emissions from seasonal sources. The adjustments to prior emissions produced by larger measurement-model disagreement that occur when seasonal sources are a small fraction of total emissions will overestimate posterior emissions from aseasonal sources. Thus these seasonal errors will bias source apportionment toward emissions that do not vary on timescales shorter than annually."

We have also added a more explicit description of the relationship between the seasonality of measurement-model disagreement and that of emissions that vary monthly before the discussion of Fig. 10.

Page 14 : line16 "the meridional gradient" of what ? emissions ? concentations ?

This sentence has been changed to clarify that we refer to the meridional gradient of X_{CH_4}.

Unit of figure 12 ? Kg/yr ? Maybe change to Tg/gridbox or Tg/yr/$\circ$latitude ?

Figure 12 plots $\mathrm{CH_4}$ column-averaged DMFs in units of ppb, as described on the labels. If referring to Fig. 12, however, the units on the figure are listed as "$\Delta\mathrm{CH_4}(\mathrm{Tg\,mo^{-1}})$." The caption has been changed from "Tg" to "summed over each zonal band, in Tg·mo^{-1}" for consistency.

Conclusions Line 3 : re-precise in the start of conclusion the you used GEOS-CHEM and what are XCH4 and XtCH4 as it has to be readable by itself.

The phrase "retrieved and modeled $X_{\mathrm{CH_4}}$ and $X^t_{\mathrm{CH_4}}$" has been changed to "TCCON and GEOS-Chem pressure-weighted total and tropospheric column-averaged DMFs of $\mathrm{CH_4}$, $X_{\mathrm{CH_4}}$ and $X^t_{\mathrm{CH_4}}$" to be more readable.

Page 15, lines 1-5 : If stratospheric ch4 is largely independent from tropospheric CH4, is it worth developing full tropospheric and stratospheric chemistry models or prescribing stratospheric CH4 based on satellite observations is enough ?

The insensitivity of the stratosphere to perturbations in tropospheric $\mathrm{CH_4}$ suggest that prescribed stratospheric $\mathrm{CH_4}$ could be prescribed in such a way that ensures mass conservation. For example, the stratospheric fields could be scaled according to the mass flux from the troposphere. As models develop their representation of stratosphere-troposphere exchange, however, the conservation of mass will need to be more carefully considered. Thus, more developed linear schemes for stratospheric $\mathrm{CH_4}$, such as the UCX mechanism we cite or Slimcat (Monge-Sanz et al., 2013), could provide computationally inexpensive ways to set stratospheric $\mathrm{CH_4}$.

References

Boering, K., Wofsy, S., Daube, B., Schneider, H., Loewenstein, M., Podolske, J., and Conway, T.: Stratospheric Mean Ages and Transport Rates from Observations of Carbon Dioxide and Nitrous Oxide, Science, 274, 1340–1343, doi:10.1126/science.274.5291.1340, 1996.

Boering, K. A., Hintsa, E. J., Wofsy, S. C., Anderson, J. G., Daube, B. C., Dessler, A. E., Loewenstein, M., McCormick, M. P., Podolske, J. R., Weinstock, E. M., and Yue, G. K.: Measurements of stratospheric carbon dioxide and water vapor at northern midlatitudes: Implications for troposphere-to-stratosphere transport, Geophysical Research Letters, 22, 2737–2740, doi:10.1029/95GL02337, http://dx.doi.org/10.1029/95GL02337, 1995.

Brewer, A.: Evidence for a world circulation provided by the measurements of helium and water vapour distribution in the stratosphere, Quarterly Journal of the Royal Meteorological Society, 75, 351–363, 1949.

Dobson, G.: Origin and distribution of the polyatomic molecules in the atmosphere, Proceedings of the Royal Society of London. Series A, Mathematical and Physical Sciences, 236, 187–193, 1956.

Fraser, A., Palmer, P. I., Feng, L., Boesch, H., Cogan, A., Parker, R., Dlugokencky, E. J., Fraser, P. J., Krummel, P. B., Langenfelds, R. L., O'Doherty, S., Prinn, R. G., Steele, L. P., van der Schoot, M., and Weiss, R. F.: Estimating regional methane surface fluxes: the relative importance of surface and GOSAT mole fraction measurements, Atmospheric Chemistry and Physics, 13, 5697–5713, doi:10.5194/acp-13-5697-2013, http://www.atmos-chem-phys.net/13/5697/2013/, 2013.

Jones, A., Walker, K. A., Jin, J. J., Taylor, J. R., Boone, C. D., Bernath, P. F., Brohede, S., Manney, G. L., McLeod, S., Hughes, R., and Daffer, W. H.: Technical Note: A trace gas climatology derived from the Atmospheric Chemistry Experiment Fourier Transform Spectrometer (ACE-FTS) data set, Atmospheric Chemistry and Physics, 12, 5207–5220, doi:10.5194/acp-12-5207-2012, http://www.atmos-chem-phys.net/12/5207/2012/, 2012.

Kirschke, S., Bousquet, P., Ciais, P., Saunois, M., Canadell, J. G., Dlugokencky, E. J., Bergamaschi, P., Bergmann, D., Blake, D. R., Bruhwiler, L., et al.: Three decades of global methane sources and sinks, Nature Geoscience, 6, 813–823, 2013.

Monge-Sanz, B. M., Chipperfield, M. P., Untch, A., Morcrette, J.-J., Rap, A., and Simmons, A. J.: On the uses of a new linear scheme for stratospheric methane in global models: water source, transport tracer and radiative forcing, Atmospheric Chemistry and Physics, 13, 9641–9660, doi:10.5194/acp-13-9641-2013, http://www.atmos-chem-phys.net/13/9641/2013/, 2013.

Mote, P. W., Rosenlof, K. H., McIntyre, M. E., Carr, E. S., Gille, J. C., Holton, J. R., Kinnersley, J. S., Pumphrey, H. C., Russell, J. M., and Waters, J. W.: An atmospheric tape recorder: The imprint of tropical tropopause temperatures on stratospheric water vapor, Journal of Geophysical Research: Atmospheres, 101, 3989–4006, doi:10.1029/95JD03422, http://dx.doi.org/10.1029/95JD03422, 1996.

Park, R. J., Jacob, D. J., Field, B. D., Yantosca, R. M., and Chin, M.: Natural and transboundary pollution influences on sulfate-nitrate-ammonium aerosols in the United States: Implications for policy, Journal of Geophysical Research: Atmospheres, 109, 2004.

Patra, P., Krol, M., Montzka, S., Arnold, T., Atlas, E. L., Lintner, B., Stephens, B., Xiang, B., Elkins, J., Fraser, P., et al.: Observational evidence for interhemispheric hydroxyl-radical parity, Nature, 513, 219–223, 2014.

Patra, P. K., Houweling, S., Krol, M., Bousquet, P., Belikov, D., Bergmann, D., Bian, H., Cameron-Smith, P., Chipperfield, M. P., Corbin, K., Fortems-Cheiney, A., Fraser, A., Gloor, E., Hess, P., Ito, A., Kawa, S. R., Law, R. M., Loh, Z., Maksyutov, S., Meng, L., Palmer, P. I., Prinn, R. G., Rigby, M., Saito, R., and Wilson, C.: TransCom model simulations of CH_4 and related species: linking transport, surface flux and chemical loss with CH_4 variability in the troposphere and lower stratosphere, Atmospheric Chemistry and Physics, 11, 12 813–12 837, doi:10.5194/acp-11-12813-2011, http://www.atmos-chem-phys.net/11/12813/2011/, 2011.

Rodgers, C. D. and Connor, B. J.: Intercomparison of remote sounding instruments, Journal of Geophysical Research, 108, 4116, doi:10.1029/2002JD002299, 2003.

Wecht, K. J., Jacob, D. J., Sulprizio, M. P., Santoni, G. W., Wofsy, S. C., Parker, R., Bösch, H., and Worden, J.: Spatially resolving methane emissions in California: constraints from the CalNex aircraft campaign and from present (GOSAT, TES) and future (TROPOMI, geostationary) satellite observations, Atmospheric Chemistry and Physics, 14, 8173–8184, doi:10.5194/acp-14-8173-2014, http://www.atmos-chem-phys.net/14/8173/2014/, 2014.

Wunch, D., Toon, G. C., Wennberg, P. O., Wofsy, S. C., Stephens, B. B., Fischer, M. L., Uchino, O., Abshire, J. B., Bernath, P., Biraud, S. C., Blavier, J.-F. L., Boone, C., Bowman, K. P., Browell, E. V., Campos, T., Connor, B. J., Daube, B. C., Deutscher, N. M., Diao, M., Elkins, J. W., Gerbig, C., Gottlieb, E., Griffith, D. W. T., Hurst, D. F., Jiménez, R., Keppel-Aleks, G., Kort, E. a., Macatangay, R., Machida, T., Matsueda, H., Moore, F., Morino, I., Park, S., Robinson, J., Roehl, C. M., Sawa, Y., Sherlock, V., Sweeney, C., Tanaka, T., and Zondlo, M. a.: Calibration of the Total Carbon Column Observing Network using aircraft profile data, Atmospheric Measurement Techniques, 3, 1351–1362, doi:10.5194/amt-3-1351-2010, http://www.atmos-meas-tech.net/3/1351/2010/, 2010.

Wunch, D., Toon, G. C., Sherlock, V., Deutscher, N. M., Liu, C., Feist, D. G., and Wennberg, P. O.: The Total Carbon Column Observing Network's GGG2014 Data Version, Tech. rep., Carbon Dioxide Information Analysis Center, Oak Ridge National Laboratory, Oak Ridge, Tennessee, U.S.A. doi: 10.14291/tccon.ggg2014.documentation.R0/1221662, doi:10.14291/tccon.ggg2014.documentation.R0/1221662, http://dx.doi.org/10.14291/tccon.ggg2014.documentation.R0/1221662, 2015.

Author Response to Review of Referee #3 for "Seasonal Variability of Stratospheric Methane: Implications for Constraining Tropospheric Methane Budgets Using Total Column Observations"

K. M. Saad[1], D. Wunch[1,2], N. M. Deutscher[3,4], D. W. T. Griffith[3], F. Hase[5], M. De Mazière[6], J. Notholt[4], D. F. Pollard[7], C. M. Roehl[1], M. Schneider[5], R. Sussmann[8], T. Warneke[4], and P. O. Wennberg[1]

[1]California Institute of Technology, Pasadena, California, USA
[2]University of Toronto, Toronto, Ontario, Canada
[3]University of Wollongong, Wollongong, NSW, Australia
[4]University of Bremen, Bremen, Germany
[5]Karlsruhe Institute of Technology, IMK-ASF, Karlsruhe, Germany
[6]Royal Belgian Institute for Space Aeronomy, Brussels, Belgium
[7]National Institute of Water and Atmospheric Research, Omakau, New Zealand
[8]Karlsruhe Institute of Technology, IMK-IFU, Garmisch-Partenkirchen, Germany

Correspondence to: K. M. Saad (katsaad@caltech.edu)

We thank Referee #3 for their comments.

The primary change in the updated manuscript is a reprocessing of the TCCON tropospheric methane (CH_4) column-averaged dry-air mole fractions (DMFs), which is described in detail in added supplement, "Updates to Tropospheric Methane Data" (Appendix A). Although some of the regression statistics and comparisons have changed as a result of measurement updates, the main conclusions, the mismatch in tropospheric seasonality and the dependence of the stratospheric contribution error on tropopause height, remain the same.

In our responses below, page and line numbers included refer to the previous discussion draft. Appendices are referred to based on their order in the revised manuscript, and their headings are noted to avoid ambiguity.

My first major concern is that the fluxes used for the "Base" case do not actually match the total column TCCON measurements all that well. This can be seen somewhat by the top row of scatter plots in Figure 4. The correlation between the the total column simulated by GEOS-Chem has a correlation with the TCCON measurements of 0.86, which is even a bit lower than the correlation of the tropospheric columns, which are arguably more relevant for flux inversions. But more worrying, in Figure 7 it can be seen that the seasonality of the total column across the TCCON northern hemisphere sites considered is completely wrong. This inability to capture the seasonal cycle in the total column means that only limited conclusions can be drawn from assessing the (slightly different) mismatch in the two parts of the column. Thus I think the main weakness of this paper is the choice of fluxes used for the forward simulation.

We chose to use the default emissions provided for the GEOS-Chem offline CH_4 simulation to demonstrate how systematic errors in the vertical profile of CH_4 (which are caused by parameters that do not vary interannually, namely OH fields and transport schemes) can alias into the optimized emissions resulting from an assimilation of total column measurements into an

atmospheric inversion. This analysis is a sensitivity study on how model biases can alias into emissions optimization. Thus, the choice of emissions would not drive results unless those emissions are somehow causing the systematic biases. The aseasonal simulation was set up as an experiment to determine if the seasonality of emissions was causing the tropospheric phase lag observed in the base simulation. As Fig. 7 illustrates, the seasonal phase was consistent between simulations even as the amplitude changed, which demonstrates that the chosen emissions fields do not drive the main result of this analysis.

These fluxes are only listed in terms of categories, with no itemization of which anthropogenic inventory (I guess EDGAR4.X?), which "other natural emissions", or which model was used for the very important seasonal wetland and rice fluxes. At very least this needs to be amended and clarified.

References were cited for the "default" offline CH_4 simulation, which included a description of these fluxes. We have since added details and references for each of the emissions categories have been added for the reader's convenience.

It's fine that the fluxes are added to the model at 60 second increments, but I guess that aside from fires and wetlands/rice the fluxes are constant throughout the year? Or did you employ a diurnal or weekly or annual cycle?

The list of emissions, which were grouped by time evolution (annual, monthly, and daily), now includes additional details that should make the time scales of their variability more apparent to the reader.

And what about the OH fields? Is there a reference for where these came from? Have they been optimized via methyl chloroform or similar?

Optimized OH fields were not available for GEOS-Chem, which led to the OH sensitivity experiments to test the dependency of CH_4 DMFs on the magnitude, seasonality, and distribution of tropospheric OH. These experiments are described in Appendix B1, "Equilibrium Sensitivity Experiments". The Northern to Southern Hemisphere ratio of 1.0 (monthly range of $0.975 - 1.02$, applying a six month lag in the Southern Hemisphere) is consistent with the ratio of 0.97 ± 0.12 found by Patra et al. (2014). The tropospheric OH are monthly-averaged output from a GEOS-Chem tropospheric chemistry simulation (Park et al., 2004). The description of tropospheric OH and stratospheric loss parameterization fields now include references.

What would have been a more relevant choice for this type of study would be to use optimized fluxes, resulting from an atmospheric inversion using the same model. There are a few groups working on methane inversions with GEOS-Chem, so such fluxes should not have been difficult to find through collaboration. Then you would have been able to start with a seasonal cycle in the column that is actually consistent at the TCCON sites, assuming that the TCCON sites were assimilated in the inversion. This would have made the analysis more relevant, and it would be my strongest recommendation for improving this study.

As you note, most of the recent optimized emissions that result from atmospheric inversions, especially those using GEOS-Chem as the forward model, assimilate TCCON total column measurements. Using these fluxes would make the measurement to model comparisons, and thus their correlations, no longer independent, and the statistics would be less meaningful.

Moreover, using optimized fluxes may not improve the seasonality of the mismatch. Fraser et al. (2011) compared TCCON total columns to GEOS-Chem run with posterior fluxes, which were derived from an inversion using GOSAT total columns and surface measurements, and found a seasonally-varying measurement-model mismatch that fell between ± 20 ppb (Fig. 6 of that paper). We agree that work that compares optimized fluxes from atmospheric inversions that assimilate data at various vertical levels would be very informative, and this approach would be an important next step.

Another concern related to the choice of fluxes relates to the method used for the aseasonal simulation. The manuscript describes that the seasonal fluxes (fires, wetlands, and rice) were "disabled" (I assume this means set to zero?), and then the other fluxes were scaled up to maintain the fluxes and the approximate (but certainly not exact, as showns in Figure 11) latitudinal distribution. Why not simply use an annual mean of the variable fluxes? Then you are not changing two things at once (geographic distribution and temporal variability) and attempting to attribute the changes to only one of the factors.

We agree that producing aseasonal emissions by changing the seasonally varying fluxes to be constant throughout each year for each grid box would be ideal. Unfortunately, the model infrastructure made such a simulation difficult to execute as it required the emissions code to be re-written, risking differences due to compiling changes. Thus the scaling technique was developed as an alternative to assess first-order impacts of emissions seasonality. We have added this explicitly as a limitation that should be improved on in the future. However, most of the notable results, especially the phase lag in the tropospheric seasonality, are consistent between the model runs despite any differences in the spatial distribution of emissions. This demonstrates the robustness of our conclusions regardless of the emissions fields used. Additionally, the analyses comparing the base and aseasonal simulations are aggregated on zonal or hemispheric scales and therefore should not vary because of the spatial differences of their emissions at smaller scales.

My next major concern is related to the numerics of how the stratospheric and tropospheric model columns are divided. I do not understand how the the statospheric column-integrated dry air mole fractions have values around 30-100 ppb (from Figure 4). This seems very, very low. Looking at the prior profiles from Wunch et al. (2011), Figure 2, the stratospheric values of CH4 range from 500-1800 ppm. I am not sure if this can be explained by the weighting with the pressure-weighted averaging kernel, as the methane column averaging kernel is actually rather flat (from Figure 4, Wunch et al., 2011). Also from Figure 1 of Saad et al. (2014), the only mixing ratios of stratospheric methane less than even 500 ppb seem to be over 40 km or so, which is far above even the highest tropopause. I had postulated that perhaps you had calculated the mixing ratio not in parts per million molecules of stratospheric air but rather of total column air (in which case it should have been explained). Although I would not advocate for such an approach, in that case the stratospheric partial column dry air mole fraction could be added directly to the tropospheric dry air mole fraction to get the total column dry air mole fraction. Looking again at Figure 4, this is clearly not the case: the tropospheric column is clearly larger than the total column. This needs to be clarified.

You correctly postulated that the stratospheric contribution is calculated in reference to the total column of air. This was done for both practical and conceptual reasons. TCCON $X_{\mathrm{CH_4}}$ and $X^t_{\mathrm{CH_4}}$ are processed to remove various spectroscopic biases and calibrated to in situ aircraft profiles, now described in Appendix A, "Updates to Tropospheric Methane Data." Thus, using these column-averaged DMFs instead of the $\mathrm{CH_4}$ columns in our proxy for stratospheric air ensures measurement biases are not the cause of any measurement-model mismatch.

Conceptually, because this paper focuses on how the model's stratospheric contribution to the total column can alter the conclusions made about tropospheric trends, we determined that stratospheric $\mathrm{CH_4}$ over the total column of air would be more relevant than the stratospheric partial column of $\mathrm{CH_4}$. We agree that if the purpose of this work was to assess modeled stratospheric profiles, the stratospheric partial column would be more appropriate. Because the stratosphere has less $\mathrm{CH_4}$, the stratospheric contribution depresses the total column value, so the tropospheric column average should be larger. We frame the stratospheric contribution as positive number to make the value more intuitive: a larger stratospheric contribution indicates the influence of the stratosphere on the total column is greater. The stratospheric contribution is also represented as a positive number for visual clarity; applying a sign change to the stratospheric contribution in Fig. 4 and adding it to $X^t_{\mathrm{CH_4}}$ does reproduce $X_{\mathrm{CH_4}}$.

We have updated the wording of the definition of the stratospheric contribution on p.5 l.21 to remove the ambiguity of how the stratospheric contribution is calculated. Additionally, we have added an appendix with the derivation of the stratospheric contribution, "Derivation of Stratospheric Contribution" (Appendix C). We have also changed usage of "stratosphere" to "stratospheric contribution" throughout the text for contexts in which the ambiguity could be confusing.

One other concern was the consistency of the model tropopause with that from the TCCON retrievals. You mention testing the impact of moving the tropopause model layer up one or two levels, but this does not allow for potential seasonal or regional variability in the match between the two. At very least the (latitude- and seasonal-dependent) correlation between the model and retrieval tropopause heights should be presented in some way.

Accurately representing GEOS-Chem's tropospheric column for the purpose of comparison to measurements depends on setting the tropopause so that the calculation from model output is consistent with the way the model defines the troposphere. Shifting the tropopause level allowed us to test the degree to which calculating $X^t_{\mathrm{CH_4}}$ using the daily average tropopause could bias the comparison. Because the vertical gradient of $\mathrm{CH_4}$ is steepest across the UTLS, choosing a lower tropopause level would change the vertical integration much less than choosing a higher level. Thus, integrating to higher pressure levels would provide a better measure of sensitivity to the integration tropopause height chosen.

Additionally, GEOS-Chem sets the top of the troposphere one level below the vertical pressure level below the tropopause, which we thought could also introduce a bias. We ran a simulation setting the top of the troposphere at the level in which the tropopause exists (now listed in Appendix B1, "Equilibrium Sensitivity Experiments"), essentially shifting the tropopause up two levels, to determine if the choice of the definition of the tropopause changed the distribution of $\mathrm{CH_4}$ concentrations. This change did not improve measurement-model agreement and, as the newly added figure demonstrates, had almost no impact on the seasonality of $X^t_{\mathrm{CH_4}}$ (Fig. 15 in the updated manuscript).

We consider other inconsistencies in the model tropopause, such as seasonal or zonal variability, as one of the model errors that can alias into $X_{\mathrm{CH_4}}$ comparisons. The calibration of TCCON measurements to in situ aircraft profiles (Wunch et al., 2015) limits any bias that errors in the TCCON tropopause heights could induce in the comparisons with the model. Moreover, the difference between calibrated TCCON and integrated aircraft $X_{\mathrm{CH_4}}$ and $X^t_{\mathrm{CH_4}}$ values have no correlation to the tropopause heights used to generate the TCCON priors or computed from the aircraft temperature and pressure profiles (uncertainty-weighted $R^2 = 0$).

P3, second paragraph: This sounds like you're describing atmospheric inversion while going out of your way not to call it "inversion". Or are you referring to optimization only by processed-based scaling of set spatial fields? Please clarify, and if you mean inversion, please say so.

We infer that the referee meant p.2 second paragraph and have added the term "atmospheric inversion" for clarity.

P2, L10: The reference to Stephens et al. (2007) here seems not to fit so well - this study was looking at aircraft profiles rather than column-integrated information.

The reference of Stephens et al. (2007) was included to illustrate the importance of assimilating observations that provide information about the vertical profile to accurately constrain chemical transport models. We agree that p.2 l.10 is not the appropriate location for this point and have moved the reference to the paragraph on p.2 l.22.

P4, L14: Although I mentioned it already above, there needs to be some citations to describe the model and fluxes used.

Citations and additional details for the GEOS-Chem offline $\mathrm{CH_4}$ emissions, tropospheric OH, and stratospheric loss fields have been added.

P5, L9-10: In Appendix A1 I coudln't find any real description of the OH sensitivity runs. Do your OH fields have seasonality? This experiment is insufficiently described.

We have added the following description of the "Updated OH" simulation (Table 2, Fig. 3) to Appendix B1, "Equilibrium Sensitivity Experiments":

> "The updated OH simulation used OH output from a 2012 GEOS-Chem standard chemistry simulation with extensive updates to the photochemical oxidation mechanisms of biogenic volatile organic compounds (VOCs), described in Bates et al. (2016) and references therein. These were converted to 3D monthly mean OH concentrations to conform to the infrastructure of the GEOS-Chem offline $\mathrm{CH_4}$ tropospheric loss mechanism. The OH was then scaled by 90% to keep the lifetime above 8 years, and emissions were scaled by 112% to maintain the same balance between sources and sinks in the base simulation. Figure 14 provides zonal averages of the difference between the base and updated OH columns."

We also ran several sensitivity experiments on different OH fields, which included scaling the default OH fields and using different scalings of the "Standard Chemistry + Biogenic VOCs" OH output. A table delineating these simulations has now been added to Appendix B1.

P5, L15: I was a bit confused here: are the means and medians for all values over the day, over just over those where TCCON measurements were made?

GEOS-Chem smoothed column-averaged DMFs were only calculated for days in which TCCON measurements were made and were smoothed using solar zenith angles, vertical scaling factors, and surface pressures for TCCON measurements used in the comparisons. The added discussion of the TCCON retrieval in Section 2.1 provides a description of the vertical scaling factor that clarifies subsequent references. To further lessen confusion, this sentence has been changed to, "For comparisons with column measurements, model vertical profiles were smoothed with corresponding TCCON CH_4 averaging kernels, interpolated for the daily mean solar zenith angles, and prior profiles, scaled with daily median vertical scaling factors and interpolated to the daily mean surface pressures measured at each site, following the methodology in Rodgers and Connor (2003) and Wunch et al. (2010)."

In general I found the use of "DMF" to mean "column-integrated dry air mole fraction" to be rather confusing. Flask measurements also measure dry air mole fraction, so DMF on its own does not tell the reader that an integrated column is being discussed. This is found throughout the manuscript and should be clarified.

The modifier "column-average" now precedes "DMF" unless referring to a surface or profile measurement to maintain consistency and avoid ambiguity.

Figure 3: The caption says that the stratosphere shows a seasonal cycle of 15 ppb at Park Falls, but in the figure looks like more like 30 ppb. Please explain. I was also surprised to see that Park Falls appears to have a larger seasonal cycle in hte stratosphere than in the troposphere for the Base case. This doesn't make sense to me. Please explain.

The text cites a seasonal amplitude of 15 ppb, referring to the peak amplitude of the seasonal cycle (i.e. the difference between the peak and the mean). The peak-to-trough amplitude, which is twice the peak amplitude, would indeed be 30 ppb. We have changed the word "amplitude" to "range" and updated the values accordingly to reduce confusion.

The model's larger seasonal cycle of the stratospheric contribution compared to that of the tropospheric column does not agree with the measurements, as illustrated by Fig. 7. The stratospheric contribution is a function of the gradient across the tropopause and CH_4 loss in the stratosphere (Appendix C, "Derivation of Stratospheric Contribution"); thus, model errors in prescribed tropopause height, stratospheric chemistry, and stratospheric transport will impact the seasonal cycle of the stratospheric contribution.

P7, L13-14: What about the significant figures on the slopes (e.g. 1.1±0.020).

The extra significant figures on the slope errors were unintended and have been removed.

P8, L5-7: I'm not sure that Figure 4 shows a good agreement between the stratospheric columns of TCCON and GEOS-Chem. Yes, the clump of points is closer to the 1:1 line, but it hardly forms a line at all. Is the correlation coefficient for this one station really notably higher?

The wording indicating good agreement has been changed to, "fall most closely to the one-to-one line." The spread across the one-to-one line seen at Lauder is partly due to seasonal variability, as the stratospheric loss parameterization in the model is monthly. Averaging GEOS-Chem daily values to correspond to the ACE-FTS and GEOS-Chem climatologies would make the relationship more compact.

Figure 5: Again I'm confused about the calculation of the stratopsheric column. For instance, we can see from Figure 4 that the stratospheric column simulated by GEOS-Chem is around 50 ppb. Then looking at Figure 5, ACE-FTS minus GEOS-Chem seems to show a difference of approximately -50 ppb around 45 degrees south. Does this mean that the ACE-FTS measurements are showing close to zero methane? In general there seems to be better agreement between TCCON and GEOS-Chem (Figure 4) than ACE-FTS and GEOS-Chem (Figure 5), but it is difficult to tell from the figures presented. Could you comment on this? How do ACE-FTS and TCCON agree?

Figure 5 illustrates differences between the $\mathrm{CH_4}$ profiles given by ACE-FTS and GEOS-Chem climatologies, not pressure-weighted column averages as in the TCCON comparison. As a point of reference, they correspond to the prior profiles from Wunch et al. (2011) you mentioned in previous comments. Thus, the ± 150 ppb range appertains to the difference of the mean $\mathrm{CH_4}$ mole fractions at each pressure level. The ACE-FTS climatology used in Fig. 5 is an older version of the measurements (v. 2.2, Jones et al., 2012), which could impact some of individual grid box differences. However, a comparison to the v.3.5 (which are used in the $X^t_{\mathrm{CH_4}}$ calculation) monthly mean $\mathrm{CH_4}$ DMFs indicate that the data version likely would not change main features illustrated in Fig. 5.

Because the comparisons between TCCON and GEOS-Chem are for pressure-weighted column averages, the agreement is therefore not directly comparable to ACE-FTS mole fraction differences at individual pressure levels. Agreement between TCCON and ACE-FTS is difficult to quantify because ACE-FTS retrievals provide vertical information solely in the upper atmosphere, and TCCON retrievals provide column averages that, due to the pressure weighting, are dominated by the troposphere. However, ACE-FTS is one of the various platforms used in the development of the empirical model that generates TCCON priors (Wunch et al., 2015), and the stratospheric $\mathrm{CH_4}$ profiles it measures are used in the calculation of the TCCON tropospheric $\mathrm{CH_4}$ product (Saad et al., 2014).

Figure 7: I am very surprised to see that the aseasonal simulations have higher seasonal cycles in both the stratosphere and the stratosphere than the base case. Are you sure of this result? What role does the (potential) seasonality of the OH sink have here?

The larger seasonal amplitude of the aseasonal $X^t_{\mathrm{CH_4}}$ is indeed a notable result. The greatest differences, from August through October, result from dampening the large summer wetland fluxes that balance high summer OH concentrations in the

base simulation. The larger variance across sites that we note is also indicative that the seasonal amplitude does not increase as drastically at the sub-tropical sites. (We did not include the figure with all site seasonalities because it was visually chaotic, given the many Northern Hemisphere sites.)

The second largest difference, during the spring, could also be a result of the source/sink balance: the aseasonal simulation introduces fluxes in the winter, when the OH concentrations are lowest. As we mention on p.10 l.18, the model may also have an error in phase with the seasonal emissions that produces the reasonable seasonal cycle amplitude in the base simulation troposphere (Fig. 7). We have added to that paragraph a discussion of the interaction between emissions and OH loss.

While the seasonal amplitude of the mean Northern Hemisphere stratospheric contribution is larger for the aseasonal versus base simulation, the maximum difference of their means is only about 2 ppb, which is within the 1σ standard deviations across sites. This similarity further demonstrates the insensitivity of the model's stratosphere to chosen emissions.

And what about the sampling throughout the year? Are there enough measurements at Bremen in December and January, or is part of this seasonality a question of shifting sampling throughout the year? Related to this: I assume you are only considering days on which there are TCCON measurements in the model analysis?

The seasonality of GEOS-Chem is computed from the smoothed pressure-weighted column-averaged DMFs, which incorporate the TCCON scaled prior profiles (see Appendix B3, "Model Smoothing for Measurement Comparisons") and thus require us to consider days on which TCCON measurements exist. While the number of measurements per month is variable throughout the year, all high latitude sites have a time series long enough to extract detrended monthly mean information. Moroever, the sites that are most susceptible to low winter sampling are the five in Europe, which are located in adjacent GEOS-Chem grid boxes. Because we average the seasonality across the Northern Hemisphere, the aggregate of these high-latitude sites would remove any impact that fewer winter measurements have. Figure 1 plots the Northern Hemispheric seasonality without the sites north of $50°$N, Bialystok and Bremen, for comparison. The only sites that are not included in the Northern Hemisphere seasonality are those which began taking measurements less than a year before the end of the model run: Saga and Réunion Island. We have rectified this omission in the text.

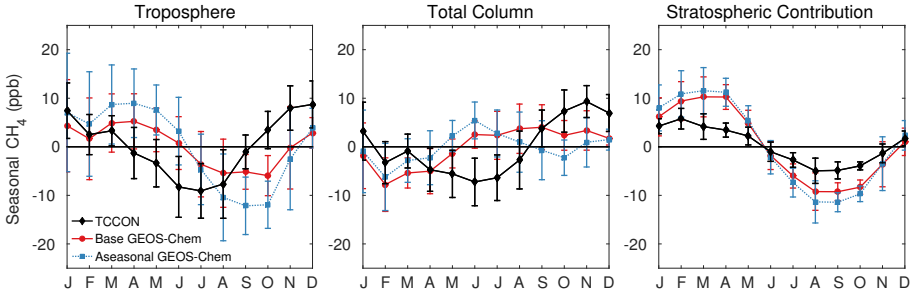

Figure 1. Detrended seasonality of TCCON (black diamonds), GEOS-Chem base (red circles), and GEOS-Chem aseasonal (blue squares) CH_4 column-averaged DMFs, averaged across Northern Hemisphere sites, except Bialystok, Bremen, Saga, and Réunion Island. Error bars denote the 1σ standard deviation across sites.

Another surprise here is that that seasonal cycle of the tropospheric and stratospheric columns in the aseasonal case are essentially in phase, yet when the total column is considered, a bimodal seasonal cycle is found. How can this be?

The stratospheric contribution is the amount by which the stratosphere decreases the total column average (via stratospheric loss and transport). Thus, the stratospheric contribution has an inverse effect on $X_{\mathrm{CH_4}}$ relative to $X^t_{\mathrm{CH_4}}$, and the balance between the stratospheric contribution and $X^t_{\mathrm{CH_4}}$ causes the seasonality in $X_{\mathrm{CH_4}}$. We define the stratospheric contribution more explicitly and include its derivation in Appendix C to prevent confusion.

P10, L11: I disagree with this statement: it seems that the seasonal cycle of the modelled stratospheric columns precede the seasonal cycle of TCCON by a good month.

The comparison of the stratospheric seasonality is difficult to assess by eye, but the stratospheric contributions of TCCON and GEOS-Chem are in phase, which is illustrated by the shared inflections point in June and December.

Figure 8: The smoothing carried out here is not informative. Why not a box and whiskers plot to show how variable the data really are? Also, Park Falls is rather a tricky station with quite a lot of local influence and not a clear seasonal cycle. Perhaps another station would be more informative?

Park Falls was chosen because of the TCCON sites that also have surface observations, the $X^t_{\mathrm{CH_4}}$ seasonality most closely matches the Northern Hemisphere mean shown in Fig. 7; thus Fig. 8 provides a good basis to compare surface and tropospheric column measurements. While the site does have a complicated seasonality near the surface, we find it notable that GEOS-Chem is able to capture several of those features, especially the local minimum in October, but still deviates from the observations, as we note on p.10 l.8. The box and whisker plots with superimposed observations and model data were difficult to follow visually. Instead, to show the variability, we have added to Fig. 8 lower and upper bounds denoting the 25th and 75th percentiles, respectively, of detrended data for each month.

Also, is the temporal sampling of the model consistent with that of the rather sparse flasks?

We had compared more frequent "Programmable Flask Package" (PFP) measurements, which have been measured at Park Falls since 2006, and found only slight differences in the seasonal cycle. Because we could not find equivalent in situ NOAA measurements, which we chose because they are on the same calibration scale as TCCON (Wunch et al., 2010), in the Southern Hemisphere, we only plot the flask measurements. Figure 2 plots Fig. 8 with the higher resolution flask data included for your reference.

In a broader sense I'm not sure what the real message here is. We see already in Figure 7 that the GEOS-Chem run does a very poor job of representing the seasonal cycle in the NH column: would you expect it to be better at the surface?

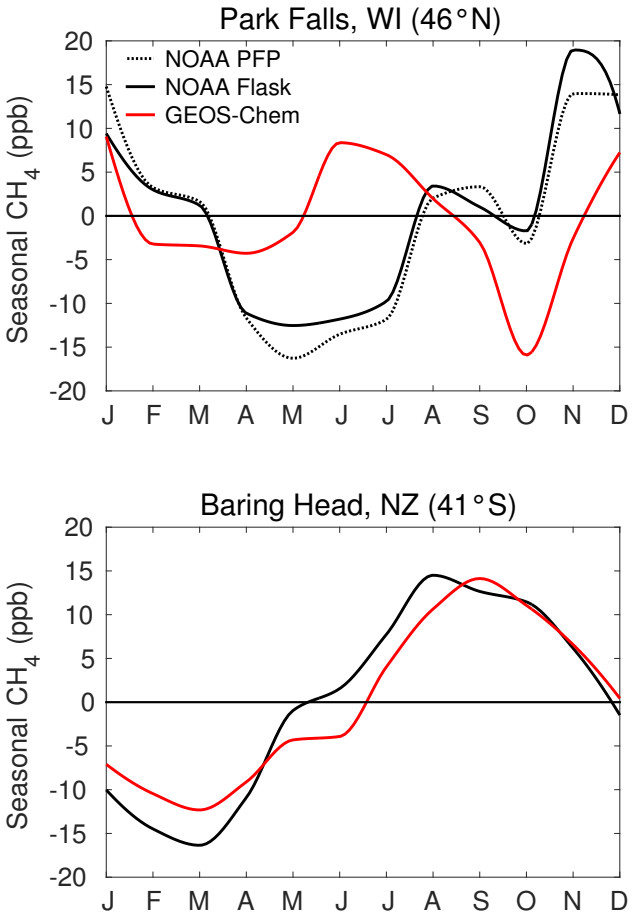

Figure 2. NOAA tall tower PFP flask (black dashed line), NOAA surface flask (black solid line), and GEOS-Chem surface level (red solid line) seasonality of CH_4 DMFs over 2005-2011 at Park Falls, WI, USA and Baring Head, NZ. PFP data is courtesy of Arlyn Andrews (NOAA): Andrews, A.E., E. Dlugokencky, and P.M. Lang (2008), Methane Dry Air Mole Fractions from the NOAA ESRL Surface Network using Programmable Flask Packages (PFP), 1992-2008, Version: 2013-07-03.

We included surface measurements (a) to demonstrate that the seasonality that we see is not due to some unknown bias in the $X^t_{\mathrm{CH_4}}$ measurements and (b) to test whether the phase shift could be due to vertical transport, which would create a smaller lag at the surface, or horizontal transport, which is our hypothesis.

Figure 9: Please label the plots (especially upper panel).

The upper panel of Fig. 9 is now labeled.

Figure 10: The y-axis should have the same scale for the top and bottom figures, even if only part of the range is shown.

The y-axes of the two subfigures in Fig. 10 have been scaled so that the latitude grid boxes are equal.

I was also not quite sure about the units here. 10^6 kg is 0.001 Tg, so the bright yellow (10 10^6 kg CH4) is 0.01 Tg CH4. But then in Figure 11 the increments between the seasonal and aseasonal run seem to be rather on the order of 1 Tg CH_4 mo^{-1}, which is two orders of magnitude higher. Or have I missed something here?

Figure 10 shows the zonally averaged wetland emissions, while Fig. 11 displays the total difference in emissions. The units in Fig. 10a have been changed to Gg, and the description of units in the caption of Fig. 11 has been changed from "Tg" to "summed over each zonal band, in Tg·mo^{-1}" to prevent confusion.

P13, L5-6: I did not quite understand the description of what you did here. You write "derived by calculating the total emissions resulting from an increase of 1 ppb of CH4 in each surface grid box". Do you mean by calculating the emissions required to cause a 1 ppb increase in each surface grid box? How often were you adding this increment? Monthly? Do you consider the effect that these emissions have on the concentrations of neibouring grid boxes? Is there a reference that explains this procedure in a bit more detail? Based on what is written here, I could not reproduce the experiment.

To show the true change in posterior emissions associated with a phase lag, the gain matrix would need to be derived for all grid boxes in the model. Because we did not have the actual sensitivity of CH_4 to wetland concentrations, which varies spatially depending on proximity to sources, we estimated that sensitivity as the mass of CH_4 associated with a 1 ppb increase in CH_4 in the surface grid box. The change in posterior emissions was then calculated as the product of this sensitivity and the fraction of the monthly mean emissions from wetlands in each surface grid box. Figure 10b mapped the difference between this change in posterior wetland emissions and the value in the same grid box three months prior, summed for each zonal band. Because this approach does not include any of the information about transport (as would exist in the linear operator that transforms model emissions to concentrations), we are not able to consider neighboring grid boxes. We have since updated the calculation as the sensitivity to 1 ppb increase in CH_4 over the tropospheric column, as the focus on this analysis is the assimilation of column data.

P14, L8: I don't think you have convincingly shown that the seasonal lag is a function of transport, and not, say, your sink, or the spatial distribution of the fluxes.

The sensitivity experiments we ran tested the model's response to a number of different emissions, OH, and meteorology fields. The seasonal phase shift in the tropospheric column appeared in all simulations, although the seasonal cycle amplitude and the shape of the springtime maximum varies. We have added a table describing these simulations and a figure that plots the tropospheric seasonality, as well as deviations from the base simulation, of each of these simulations to Appendix B1, "Equilibrium Sensitivity Experiments." We have also removed the sentence in the conclusion referred to by this comment.

P15, L1-2: While I agree that prescribing the stratospheric CH4 fields based on satellite observations might help, this will lead to transport that is not mass conserving, which is a problem for flux inversion. Please comment.

The insensitivity of the stratosphere to perturbations in tropospheric CH_4 suggest that prescribed stratospheric CH_4 would not need complicated adjustment to enforce mass conservation. We agree that the mechanism by which a model would set these CH_4 fields in the stratosphere would require careful consideration of how best to ensure the conservation of mass. For example, the stratospheric fields could be scaled according to the mass flux from the troposphere. As models develop their representation of stratosphere-troposphere exchange, however, the conservation of mass will become a more complicated problem. In addition to the UCX mechanism we suggested, a variety of linear schemes for stratospheric CH_4 have been tested for other models, such as Slimcat (Monge-Sanz et al., 2013).

Perhaps also mention that MIPAS and ACE-FTS are both good candidates for such an approach, but the former is not flying right now, and the latter has already been flying for 11 years and there is no replacement in sight.

This sentence now reads, "satellite observations from ACE-FTS, MIPAS (von Clarmann et al., 2009), or a compilation of remote sensing instruments (Buchwitz et al., 2015)." While stratospheric CH_4 fields for specific years would be ideal, even a monthly climatology with a secular increase applied would be an improvement on the current loss parameterization, which are monthly fields that do not vary interannually.

Typographical/language comments:

P3, L9: add "the" before "assimilation"

Table 1: The sign on the latitude of Darwin is wrong in this table.

P4, L11: Add degree symbol on both 4 and 5.

P5, L5: "data WERE available" (plural)

P5, L13: "and initial conditions" -> "and used as initial conditions"

There is no reference to Appendix A2 in the text.

P5, L18: "test the dependence of our results ON the"

p6, L1, L5, and a few other places: "emissions seasonality" isn't quite right. It should either be "the emissions' sensitivity" or "the seasonality of the emissions".

p11, L6: emissions -> emission

The above changes were made, and Appendix A2 (now B2) is now referenced in Section 2.2.1

References

Bates, K. H., Nguyen, T. B., Teng, A. P., Crounse, J. D., Kjaergaard, H. G., Stoltz, B. M., Seinfeld, J. H., and Wennberg, P. O.: Production and Fate of C4 Dihydroxycarbonyl Compounds from Isoprene Oxidation, The Journal of Physical Chemistry A, 120, 106–117, doi:10.1021/acs.jpca.5b10335, http://dx.doi.org/10.1021/acs.jpca.5b10335, 2016.

Buchwitz, M., Reuter, M., Schneising, O., Boesch, H., Guerlet, S., Dils, B., Aben, I., Armante, R., Bergamaschi, P., Blumenstock, T., Bovensmann, H., Brunner, D., Buchmann, B., Burrows, J. P., Butz, A., Chédin, A., Chevallier, F., Crevoisier, C. D., Deutscher, N. M., Frankenberg, C., Hase, F., Hasekamp, O. P., Heymann, J., Kaminski, T., Laeng, A., Lichtenberg, G., De Mazière, M., Noël, S., Notholt, J., Orphal, J., Popp, C., Parker, R., Scholze, M., Sussmann, R., Stiller, G. P., Warneke, T., Zehner, C., Bril, A., Crisp, D., Griffith, D. W. T., Kuze, A., O'Dell, C., Oshchepkov, S., Sherlock, V., Suto, H., Wennberg, P., Wunch, D., Yokota, T., and Yoshida, Y.: The Greenhouse Gas Climate Change Initiative (GHG-CCI): Comparison and quality assessment of near-surface-sensitive satellite-derived CO_2 and CH_4 global data sets, Remote Sensing of Environment, 162, 344–362, 2015.

Fraser, A., Chan Miller, C., Palmer, P. I., Deutscher, N. M., Jones, N. B., and Griffith, D. W. T.: The Australian methane budget: Interpreting surface and train-borne measurements using a chemistry transport model, Journal of Geophysical Research: Atmospheres, 116, n/a–n/a, doi:10.1029/2011JD015964, http://dx.doi.org/10.1029/2011JD015964, d20306, 2011.

Jones, A., Walker, K. A., Jin, J. J., Taylor, J. R., Boone, C. D., Bernath, P. F., Brohede, S., Manney, G. L., McLeod, S., Hughes, R., and Daffer, W. H.: Technical Note: A trace gas climatology derived from the Atmospheric Chemistry Experiment Fourier Transform Spectrometer (ACE-FTS) data set, Atmospheric Chemistry and Physics, 12, 5207–5220, doi:10.5194/acp-12-5207-2012, http://www.atmos-chem-phys.net/12/5207/2012/, 2012.

Monge-Sanz, B. M., Chipperfield, M. P., Untch, A., Morcrette, J.-J., Rap, A., and Simmons, A. J.: On the uses of a new linear scheme for stratospheric methane in global models: water source, transport tracer and radiative forcing, Atmospheric Chemistry and Physics, 13, 9641–9660, doi:10.5194/acp-13-9641-2013, http://www.atmos-chem-phys.net/13/9641/2013/, 2013.

Park, R. J., Jacob, D. J., Field, B. D., Yantosca, R. M., and Chin, M.: Natural and transboundary pollution influences on sulfate-nitrate-ammonium aerosols in the United States: Implications for policy, Journal of Geophysical Research: Atmospheres, 109, 2004.

Patra, P., Krol, M., Montzka, S., Arnold, T., Atlas, E. L., Lintner, B., Stephens, B., Xiang, B., Elkins, J., Fraser, P., et al.: Observational evidence for interhemispheric hydroxyl-radical parity, Nature, 513, 219–223, 2014.

Rodgers, C. D. and Connor, B. J.: Intercomparison of remote sounding instruments, Journal of Geophysical Research, 108, 4116, doi:10.1029/2002JD002299, 2003.

Saad, K. M., Wunch, D., Toon, G. C., Bernath, P., Boone, C., Connor, B., Deutscher, N. M., Griffith, D. W. T., Kivi, R., Notholt, J., Roehl, C., Schneider, M., Sherlock, V., and Wennberg, P. O.: Derivation of tropospheric methane from TCCON CH_4 and HF total column observations, Atmospheric Measurement Techniques, 7, 2907–2918, doi:10.5194/amt-7-2907-2014, http://www.atmos-meas-tech.net/7/2907/2014/, 2014.

Stephens, B. B., Gurney, K. R., Tans, P. P., Sweeney, C., Peters, W., Bruhwiler, L., Ciais, P., Ramonet, M., Bousquet, P., Nakazawa, T., Aoki, S., Machida, T., Inoue, G., Vinnichenko, N., Lloyd, J., Jordan, A., Heimann, M., Shibistova, O., Langenfelds, R. L., Steele, L. P., Francey, R. J., and Denning, A. S.: Weak Northern and Strong Tropical Land Carbon Uptake from Vertical Profiles of Atmospheric CO2, Science, 316, 1732–1735, doi:10.1126/science.1137004, http://science.sciencemag.org/content/316/5832/1732, 2007.

von Clarmann, T., Höpfner, M., Kellmann, S., Linden, A., Chauhan, S., Funke, B., Grabowski, U., Glatthor, N., Kiefer, M., Schieferdecker, T., Stiller, G. P., and Versick, S.: Retrieval of temperature, H₂O, O₃, HNO₃, CH₄,

N₂O, ClONO₂ and ClO from MIPAS reduced resolution nominal mode limb emission measurements, Atmospheric Measurement Techniques, 2, 159–175, doi:10.5194/amt-2-159-2009, http://www.atmos-meas-tech.net/2/159/2009/, 2009.

Wunch, D., Toon, G. C., Wennberg, P. O., Wofsy, S. C., Stephens, B. B., Fischer, M. L., Uchino, O., Abshire, J. B., Bernath, P., Biraud, S. C., Blavier, J.-F. L., Boone, C., Bowman, K. P., Browell, E. V., Campos, T., Connor, B. J., Daube, B. C., Deutscher, N. M., Diao, M., Elkins, J. W., Gerbig, C., Gottlieb, E., Griffith, D. W. T., Hurst, D. F., Jiménez, R., Keppel-Aleks, G., Kort, E. a., Macatangay, R., Machida, T., Matsueda, H., Moore, F., Morino, I., Park, S., Robinson, J., Roehl, C. M., Sawa, Y., Sherlock, V., Sweeney, C., Tanaka, T., and Zondlo, M. a.: Calibration of the Total Carbon Column Observing Network using aircraft profile data, Atmospheric Measurement Techniques, 3, 1351–1362, doi:10.5194/amt-3-1351-2010, http://www.atmos-meas-tech.net/3/1351/2010/, 2010.

Wunch, D., Toon, G. C., Blavier, J.-F. L., Washenfelder, R. a., Notholt, J., Connor, B. J., Griffith, D. W. T., Sherlock, V., and Wennberg, P. O.: The Total Carbon Column Observing Network, Philosophical transactions. Series A, Mathematical, physical, and engineering sciences, 369, 2087–2112, doi:10.1098/rsta.2010.0240, http://www.ncbi.nlm.nih.gov/pubmed/21502178, 2011.

Wunch, D., Toon, G. C., Sherlock, V., Deutscher, N. M., Liu, C., Feist, D. G., and Wennberg, P. O.: The Total Carbon Column Observing Network's GGG2014 Data Version, Tech. rep., Carbon Dioxide Information Analysis Center, Oak Ridge National Laboratory, Oak Ridge, Tennessee, U.S.A. doi: 10.14291/tccon.ggg2014.documentation.R0/1221662, doi:10.14291/tccon.ggg2014.documentation.R0/1221662, http://dx.doi.org/10.14291/tccon.ggg2014.documentation.R0/1221662, 2015.

Seasonal Variability of Stratospheric Methane: Implications for Constraining Tropospheric Methane Budgets Using Total Column Observations

K. M. Saad[1], D. Wunch[1,2], N. M. Deutscher[3,4], D. W. T. Griffith[3], F. Hase[5], M. De Mazière[6], J. Notholt[4], D. F. Pollard[7], C. M. Roehl[1], M. Schneider[5], R. Sussmann[8], T. Warneke[4], and P. O. Wennberg[1]

[1]California Institute of Technology, Pasadena, California, USA
[2]University of Toronto, Toronto, Ontario, Canada
[3]University of Wollongong, Wollongong, NSW, Australia
[4]University of Bremen, Bremen, Germany
[5]Karlsruhe Institute of Technology, IMK-ASF, Karlsruhe, Germany
[6]Royal Belgian Institute for Space Aeronomy, Brussels, Belgium
[7]National Institute of Water and Atmospheric Research, Omakau, New Zealand
[8]Karlsruhe Institute of Technology, IMK-IFU, Garmisch-Partenkirchen, Germany

Correspondence to: K. M. Saad (katsaad@caltech.edu)

Abstract. Global and regional methane budgets are ~~uncertain due to the large number of highly variable sources. Current estimates~~ markedly uncertain. Conventionally, estimates of methane sources are derived by bridging emissions inventories with atmospheric observations ~~using~~ employing chemical transport models. ~~This approach requires accurately~~ The accuracy of this approach requires correctly simulating advection and chemical loss ~~to produce valid distributions of methane concentrations resulting from surface fluxeswhen assimilating~~ such that modeled methane concentrations scale with surface fluxes. When total column measurements ~~. To assess~~ are assimilated into this framework, modeled stratospheric methane introduces additional potential for error. To evaluate the impact of ~~model stratospheric errorson inversions that assimilate total columns, we compare the agreement between~~ such errors, we compare Total Carbon Column Observing Network (TCCON) and GEOS-Chem total and tropospheric column-averaged dry-air mole fractions of methane. We find ~~both a mismatch in the Northern Hemisphere stratospheric contribution that~~ that the model's stratospheric contribution to the total column is insensitive to perturbations to the seasonality or distribution of *tropospheric* emissions or loss. In the Northern Hemisphere, we identify disagreement between the measured and modeled stratospheric contribution, which increases as the tropopause altitude decreases, and a temporal phase lag in the model's tropospheric seasonality driven by transport errors. ~~These tropospheric errors particularly compensate the stratospheric discrepancies between measurements and models, thereby producing agreement in the total columns masking inconsistencies in methanevertical profiles. These~~ Within the context of GEOS-Chem, we find that the errors in tropospheric advection partially compensate for the stratospheric methane errors, masking inconsistencies between the modeled and measured tropospheric methane. These seasonally-varying errors alias into source ~~attribution~~ attributions resulting from model inversions. ~~We estimate~~ In particular, we suggest that the tropospheric ~~time lag~~ phase lag error leads to large ~~errors in posterior~~ misdiagnoses of wetland emissions in the high latitudes of the Northern Hemisphere.

1 Introduction

Identifying the processes that have driven changes in atmospheric methane (CH_4), a potent radiative forcing agent and major driver of tropospheric oxidant budgets, is critical for understanding future impacts on the climate system. Methane's growth rate, which had been decreasing through the 1990s from about 10 to 0 ppb per year, began to increase again in 2006 and over the past decade has averaged 5 ppb per year (Dlugokencky et al., 2011). Developing robust constraints on the global CH_4 budget is integral for understanding which processes produced these decadal trends (e.g., Bergamaschi et al., 2013; Wecht et al., 2014a, b; Turner et al., 2015).

One common approach to quantifying changes in the spatial distribution of sources ~~incorporates~~ are atmospheric inversions, which incorporate surface fluxes estimated by bottom-up inventories as boundary conditions for a chemical transport model (CTM). The modeled CH_4 concentrations are compared to observations within associated grid boxes, and prior emissions are scaled to minimize differences with measured dry-air mole fractions (DMFs), producing posterior estimates. ~~This method assumes that each source's relative contribution to a given grid box's concentration are known at any point in time.~~ The accuracy of these optimized emissions depends on how well the CTM simulates atmospheric transport and CH_4 sinks, which are generally prescribed.

Pressure-weighted total column-averaged DMFs (X_{gas}) provide a relatively new constraint and have previously been shown to improve estimates of regional and interhemispheric gradients in trace gases ~~(Stephens et al., 2007; Yang et al., 2007)~~ (Yang et al., 2007). Fourier transform infrared spectrometers can measure CH_4 DMFs (X_{CH_4}) from ground-based sites, such as those in the Total Carbon Column Observing Network (TCCON) and Network for the Detection of Atmospheric Composition Change (NDACC), and satellites, including SCanning Imaging Absorption spectroMeter for Atmospheric CartograpHY (SCIAMACHY) (Bergamaschi et al., 2007), Greenhouse gases Observing SATellite (GOSAT) (Parker et al., 2011), and the upcoming TROPOspheric Monitoring Instrument (TROPOMI) (Butz et al., 2012). These observations complement surface measurements because they add information about the vertically-averaged profile and are sensitive in the free troposphere (Yang et al., 2007). Additionally, they complement aircraft observations by measuring trace gases at higher temporal frequency~~.~~, ~~Satellite measurements also~~ although they share the limitation of not measuring in inclement weather. Satellite measurements add global coverage that can fill in gaps where in situ observations are sparse. Fraser et al. (2013) found ~~that~~ assimilating GOSAT CH_4 columns into the GEOS-Chem CTM with an ensemble Kalman filter reduced posterior emissions uncertainties by ~~up to 45% compared to~~ $9-48\%$ for individual source categories and by more than three times those of inversions that only assimilated surface data for most regions. Wecht et al. (2014b) determined from their analysis of observing system simulation experiments (OSSEs) that TROPOMI's ~~global daily measurements will~~ daily frequency and global coverage performs similarly to aircraft campaigns on sub-regional scales and could provide a constraint on California's CH_4 emissions similar to CalNex aircraft observations (Santoni et al., 2014; Gentner et al., 2014).

Incorporating total columns into modeling assessments can also be used to diagnose systematic issues with model transport. ~~Comparing~~ For example, comparing carbon dioxide (CO_2) from TCCON and TransCom (Baker et al., 2006), Yang et al. (2007) found that most ~~TransCom models~~ models included in the comparison lack sufficiently strong vertical ~~transport~~

from exchange between the planetary boundary layer (PBL) to the mixed layerand the free troposphere, thereby dampening the seasonal cycle amplitude of X_{CO_2}. The limitations of models to accurately represent vertical transport can lead to radically different spatial distributions of fluxes; Stephens et al. (2007) found, for example, that the northern terrestrial carbon land sink and tropical emissions were overestimated by 0.9 and 1.7 PgC·year^{-1}, respectively, when constraining models with aircraft CO_2 in the free troposphereprofiles. More recent studies attribute to model transport errors the tendency of simulated CH_4 in the Southern Hemisphere to be higher at the surface than the free troposphere, in contrast with measurements (Patra et al., 2011; Fraser et al., 2011) (Fraser et al., 2011; Patra et al., 2011) .

Tropospheric CH_4 typically does not vary radically with height above the PBL; above the tropopause, however, the vertical profile of CH_4 exhibits a rapid decline with altitude as a result of its oxidation and the lack of any source beyond advection from the troposphere. Fluctuations in stratospheric dynamics, including the height of the tropopause, change the contribution of the stratosphere to the total column. CH_4 profiles with similar tropospheric values can thus have significant differences in X_{CH_4} (Saad et al., 2014; Washenfelder et al., 2003; Wang et al., 2014).

Insofar as Provided that simulations replicate seasonal and zonal variability of stratospheric CH_4 loss, tropopause heights, and vertical exchange across the upper troposphere and lower stratosphere (UTLS), posterior flux estimates from inversions incorporating X_{CH_4} measurements would not be sensitive to stratospheric processes. However, most models do not accurately represent stratospheric transport, producing low age of air values and zonal gradients in the subtropical lower stratosphere that are less steep than observations (Waugh and Hall, 2002). The TransCom-CH_4 CTM intercomparison assessment of transport using sulfur hexafluoride SF_6 showed a strong correlation between the stratosphere-troposphere exchange (STE) rate and the model's CH_4 budget and a weaker correlation between the CH_4 growth rate and vertical gradient in the model's equatorial lower stratosphere (Patra et al., 2011) . These forward model dependencies of CH_4 concentrations to vertical transport, both within the troposphere and across the tropopause, have the potential to introduce substantial errors in atmospheric inversions. As temporal and spatial biases in a model's vertical profile will alias into posterior emissions, inversions that incorporate total column measurements must ensure that the stratosphere is sufficiently well described so as to not introduce spurious seasonal, zonal and interhemispheric trends in CH_4 concentrations and consequently emissions.

In this analysis, we identify systematic model biases errors in the seasonal cycle and spatial distribution of CH_4 DMFs by comparing TCCON total and tropospheric columns (Saad et al., 2014) to vertically integrated profiles derived from the GEOS-Chem CTM (Bey et al., 2001; Wang et al., 2004; Wecht et al., 2014a). We assess the impact of errors in the characterization of stratospheric processes on the assimilation of X_{CH_4} and resulting posterior emissions estimates. In Section 2 we describe the TCCON column measurements and GEOS-Chem set up and characteristics. In Section 3 we present the results of the measurement-model comparison. In Section 4 we compare the base case simulation to one in which emissions fluxes do not vary within each year and quantify the sensitivity of source attribution of the biggest seasonal emissions sector, wetlands, to the tropospheric seasonal delay.

Figure 1. Map of TCCON sites used in this analysis. Site colors are on a spectral color scale in order of latitude, with Northern Hemisphere sites designated by cool colors and Southern Hemisphere sites designated by warm colors.

2 Methods

2.1 Tropospheric Methane Columns

TCCON has provided precise measurements of X_{CH_4} and other atmospheric trace gases for over ten years ~~(Wunch et al., 2011a)~~ (Wunch et
Developed to address open questions in carbon cycle science, the earliest sites are located in Park Falls, Wisconsin, United States and Lauder, New Zealand at about 45° North and South, respectively. Since 2004, the ground-based network of Fourier transform spectrometers has expanded greatly. X_{CH_4} are processed with the current version of the TCCON software, GGG2014, to be consistent, and thereby comparable, across sites. Total column retrievals are generated with the GFIT nonlinear least-squares fitting algorithm, which calculates the best spectral fit of the solar absorption signal to an a priori vertical profile and outputs a vertical scaling factor. The pressure-weighted integration of the scaled a priori profile produces column abundances, which are then divided by the dry air column, calculated using concurrently retrieved oxygen (O_2) columns (Wunch et al., 2010, 2011a, 2015) . Trace gas a priori profiles are derived with empirical models, which are generated incorporating aircraft and balloon in situ and satellite measurements (see Wunch et al., 2015, for a complete list) , and for CH_4 include a secular increase of 0.3% per year and an interhemispheric gradient in the altitude dependence of the vertical profiles (Toon and Wunch, 2014) . These models are fit to daily noontime National Centers for Environmental Protection and National Center for Atmospheric Research (NCEP/NCAR) reanalysis pressure grids (Kalnay et al., 1996) , interpolated to the surface pressure measured real-time on site. Because the profile of CH_4 drops off rapidly in the stratosphere, the accuracy of the a priori shape, and thus the retrieved column, depends on correctly determining the tropopause.

Tropospheric columns have been shown to represent the magnitude and seasonality of in situ measurements (Saad et al., 2014; Washenfel
The tropospheric CH_4 ~~columns~~ column-averaged DMFs ($X^t_{CH_4}$) are derived by the ~~hydrogen fluoride () proxy~~ HF-proxy method described in Saad et al. (2014), which uses the relationship between CH_4 and HF in the stratosphere, derived from ACE-FTS satellite measurements (Bernath, 2005; De Mazière et al., 2008; Mahieu et al., 2008; Waymark et al., 2014), to cal-

culate and remove the stratospheric contribution to X_{CH_4}. ~~Tropospheric columns have been shown to represent the magnitude and seasonality of in situ measurements (Saad et al., 2014; Washenfelder et al., 2003; Wang et al., 2014) .~~ The $X^t_{CH_4}$ used in this analysis have been processed consistently with the GGG2014 TCCON products, with airmass dependence and calibration factors calculated for and applied to $X^t_{CH_4}$ (Wunch et al., 2010, 2015). Additional details about the tropospheric CH_4 measurements can be found in Appendix A.

With the exception of Eureka and Sodankylä, which are highly influenced by the stratospheric polar vortex, all TCCON sites that provide measurements before December 2011 are included in this analysis (Fig. 1). Table 1 lists locations and data collection start dates for each of the sites.

Table 1. TCCON sites, coordinates, altitudes, start date of measurements and locations used in this analysis.

Site	Latitude (°)	Longitude (°)	Elevation (km)	Start Date	Location	Data Reference
Bialystok	53.2	23.0	0.18	Mar 2009	Bialystok, Poland	Deutscher et al. (2014)
Bremen	53.1	8.9	0.03	Jan 2007	Bremen, Germany	Notholt et al. (2014)
Karlsruhe	49.1	8.4	0.11	Apr 2010	Karlsruhe, Germany	Hase et al. (2014)
Orleans	48.0	2.1	0.13	Aug 2009	Orleans, France	Warneke et al. (2014)
Garmisch	47.5	11.1	0.75	Jul 2007	Garmisch, Germany	Sussmann and Rettinger (2014)
Park Falls	45.9	-90.3	0.47	Jan 2005	Park Falls, WI, USA	Wennberg et al. (2014b)
Lamont	36.6	-97.5	0.32	Jul 2008	Lamont, OK, USA	Wennberg et al. (2014c)
JPL	34.2	-118.2	0.39	Jul 2007	Pasadena, CA, USA	Wennberg et al. (2014d, a)
Saga	33.2	130.3	0.01	Jul 2011	Saga, Japan	Kawakami et al. (2014)
Izaña	28.3	-16.5	2.37	May 2007	Tenerife, Canary Islands	Blumenstock et al. (2014)
Darwin	~~12.4~~ -12.4	130.9	0.03	Aug 2005	Darwin, Australia	Griffith et al. (2014a)
Réunion Island	-20.9	55.5	0.09	Sep 2011	Saint-Denis, Réunion	De Maziere et al. (2014)
Wollongong	-34.4	150.9	0.03	Jun 2008	Wollongong, Australia	Griffith et al. (2014b)
Lauder	-45.0	169.7	0.37	Jan 2005	Lauder, New Zealand	Sherlock et al. (2014a, b)

2.2 GEOS-Chem Model

Model comparisons use the offline CH_4 GEOS-Chem version 9.02 at ~~4 × 5°~~ $4° \times 5°$ horizontal resolution on a reduced vertical grid (47L). CH_4 loss is calculated on 60 minute intervals and is set by ~~3D monthly~~ annually-invariable monthly 3D fields: hydroxyl radical (OH) concentrations in the troposphere (Park et al., 2004) and parameterized CH_4 loss rates per unit volume in the stratosphere ~~.~~ (Considine et al., 2008; Allen et al., 2010; Murray et al., 2012) . Emissions are released at 60-minute time steps and are ~~split between~~ provided by the GEOS-Chem development team for 10 sectors: gas and oil, coal, livestock, waste, biofuel, ~~other anthropogenic, and other natural emissions annual values~~and other anthropogenic annual emissions from EDGAR v4.2 (European Commission Joint Research Centre, Netherlands Environmental Assessment Agency, 2011; Wecht et al., 2014a)

other natural annual emissions from (Fung et al., 1991) ; rice agriculture ~~and wetland monthly~~ (European Commission Joint Research Centr wetland (Pickett-Heaps et al., 2011) monthly emissions, which incorporate GEOS5 annual and monthly mean soil moisture values; and biomass burning daily ~~values using~~ emission from GFED3 ~~emissions estimates~~ estimates (Mu et al., 2011; van der Werf et al., 2 Loss via soil absorption (Fung et al., 1991) , set annually, is subtracted from the total emissions at each time step.

2.2.1 Model Set Up

We initialized zonal CH_4 distributions with GGG2014 data version a priori profiles (Wunch et al., 2015) produced at horizontal grid centers, which we adjusted vertically to match the zonally averaged daily mean ~~GEOS5 tropopause~~model's tropopause, derived from the National Aeronautics and Space Administration Global Modeling and Assimilation Office (NASA/GMAO) Goddard Earth Observing System Model, Version 5 (GEOS5). The model was run from December 2003, the first month in which GEOS5 meteorological data ~~was~~ were available, to June 2004, the beginning of the TCCON time series; we then ran the model repeatedly over the June 2004-May 2005 time frame, which allowed us to make comparisons with the TCCON data at Park Falls and Lauder, until CH_4 concentrations reached equilibrium. A number of perturbation experiments were run in this way to quantify the sensitivity of CH_4 distribution and seasonality to the offline OH fields, prescribed emissions, and tropopause levels (Table 2). These model experiments are described in greater detail in Appendix B1.

Using CH_4 fields for 1 January 2005 from the equilibrium simulation as initial conditions, model daily mean CH_4 mole fractions were computed through 2011. These were converted to dry mole fractions, as described in Appendix B2. In addition to the default emissions scheme, an aseasonal simulation setup, in which rice, wetland, and biomass burning emissions were disabled and aseasonal emissions scaled up such that total annual zonal fluxes approximate those in the base simulation, was similarly run to equilibrium and used as initial conditions for the 2005-2011 run.

For comparisons with column measurements, model vertical profiles were smoothed with corresponding TCCON CH_4 averaging kernels~~and~~ , interpolated for the daily mean solar zenith angles, and prior profiles, scaled with daily median vertical scaling factors and interpolated to the daily ~~median scaled priors using daily~~ mean surface pressures ~~and solar zenith angles for~~ measured at each site, following the methodology in Rodgers and Connor (2003) and Wunch et al. (2010). Tropospheric columns were integrated in the same manner as the total columns up to the grid level completely below the daily mean tropopause, consistent with how GEOS-Chem partitions the atmosphere in the offline CH_4 simulation. To test the dependence of our results ~~to~~ on the chosen vertical integration level, tropospheric columns were also calculated assuming the tropopause was

Table 2. ~~Table of~~ Sensitivity Experiments

Run Name	Description	CH_4 Lifetime (years)	Final CH_4 Burden (Tg)
Base	Default OH and Emissions	9.55	4825
Aseasonal	Constant Monthly Emission Rates	9.57	4872
Updated OH	Monthly OH fields from Standard Chemistry + Biogenic ~~VOCS~~ VOCs	8.53	4828

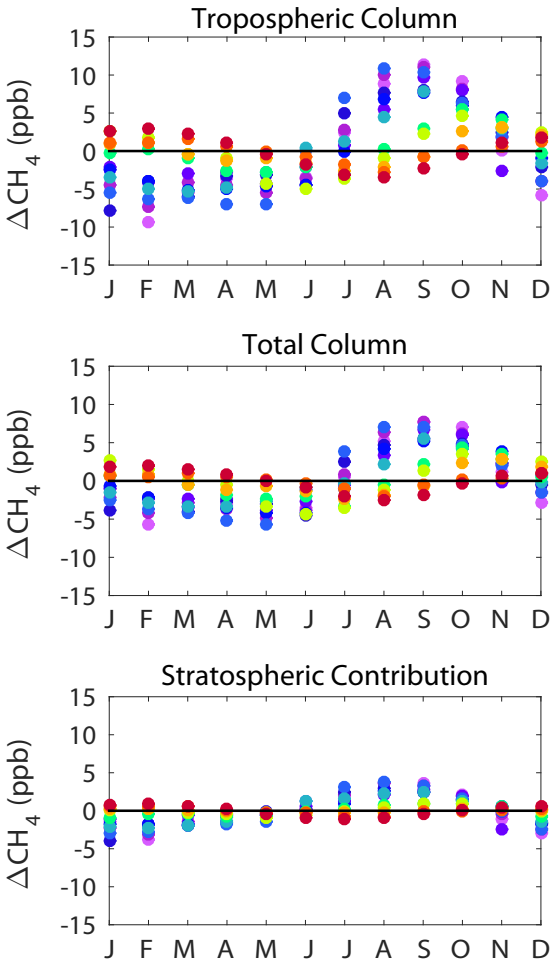

Figure 2. Seasonality of the difference between base and aseasonal CH_4 for tropospheric, total and stratospheric contribution to total columns. Site colors are as in Fig. 1.

one and two grid cells above this level. While $X^t_{CH_4}$ changed slightly, by a median of about 1 and 5 ppb for a one and two-level increase respectively, shifting the tropopause did not alter the findings discussed in this paper. ~~The stratospheric contribution is calculated as the residual between the tropospheric and total columns.~~ A description of the model smoothing methodology and assumptions is provided in Appendix B3. The stratospheric contribution to the total column, which is calculated as the residual between the $X^t_{CH_4}$ and X_{CH_4}, is the amount by which the stratosphere attenuates X_{CH_4} via stratospheric loss and transport (see Appendix C for the derivation).

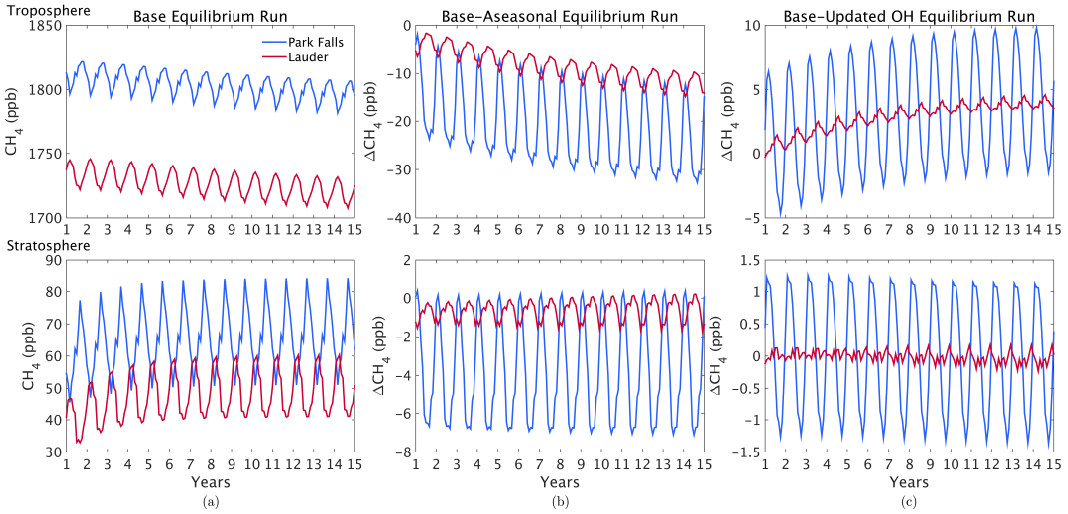

Figure 3. Smoothed daily mean ~~DMFs~~ $X^t_{CH_4}$ and stratospheric contribution to X_{CH_4} at Park Falls (blue) and Lauder (red) for (a) base equilibrium simulation and the difference between the base and (b) aseasonal and (c) updated OH simulations.

2.2.2 Model Features

The seasonal amplitude of the differences between base and aseasonal simulations are ~~small for~~ small–within ±4 ppb–for all vertical levels in the Southern Hemisphere (Fig. 2). In the Northern Hemisphere, however, the difference ~~in the amplitude~~ is much larger and primarily impacts the troposphere, where it varies between −10 and +13 ppb. The insensitivity of the stratosphere to ~~emissions seasonality~~ the seasonality of emissions is due to the common source of stratospheric air in the tropics (Boering et al., 1995) and the loss of seasonal information as the age of air increases ~~.~~ (Mote et al., 1996) .

~~Seasonality of the difference between base and aseasonal for tropospheric, total and stratospheric contribution to total columns. Site colors are as in Fig. 1.~~

Due to the relatively short photochemical lifetime of CH_4 in the stratosphere, about 22 months in the base simulation, stratospheric CH_4 concentrations stabilize much more quickly than in the troposphere (Fig. 3a). This rapid response time of the stratosphere occurs regardless of perturbations to the troposphere, such as ~~emissions seasonality~~ the seasonality of emissions (Fig. 3b) or tropospheric OH fields (Fig. 3c). In both hemispheres the differences between the base and experimental simulations asymptotically approach steady state with seasonal variability over a decade in the troposphere, but oscillate seasonally around a constant mean in the stratosphere. Stratospheric differences between simulations are considerably ~~lower~~ smaller than the seasonal amplitude of the base run: within six and one ppb, respectively, versus a seasonal ~~amplitude of 15~~ range of 30 ppb at Park Falls. By contrast, $X^t_{CH_4}$ have differences within 30 and 10 ppb, respectively, versus a seasonal ~~amplitude of 10~~ range of 20 ppb at Park Falls. The stratosphere at Lauder is even less sensitive to tropospheric perturbations.

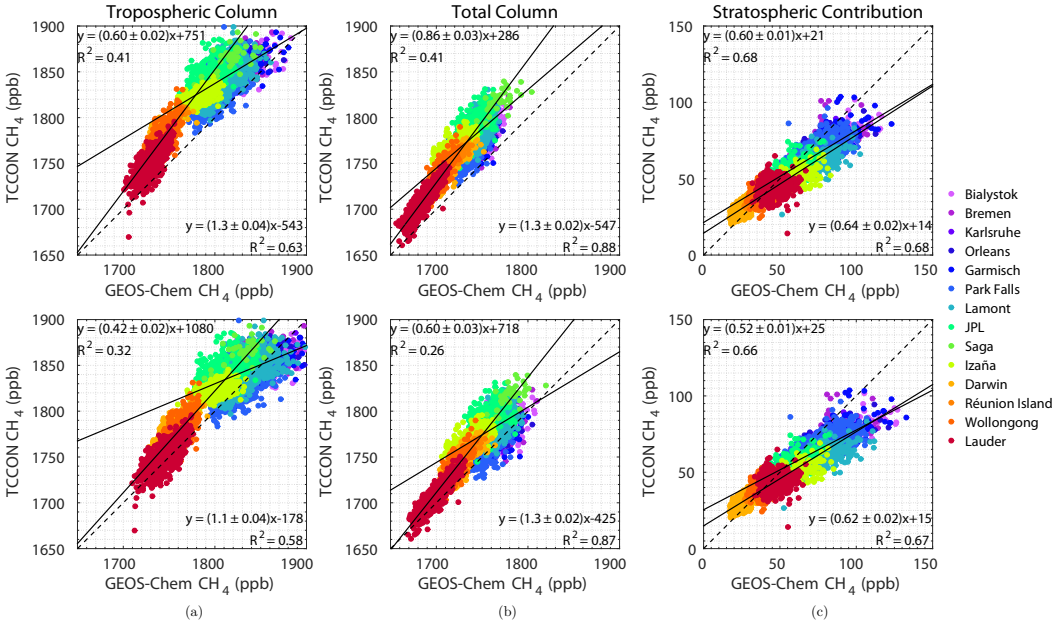

Figure 4. Daily median TCCON and smoothed daily mean GEOS-Chem base (top) and aseasonal (bottom) DMFs for (a) $X^t_{CH_4}$, (b) X_{CH_4}, and (c) stratospheric contribution. Site colors are as in Fig. 1. Northern Hemisphere least squares regression equations are in the top left, and Southern Hemisphere least squares regression equations are in the bottom right of each plot. Dashed lines mark the one-to-one lines.

3 Measurement-Model Comparison

The TCCON daily median and GEOS-Chem daily mean CH_4 ~~DMFs are highly correlated for both the tropospheric and total columns, with R^2 values of 0.89~~ column-averaged DMFs demonstrate a strong interhemispheric difference for $X^t_{CH_4}$ and ~~0.86 for their respective least squares linear regressions~~ X_{CH_4} in the both the base and aseasonal simulations (Fig. 4~~, top). However, the tropospheric slope is less than one while the total column slope is greater than one, indicating that the temporal variability differs~~). The Northern Hemisphere $X^t_{CH_4}$ slope deviates from the one-to-one line more than the X_{CH_4} slope (0.60 ± 0.02 versus 0.86 ± 0.03), and the correlation coefficients are equivalent ($R^2 = 0.41$), which indicates that the poorer agreement between measurements and models in the troposphere ~~and stratosphere. While no hemispheric difference is apparent for either~~ drive the scatter in the total column.

The stratospheric contribution comparison between TCCON and the base simulation for the Northern Hemisphere sites has an equivalent slope (0.60 ± 0.1) and higher correlation coefficient ($R^2 = 0.68$) compared to $X^t_{CH_4}$ ~~or X_{CH_4}, the stratospheric relationship between the measurements and model bifurcate between the Northern and Southern Hemispheres, as evidenced by the lower correlation coefficient of 0.75 (~~(Fig. 4c~~, top). TCCON and~~). GEOS-Chem ~~are consistent across the Southern Hemisphere sites; the slope, intercept and correlation coefficient are 1.1±0.020, 6, and 0.84, respectively. By contrast, in the Northern Hemisphere the TCCON stratospheric contribution is less than that of GEOS-Chem, the linear regression has a slope of 0.50±0.012, and the relationship exhibits more scatter, as shown by the correlation coefficient of 0.66.~~ 's larger

stratospheric contribution to the total column, coupled with lower tropospheric values, depresses X_{CH_4}. Because this effect on X_{CH_4} occurs more at higher latitudes, zonal errors in the model's stratosphere balances those in the troposphere. The result is better measurement-model agreement in the total columns.

~~Daily median TCCON and smoothed daily mean GEOS-Chem base (top) and aseasonal (bottom) DMFs for (a) $X^t_{CH_4}$, (b) X_{CH_4}, and (c) stratospheric contribution. Site colors are as in Fig. 1. Dashed lines mark the one-to-one lines.~~

The aseasonal simulation ~~retains similarly strong correlations with TCCON for~~produces lower slopes and correlation coefficients for, $X^t_{CH_4}$ ~~and~~ (slope=0.42 ± 0.02, $R^2 = 0.32$), X_{CH_4} (~~Fig. 4, bottom~~)slope=0.60 ± 0.03, $R^2 = 0.26$), and the stratospheric contribution (slope=0.52 ± 0.01, $R^2 = 0.66$) in the Northern Hemisphere. Removing the seasonality of emissions increases both measurement-model differences and scatter, as we would expect given the seasonality of Northern Hemisphere emissions noted in bottom-up studies (Kirschke et al., 2013) . The aseasonal simulation also reduces the offset between TCCON and GEOS-Chem, whereby modeled $X^t_{CH_4}$ and ~~Northern Hemisphere~~ X_{CH_4} ~~.~~are systematically low. TransCom-CH_4 showed that GEOS-Chem CH_4 concentrations tend to be lower than the model median, and much lower than the range of other models when using the same OH fields (Patra et al., 2011) . The aseasonal emissions used in this analysis likely reduce this documented imbalance with the model's tropospheric OH fields. ~~The northern mid-latitude sites depress the~~

The X_{CH_4} and $X^t_{CH_4}$ ~~slope to 0.74 and reduce the goodness of fit of the linear regression,~~ regression equations across Southern Hemisphere sites are nearly equivalent, which suggests that the Southern Hemisphere is not as impacted by the STE errors as the Northern Hemisphere. This consistency between X_{CH_4} and ~~thus the correlation coefficient, slightly. The scatter about~~ $X^t_{CH_4}$ could also be a function of the zonal dependence of the stratospheric error: whereas more than half of the Northern Hemisphere sites are north of $45°$N, the most poleward site in the Southern Hemisphere is located at $45°$S. The increased scatter associated with the slightly lower $X^t_{CH_4}$ R^2 value of 0.63, compared to the X_{CH_4} ~~linear regression increases for the Northern~~ R^2 value of 0.88, does indicate that the Southern Hemisphere is not exempt from model errors associated with emissions, the OH distribution, or transport. The lower $X^t_{CH_4}$ slope of the aseasonal simulation (1.1 versus 1.3) illustrates the influence of emissions: removing their seasonality leads to better measurement-model agreement, evidenced by a slope closer to both the one-to-one line and the zero-intercept. We hypothesize that either the seasonality of Southern Hemispheric emissions is too strong or, more likely, errors in the Northern Hemispheric seasonality of emissions drive measurement-model mismatch in the Southern Hemisphere via interhemispheric transport. If this effect was solely due to a changed emissions distribution, we would expect the X_{CH_4} slope to also change for the Southern Hemisphere sites, ~~but otherwise the fit improves markedly: the slope is 1.0 and the intercept is -47ppb.~~ if only slightly; instead the slope is equivalent to the base simulation $X^t_{CH_4}$ and X_{CH_4} slopes, and $R^2 = 0.87$, only marginally less than the base simulation X_{CH_4} correlation coefficient.

The stratospheric contribution ~~has nearly the same slope, intercept, and R^2 values as and retains the interhemispheric differences seen in the base simulation~~regression equations differ only slightly between the base and aseasonal simulations: $(0.64 \pm 0.02)x + 14$, $R^2 = 0.68$, versus $(0.62 \pm 0.02)x + 15$, $R^2 = 0.67$. The insensitivity of both the stratospheric contribution and the total columns in the Southern Hemisphere to perturbations in the seasonality of tropospheric emissions could be driven by the smaller vertical gradient across the UTLS that results from the influence of Northern Hemispheric air both in the free

troposphere (Fraser et al., 2011) and the stratosphere (Boering et al., 1995) . This effect would also support the interpretation of Northern Hemispheric emissions errors driving disagreement between observations and the model in the Southern Hemisphere.

In the troposphere, CH_4 increases from south to north; the stratospheric contribution of CH_4, however, increases from the equator to the poles due to the zonal gradient in tropopause height. In the Northern Hemisphere total column, the zonal gradient largely disappears: at high latitudes, the larger tropospheric emissions balances the larger stratospheric contribution. By contrast, zonal gradients in the Southern Hemisphere troposphere and stratosphere are additive, and greater south to north differences are apparent in the total column.

Figure 5 illustrates how the model differs from ACE-FTS CH_4 measurements in the stratosphere ~~. Excepting the top of the atmosphere in the tropics~~over boreal spring (March-April-May) and fall (September-October-November). Excepting above the tropical tropopause, CH_4 is considerably lower in the ACE-FTS climatology (v. 2.2, Jones et al., 2012) compared to GEOS-Chem. The difference varies both with altitude and latitude, especially in the Northern spring poleward of $40°$N. The vertical gradient is the least pronounced in Lauder, where the stratospheric contributions of TCCON and GEOS-Chem ~~agree well~~ fall most closely to the one-to-one line (Fig. 4).The low CH_4 in the tropical mid and upper stratosphere in GEOS-Chem could be a result of too weak vertical ascent to the stratosphere; however, the ACE-FTS data gaps in the tropical troposphere make this hypothesis difficult to test.

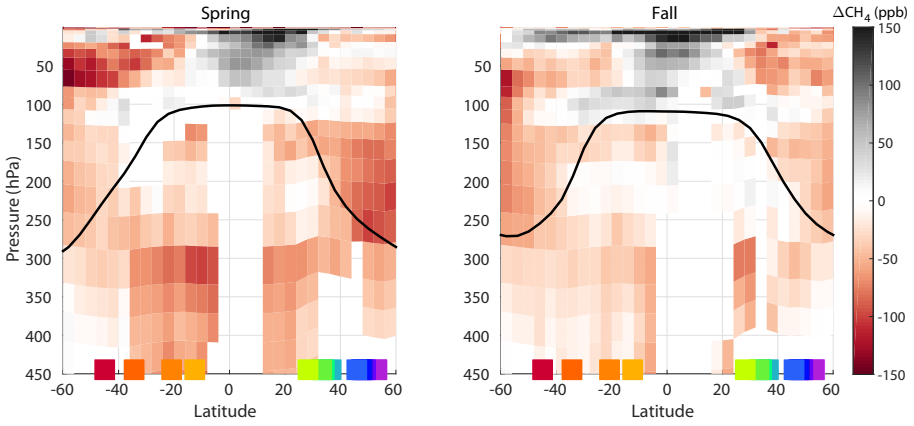

Figure 5. Zonally averaged ACE minus GEOS-Chem climatological CH_4 mole fractions for boreal spring and fall. Black line represents the mean zonal tropopause level. Site colors of squares on the x-axis are as in Fig. 1.

3.1 Dependence on Tropopause Height

In the Northern Hemisphere, the measurement-model mismatch of the ~~stratosphere~~ stratospheric contribution increases as the tropopause altitude shifts downward (Fig. 6). As the model's stratospheric portion of the pressure-weighted total column increases~~in the model~~, the error in stratospheric CH_4 ~~produces~~ is amplified, causing a larger disagreement with measurements. ~~This introduces both zonal and seasonal biases because~~ Because the tropopause height decreases with latitude, and this gradient

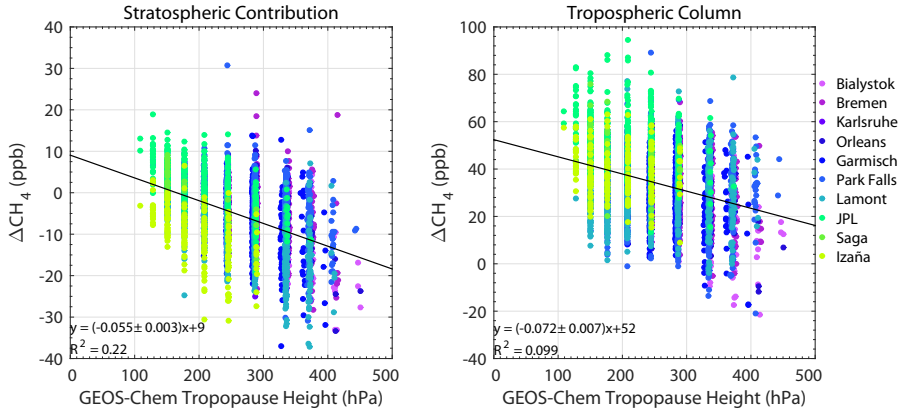

Figure 6. TCCON minus GEOS-Chem CH_4 column-averaged DMFs as a function of the effective GEOS-Chem tropopause height, shown for Northern Hemisphere sites. Site colors are as in Fig. 1.

increases during winter and spring~~. As the~~, this introduces both zonal and seasonal biases. The disagreement exhibits a large spread for relatively few tropopause pressure heights because the model's effective tropopause, that is, the pressure level at which the model divides the troposphere from the stratosphere in GEOS-Chem, is defined at discrete grid level pressure boundaries~~, the disagreement exhibits a large spread for relatively few tropopause pressure heights~~.

The tropospheric mismatch ($\Delta X^t_{CH_4}$)~~shows~~, by contrast, decreases with tropopause height for the majority of days and exhibits a much weaker correlation to tropopause height, ~~as the~~ 0.099 versus 0.22 for the stratospheric contribution. Thus, as expected, the tropopause height explains less of the variance in the measurement-model mismatch in $X^t_{CH_4}$: the upper troposphere is generally well-mixed, and chemical loss does not vary with altitude as much as in the lower stratosphere. ~~The~~ This weaker relationship also demonstrates that the choice of tropopause used in the tropospheric profile integration does not strongly impact $\Delta X^t_{CH_4}$.

The relationship between $\Delta X^t_{CH_4}$ and tropopause height has a clear zonal component that indicates that the correlation is instead a result of another parameter that varies with latitude. The tropospheric slope is dominated by high-latitude sites; the subtropical sites exhibit a much weaker correlation. At Izaña, which is in the sub-tropics at an altitude of 2.4 km, the correlation between $\Delta X^t_{CH_4}$ and tropopause ~~pressure~~ position is weak: the slope of ~~-0.034 ± 0.028~~ -0.035 ± 0.03 is nearly flat within error, and R^2 is ~~0.028~~0.025. By contrast, the stratospheric relationship at Izaña corresponds ~~within error~~ more closely with the other Northern Hemisphere sites: the slope is ~~-0.087 ± 0.015, and $R^2 = 0.39$. This weaker relationship also demonstrates that the choice of tropopause used in the tropospheric profile integration does not govern $\Delta X^t_{CH_4}$.~~ -0.088 ± 0.02, and $R^2 = 0.36$.

3.2 Seasonal Agreement

The tropospheric difference between TCCON and GEOS-Chem, $\Delta X^t_{CH_4}$, has a periodic trend ~~,~~indicating that the model error has a strong seasonal component in the troposphere. To isolate stable seasonal patterns from the cumulative influence of emissions, we calculate the detrended seasonal mean ~~DMFs~~column-averaged DMFs for each site. In the Southern Hemisphere,

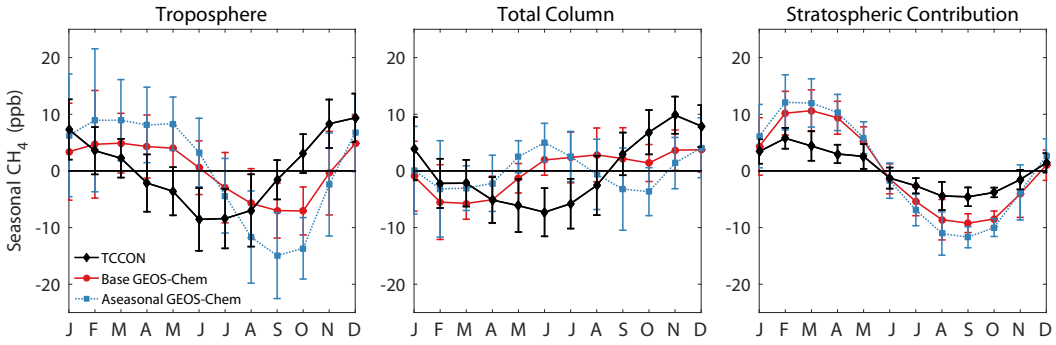

Figure 7. Detrended seasonality of TCCON (black diamonds), GEOS-Chem base (red circles), and GEOS-Chem aseasonal (blue squares) CH_4 column-averaged DMFs, averaged across Northern Hemisphere sites~~.~~, except Saga and Réunion Island, which have less than one year of measurements prior to 2012. Error bars denote the 1σ standard deviation across sites.

the measurements and model agree well. Across the Northern Hemisphere sites, however, the seasonality differs (Fig. 7). The seasonal amplitude of GEOS-Chem $X^t_{CH_4}$ is about equal to that of TCCON, but the ~~phase trails TCCON by two to three months. The TCCON~~ TCCON $X^t_{CH_4}$ seasonal minimum is in June/July while the GEOS-Chem seasonal minimum is in September/October. Additionally, while TCCON $X^t_{CH_4}$ begins to decrease in January, GEOS-Chem shows some persistence into the spring.

The seasonal delay also appears in comparisons of GEOS-Chem surface CH_4 with ~~NOAA~~ National Oceanic and Atmospheric Administration (NOAA) surface flask measurements at the LEF site in Park Falls (Fig. 8). The seasonality of GEOS-Chem's surface is regulated more by ~~production and loss~~ emissions than transport: CH_4 peaks in the summer, when wetland emissions are highest (Fig. 10). This contrasts with the flask measurements, which reach a minimum in the summer (Fig. 8). The seasonality covaries remarkably closely with respect to other features: the late winter decrease, spring persistence, and local minimum in October. The spring plateau lasts twice as long as seen in observations, however, and matches $X^t_{CH_4}$, indicating that feature is not the result of vertical transport between the PBL and free troposphere.

Not surprisingly, a time lag does not occur in the stratosphere; the TCCON stratospheric seasonal amplitude is less than half but in phase with that of GEOS-Chem (Fig. 7). The vertical inconsistency of the seasonality produces unusual features in the model total column. From January through April, the TCCON and GEOS-Chem X_{CH_4} are consistent because the model's bias in the troposphere is balanced by the ~~low tropopause~~larger stratospheric contribution. Starting in May, however, the model diverges from the measurements as the higher tropopause limits the stratosphere's influence, and the phase lag in the troposphere dominates. This balancing effect is also demonstrated by the greater variance across sites in the model $X^t_{CH_4}$ and stratospheric contribution compared to measurements, but about the same variance in X_{CH_4}.

For the aseasonal simulation, the tropospheric seasonal cycle amplitude and variance across sites increase ~~, suggesting that the seasonality of emissions in the base simulation has~~ (Fig. 7). The greatest model differences, from August through October, are a result of dampening the large wetland fluxes in the base simulation that balance higher OH concentrations.

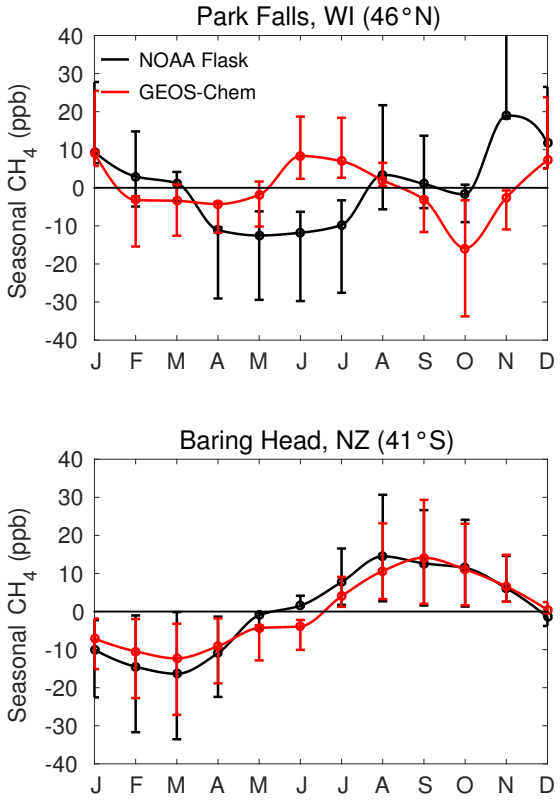

Figure 8. NOAA surface flask (black) and GEOS-Chem surface level (red) seasonality of CH_4 DMFs over 2005-2011 at Park Falls, WI, USA and Baring Head, NZ. Lower and upper bounds denote the 25th and 75th percentiles, respectively, of detrended data for each month.

The seasonal amplitude does not increase as drastically in the sub-tropics, where the total emissions are not as impacted by seasonally-varying sources, leading to the greater variance across sites. The second largest difference between simulation amplitudes occurs in the spring, and OH loss could potentially be driving in these months also. The aseasonal simulation spreads the wetland fluxes so as to introduce emissions in the winter and spring, when the OH concentrations are lowest. Another possibility is that the model could be subject to errors that are in phase with the base simulation seasonal emissions, which would then have an ameliorating effect ~~on model error (Fig. 7).~~ that produces the reasonable seasonal cycle amplitude. The stratospheric contribution does not change, however, further demonstrating that the stratosphere is insensitive to perturbations to Northern Hemisphere emissions.

The impact of a static stratosphere and changing troposphere is to make the seasonality of the aseasonal simulation X_{CH_4} bimodal: the October local minimum in the base simulation becomes a fall absolute minimum. The aseasonal X_{CH_4} agrees with TCCON in late winter, masking the greater disagreement in the troposphere. Notably, the main tropospheric features of the base simulation, the seasonal phase lag and spring persistence, are still apparent. Thus, the seasonality of emissions prescribed in the forward model is not the driver of the discrepancies between measurement and model $X^t_{CH_4}$ seasonalities.

OH is not likely the driver of these features, as the Northern Hemisphere phase shift also occurs in simulations performed with large changes in OH (~~not shown~~Fig. 15, in Appendix B1). Transport is thus the most likely driver of these tropospheric trends in the model.

4 Discussion

The stratospheric insensitivity to changes in emissions and tropospheric loss has significant implications for flux inversions. Model inversions use the sensitivity of trace gas concentrations at a given location to perturbations of different ~~emissions~~ emission sources to adjust those emissions so as to match observations at that location. The ~~model sensitivity kernel implicitly includes uncertainties in transport ,~~ response of modeled CH_4 DMFs to changing emissions depends on the model's transport and chemical loss, ~~and~~ as well as assumptions about the seasonal and spatial distribution of emissions relative to each other~~,~~ ~~which are compounded if vertical levels are~~ . Thus the model sensitivity kernel, the linear operator that maps emissions to CH_4 concentrations, implicitly includes uncertainties in these terms. The model's stratospheric response to emissions perturbations differ from that of the troposphere and are subject to different transport and loss errors. Because the tropospheric transport errors covary with emissions, they alias into the resulting source attribution.

Comparing measurement and model stratospheric CH_4 as a fraction of the total column provides a normalized comparison that isolates differences in the vertical structure from those caused by initial conditions and unbalanced sources and sinks. Figure 9 illustrates the error associated with the normalized stratospheric column and the associated stratospheric contribution to X_{CH_4} at Park Falls. Although the stratosphere accounts for ~~about~~ less than 30% of X_{CH_4}, a relatively small error can produce significant seasonal differences; the springtime error of ~~4×10^{17} molec~~ 4.5×10^{17} molec$\cdot$cm^{-2} (~~25~~ 23 ppb) is more than twice the seasonal cycle amplitude. Winter and spring are also when $X^t_{CH_4}$ is least sensitive to seasonal emissions; by contrast, the error is about 15 ppb in the summer, when seasonal emissions have the greatest influence (Fig. 9, top panel). The seasonality of the stratospheric error will therefore distort the inversion mechanism and thus posterior emissions estimates.

Additional bias is introduced by differences in the seasonal patterns of $\Delta X^t_{CH_4}$ and ΔX_{CH_4}. Wetlands are the largest seasonal source of CH_4 in models and the largest natural source in flux inventories, and their emissions are very uncertain~~.~~: estimates range between 142 and 284 TgC$\cdot$year^{-1} for the 2000-2009 time period (Kirschke et al., 2013) . A priori GEOS-Chem CH_4 emissions from northern high-latitude wetlands are extremely variable, with large fluxes in June, July and August, moderate fluxes in May and September, and almost no fluxes the remainder of the year (Fig. 10a). Surface CH_4 concentrations in models depend on the assumed seasonally-varying emissions. Patra et al. (2011) found that correlations between the seasonal cycles of the forward model averages and in situ observations of CH_4 DMFs at the surface varied for a given site by up to 0.78 ± 0.4 depending on wetland and biomass burning fields used. Model inversions that scale emissions in a given grid box based on the incorrect seasonality will invariably change the posterior attribution of seasonal emissions. ~~A~~ Fraser et al. (2013) found that optimized wetland emissions from inversions that assimilate surface data only are smaller than the priors, while those from inversions that assimilate GOSAT total columns are larger, even if surface measurements are also

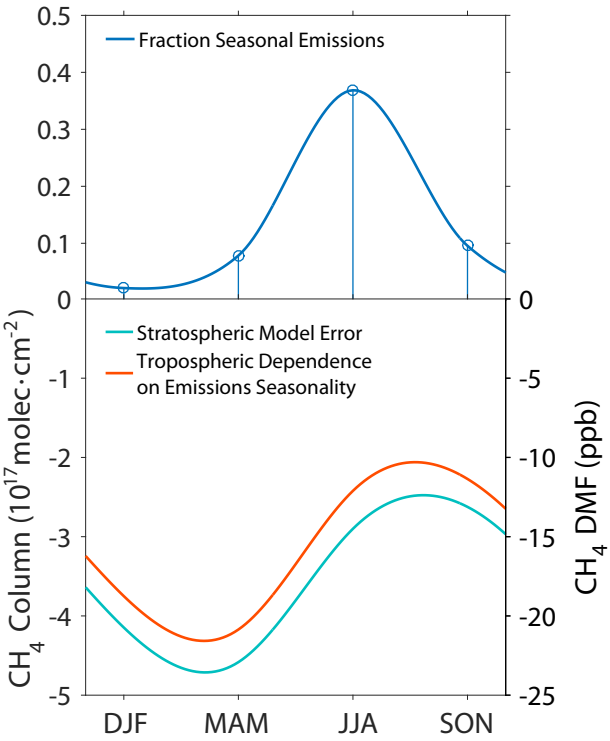

Figure 9. Top: Seasonally-averaged fraction of model emissions from seasonally-varying sources, north of 40°N. Bottom: Seasonally-averaged normalized model stratospheric column error (teal) and the difference between base and aseasonal simulation tropospheric columns (orange) at Park Falls.

assimilated. From this we infer that the transport errors in the model's free troposphere lead to an "optimization" of the prior fluxes of opposite sign to that of the emissions errors that the inversion attempts to correct.

A two to three-month shift in the ~~troposphere~~ phase of the $X^t_{CH_4}$ seasonality will produce a strong under- or overestimation of posterior wetland fluxes in late spring through early fall. In an inversion, prior emissions are adjusted in proportion to the deviation of the model's CH_4 DMFs from observed values. These posterior emissions are scaled for each sector according to their a priori fraction of total emissions in each grid box. Thus, an increase in posterior emissions relative to the prior in the northern mid and high latitudes during winter will not change emissions from wetlands. For example, Fig. 10b illustrates the sensitivity of posterior wetland emissions to a three-month lag in the Northern Hemisphere (derived by calculating the total emissions resulting from an increase of 1 ppb of CH_4 in each ~~surface grid box~~ tropospheric column and scaling those emissions according to the a priori contribution of wetlands). The tropics and subtropics are less sensitive to a phase shift, but polewards of 40°N, both the magnitude and seasonality of the difference is significant. ~~The largest disagreements~~ Large differences between measured and modeled $X^t_{CH_4}$ are concurrent with low emissions from seasonal sources. The adjustments to prior emissions produced by larger measurement-model disagreement that occur when seasonal sources are a small fraction

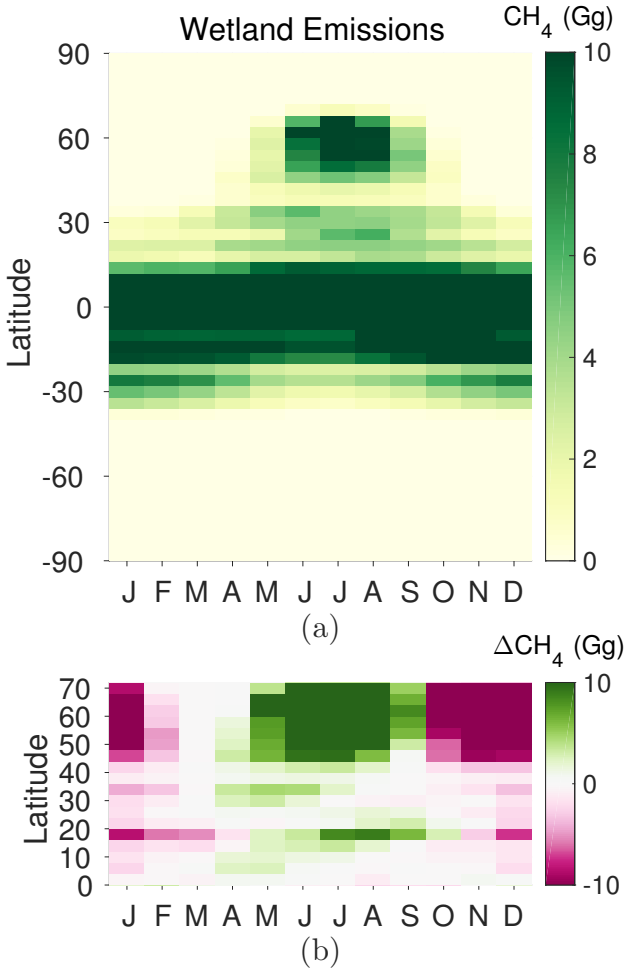

Figure 10. (a) GEOS-Chem monthly zonal mean wetland emissions, in ~~million kg~~Gg. (b) The Northern Hemisphere sensitivity of GEOS-Chem wetland emission attribution caused by a 3-month lag for each 1 ppb increase of CH_4 ~~at~~ in the ~~surface~~tropospheric column, in ~~thousand kg~~Gg.

of total emissions ~~, and~~ will overestimate posterior emissions from aseasonal sources. Thus these seasonal errors will bias source apportionment toward emissions that do not vary on timescales shorter than annually.

5 Conclusions

Assimilation of ~~X_{CH_4} measurements into global CTMs can help to quantify~~ total column measurements into CTMs can improve constraints on the global CH_4 budget; however, the model's treatment of stratospheric chemistry and dynamics must be carefully considered. This work has compared ~~retrieved and modeled~~ TCCON and GEOS-Chem pressure-weighted total and tropospheric column-averaged CH_4 DMFs, X_{CH_4} and $X^t_{CH_4}$ respectively, parsing out the seasonality of the troposphere and

stratosphere and the resulting impacts on X_{CH_4} (Fig. 9a). ~~While the~~ The Southern Hemisphere measurement-model agreement is robust ~~, in~~ to changes in emissions or tropospheric OH. In the Northern Hemisphere the model's stratospheric contribution is larger than that of the measurements, and the mismatch increases as the tropopause ~~height~~ altitude decreases. The result is greater model error at high-latitude sites, with the magnitude of ~~the mismatch~~ this error varying seasonally. Moreover, in the Northern Hemisphere the GEOS-Chem ~~has a lag in Northern Hemisphere~~ $X^t_{CH_4}$ ~~, which occurs regardless of changes in emissions seasonality and thus seems to be a product of transport errors. Furthermore, the stratosphere is insensitive to changes in the tropospheric emissions or chemical loss. These features~~ exhibits a 2-3 month phase lag. The combined tropospheric and stratospheric errors smooth the model X_{CH_4} such that they may agree with total column measurements despite having an incorrect vertical distribution.

Model transport errors coupled with spatial and seasonal measurement sparsity can limit the accuracy of the location and timing of emissions scaling. The differences in the seasonality mismatch across vertical levels amplifies the error uncertainty because the timing of optimized fluxes will be especially susceptible to limitations in model transport. The stronger influence of the stratosphere at higher latitudes due to lower tropopause heights, together with the higher temporal variability of the stratospheric fraction of the total column due to the stronger seasonal cycle of the tropopause, also impacts the seasonality of the meridional gradient of X_{CH_4}.

The influence of stratospheric variability on emissions is not unique to the model chosen for this analysis. Bergamaschi et al. (2013) ran TM5-4DVAR inversions using SCIAMACHY column and NOAA surface measurements and found that the mean biases between the optimized CH_4 profiles and aircraft measurements differ between the PBL, free troposphere, and UTLS. Seasonal emissions from wetlands and biomass burning vary by ± 10 and ± 7 TgCH_4, respectively, from year to year, and the zonal partitioning of posterior emissions is sensitive to the wetland priors chosen. Moreover, the larger changes to emissions and sensitivity to assumptions in the Northern Hemisphere indicate that TM5 is also subject to the strong hemispheric differences found in GEOS-Chem. The TransCom-CH_4 model comparison found that the interhemispheric exchange time in GEOS-Chem was near the model median over the 1996-2007 time series (Patra et al., 2011) , which suggests that GEOS-Chem's interhemispheric transport, and thus associated errors, is not particularly distinct. Ostler et al. (2015) found that ACTM and other CTMs used in ~~TransCom-CH4~~ TransCom-CH_4 are also subject to transport errors that impact emissions optimization. Furthermore, ACTM profiles show a similar over-estimation of stratospheric CH_4, zonally-varying measurement-model mismatch dependent on tropopause height, and a smaller seasonal cycle for Northern Hemisphere X_{CH_4} compared to TCCON.

In this analysis we have used TCCON $X^t_{CH_4}$ derived with the HF-proxy method; however, $X^t_{CH_4}$ calculated using other stratospheric tracers such as nitrous oxide (N_2O) (Wang et al., 2014) would provide an additional constraint on models' representations of the stratosphere, as N_2O is not subject to the spectral interference with water vapor that impacts HF. Information about the vertical tropospheric CH_4 profile directly retrieved from NDACC spectra (Sepúlveda et al., 2014) can also be used to assess whether transport errors differ at different levels of the free troposphere. Ideally, information from these tropospheric products could be integrated to overcome the limitations of each: the sensitivity of $X^t_{CH_4}$ to prior assumptions of stratospheric-tropospheric exchange and the sensitivity of profile retrievals to UTLS variability (Ostler et al., 2014).

A limitation of the aseasonal simulation was that the distribution of emissions was not identical to that of the base simulation due to the scaling approach we employed. Ideally, the aseasonal emissions for each sector would have been fluxes calculated for each grid box from the base simulation annual emissions. The robustness of the model's tropospheric phase shift that was apparent regardless of the emissions used demonstrates that this feature is not a product of the chosen emissions fields. However, more nuanced analysis on smaller spatial scaled would benefit from simulations that prescribe the annual mean for each of the seasonal sources. The most recent version of GEOS-Chem has a much more flexible emissions scheme (Keller et al., 2014) that allows these more nuanced experiments to be performed and analyzed.

The insensitivity of model stratospheres to tropospheric change allows for a straightforward solution: prescribed stratospheric CH_4 fields based on satellite observations ~~. As~~ from ACE-FTS, MIPAS (von Clarmann et al., 2009) , or a compilation of remote sensing instruments (Buchwitz et al., 2015) . As the representation of tropical convection and exchange across the UTLS ~~improve~~ advances in models and reduce stratospheric isolation, chemical loss, and transport mechanisms would need to be improved. The output from more accurate stratospheric models over the time period of interest could be used to set the stratospheric component in the offline CH_4 simulation. For instance, the Universal tropospheric-stratospheric Chemistry eXtension (UCX) mechanism, which has been added to more recent versions of GEOS-Chem, updates the stratospheric component of the standard full chemistry simulation such that CH_4 has more sophisticated upwelling, advection and chemical reaction schemes (Eastham et al., 2014). Models that account for interannual variability in both stratospheric and tropospheric dynamics can then assimilate total column measurements to develop more accurate global CH_4 budgets.

Appendix A: Updates to Tropospheric Methane Data

The TCCON $X^t_{CH_4}$ data used in this analysis were developed as in Saad et al. (2014) with several adjustments to both the parameters used and methodology.

The HF-proxy method for determining $X^t_{CH_4}$ incorporates the relationship between CH_4 and HF in the stratosphere, which is calculated using ACE-FTS data. These CH_4-HF slopes now use updated ACE-FTS version 3.5 measurements with v.1.1 flags (Boone et al., 2013; Sheese et al., 2015) . The data quality flags are provided for profile data on a 1 km vertical grid, which uses a piecewise quadratic method to interpolate from the retrievals (Boone et al., 2013) . Additionally, the CH_4 and HF measurement errors are now considered in the pressure-weighted linear regression that determines the slopes. All other data processing to produce the CH_4-HF slopes followed methods described in Saad et al. (2014) . Figure 11 shows the updated annual zonal values used to calculate $\hat{X}^t_{CH_4}$ with Washenfelder et al. (2003) and MkIV (retrieved from http://mark4sun.jpl.nasa.gov/m4data.html) values included for reference (c.f. Saad et al., 2014, Fig. 2) . These updates altered $\hat{X}^t_{CH_4}$ for the sites and time period covered in this paper by less than 2 ppb.

The derivation of the tropospheric column in Washenfelder et al. (2003) , Saad et al. (2014) , and Wang et al. (2014) implicitly assumed that the CH_4 profile is continuous across the tropopause; however, the boundary condition for stratospheric CH_4 is rather set by tropospheric air transported through the tropical tropopause (Brewer, 1949; Dobson, 1956) . Boering et al. (1996) showed that the concentration of CO_2 directly above the tropopause can be approximated by introducing a two-month phase lag to

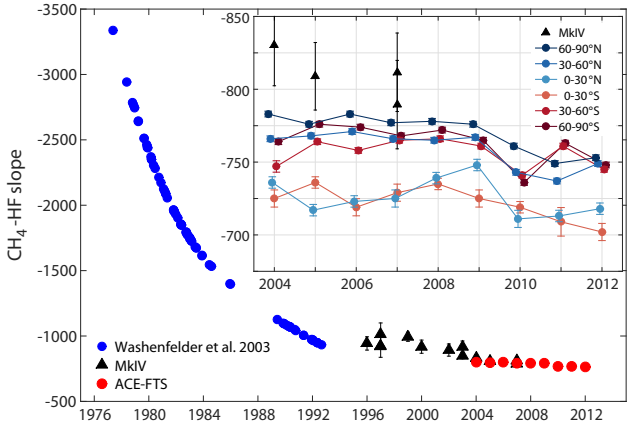

Figure 11. Long-term CH_4–HF slopes from Washenfelder et al. (2003) , MkIV, and updated ACE-FTS measurements. Inset: Time series of zonal pressure-weighted ACE-FTS slopes (β) used to calculate $\hat{X}^t_{CH_4}$, with error bars denoting the 2σ standard error. Zonal slopes are offset each year for visual clarity.

the average concentration at northern and southern tropical surface sites: Mauna Loa, Hawaii (MLO) and Tutuila, American Samoa (SMO), respectively. As the CH_4 entering the stratosphere originates in both hemispheres (Boering et al., 1995) , stratospheric CH_4 exhibits a smaller interhemispheric gradient than in the troposphere: about 20ppb, as calculated from ACE-FTS measurements, versus about 50 ppb, taken as the difference at MLO and SMO. To calculate the stratospheric boundary condition for CH_4 we remove the seasonal component of the mean of CH_4 DMFs at MLO and SMO, which are made available through 2014 by the NOAA Earth System Research Laboratory (ESRL) Global Monitoring Division (Dlugokencky et al., 2016) . To capture the interhemispheric gradient observed in ACE stratospheric CH_4 measurements, we add and subtract 10 ppb, in the northern and southern extratropics respectively, the limits of which we choose as the Tropic of Cancer (23°N) and the Tropic of Capricorn (23°S). A constant value is chosen in each hemisphere to reflect the rapid mixing time of air from the extra-tropics in the region directly above the tropopause, which Boering et al. (1996) found to be less than one month. Within the tropics, we interpolate the boundary condition as a linear function of altitude such that $x_{CH_4}(P^t) = \bar{x}^s_{CH_4} + \frac{10}{23}\lambda$, where $x_{CH_4}(P^t)$ is the boundary condition at the tropopause, $\bar{x}^s_{CH_4}$ is the mean DMF of CH_4 at the surface, and λ is the latitude of the site.

Assuming hydrostatic equilibrium, the tropospheric column of CH_4, $c^t_{CH_4}$, can be calculated as the integral of the vertical profile, $x_{CH_4} \equiv x_{CH_4}(P)$, from the surface, P^s, to the tropopause, P^t:

$$c^t_{CH_4} = \int_{P^t}^{P^s} x_{CH_4} \frac{dP}{gm} = X^t_{CH_4} \frac{P^s - P^t}{g^t_* m} \tag{A1}$$

where P is the pressure height, g is the gravitational acceleration, g^t_* is the pressure-weighted tropospheric value of g, and m is the mean molecular mass of CH_4 (Washenfelder et al., 2006) . The profile of CH_4 in the stratosphere can be expressed as

a linear function of pressure altitude, $x_{\mathrm{CH_4}}(P) = x_{\mathrm{CH_4}}(P^t) + \delta \cdot P$, where $\delta = \frac{dx_{\mathrm{CH_4}}}{dP}$ is the stratospheric loss of $\mathrm{CH_4}$. This stratospheric loss term is estimated by the HF-proxy method to produce the retrieved tropospheric column-averaged DMF, $\hat{X}^t_{\mathrm{CH_4}}$, such that

$$\hat{X}^t_{\mathrm{CH_4}} \frac{P^s}{g_* m} = \hat{c}^t_{\mathrm{CH_4}} = \int_0^{P^s} x_{\mathrm{CH_4}} \frac{dP}{gm} - \int_0^{P^t} \delta \cdot P \frac{dP}{gm} \tag{A2}$$

where g_* is the pressure-weighted column average of g. The stratospheric boundary condition can thus be related to the retrieved tropospheric column as

$$\int_0^{P^t} x_{\mathrm{CH_4}} \frac{dP}{gm} = \int_0^{P^t} x_{\mathrm{CH_4}}(P^t) \frac{dP}{gm} - \hat{c}^t_{\mathrm{CH_4}} + \int_0^{P^s} x_{\mathrm{CH_4}} \frac{dP}{gm}. \tag{A3}$$

Given the total column integration is the sum of the tropospheric and stratospheric partial columns, and substituting Equation A3:

$$\int_{P^t}^{P^s} x_{\mathrm{CH_4}} \frac{dP}{gm} = \int_0^{P^s} x_{\mathrm{CH_4}} \frac{dP}{gm} - \int_0^{P^t} x_{\mathrm{CH_4}} \frac{dP}{gm} \tag{A4}$$

$$= \int_0^{P^s} x_{\mathrm{CH_4}} \frac{dP}{gm} - \int_0^{P^t} x_{\mathrm{CH_4}}(P^t) \frac{dP}{gm} + \hat{c}^t_{\mathrm{CH_4}} - \int_0^{P^s} x_{\mathrm{CH_4}} \frac{dP}{gm} \tag{A5}$$

$$= \hat{c}^t_{\mathrm{CH_4}} - \int_0^{P^t} x_{\mathrm{CH_4}}(P^t) \frac{dP}{gm} \tag{A6}$$

$$X^t_{\mathrm{CH_4}} \frac{P^s - P^t}{g^t_* m} = \hat{X}^t_{\mathrm{CH_4}} \frac{P^s}{g_* m} - x_{\mathrm{CH_4}}(P^t) \frac{P^t}{g^0_* m} \tag{A7}$$

where g^0_* is the pressure-weighted average of g from the tropopause to the top of the atmosphere. While the molecular mass of air changes as a function of water vapor and thus altitude and gravity changes as a function of both altitude and latitude, assuming constant values of g and m changes $X^t_{\mathrm{CH_4}}$ by less than 2 ppb. Thus, to good approximation these variables can be canceled out:

$$X^t_{\mathrm{CH_4}}[P^s - P^t] = \hat{X}^t_{\mathrm{CH_4}} \cdot P^s - x_{\mathrm{CH_4}}(P^t) \cdot P^t \tag{A8}$$

$$X^t_{\mathrm{CH_4}} = \frac{\hat{X}^t_{\mathrm{CH_4}} \cdot P^s - x_{\mathrm{CH_4}}(P^t) \cdot P^t}{P^s - P^t}. \tag{A9}$$

The surface pressure is measured at each site, and the tropopause pressure is calculated from the TCCON prior temperature profiles. The uncertainties associated with the interpolated value of the tropopause height are determined by calculating $X^t_{CH_4}$ for $\pm 30\%$ of P^t and adding these confidence intervals in quadrature to the precision error of $\hat{X}^t_{CH_4}$. The aforementioned deseasonalization of $x_{CH_4}(P^t)$ is an approximation that adds another uncertainty. The signal of the tropospheric seasonal cycle of a trace gas entering the stratosphere is apparent directly above the tropopause and both dampens in amplitude and shifts in time with increasing altitude (Mote et al., 1996) . Thus, the stratospheric boundary condition is not truly constant throughout the column, but rather the pressure-weighted sum of these attenuated signals. Calculating $x_{CH_4}(P^t)$ without removing the seasonality, which provides the maximum impact of this uncertainty, decreases $X^t_{CH_4}$ by an average of 1 ppb and 4 ppb in the Northern and Southern Hemispheres, respectively, and does not alter the seasonal cycle of $X^t_{CH_4}$. Moreover, as described below, the mismatch between the calibrated TCCON $X^t_{CH_4}$ and the in situ aircraft $X^t_{CH_4}$ does not correlate with season ($R^2 = 0.017$). Thus, we retain the simpler computation of deseasonalized $x_{CH_4}(P^t)$ in Equation A9.

Airmass-dependent artifacts were derived for updated values consistently with the total column CH_4 (Wunch et al., 2015) . Removing these artifacts, the $X^t_{CH_4}$ was then calibrated with in situ aircraft profiles using the same methodology described in Wunch et al. (2010) and including the updates delineated in (Wunch et al., 2015) to produce a calibration correction factor of 0.9700 (Fig. 12). The covariance between the difference between the calibrated TCCON and aircraft $X^t_{CH_4}$ and several parameters were assessed to ensure biases were not introduced into the measurements. These differences had an uncertainty-weighted correlation coefficient of 0.1 for solar zenith angle and uncertainty-weighted correlation coefficients of less that 0.02 for

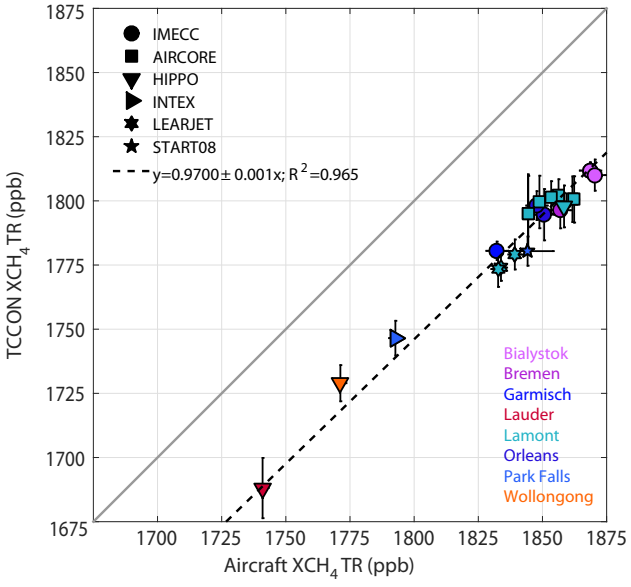

Figure 12. Calibration curve of TCCON $X^t_{CH_4}$ (c.f. Wunch et al., 2015, Fig. 8) . Site colors are as in Fig. 1. Aircraft campaigns are described in Table 6 of Wunch et al. (2015) .

tropopause and surface pressures, year, and season. Measurement precisions and errors were determined as in Saad et al. (2014) , with the additional uncertainties mentioned in this section included. Individual TCCON sites have median $X^t_{CH_4}$ precisions in the range of 0.1-0.8%, and mean and median precisions are 0.3 and 0.2%, respectively, for all sites through May 2016.

Appendix B: GEOS-Chem Simulations

B1 Equilibrium Sensitivity Experiments

All equilibrium runs for a given simulation have identical meteorology, emissions, and OH fields over June 2004-May 2005. Initial conditions for each year are set by the restart files of the previous run. To calculate columns at each site, GEOS-Chem monthly mean mole fractions are adjusted for the monthly medians of the site's daily mean surface pressures and smoothed with the monthly median scaled prior profiles and averaging kernels, interpolated using the monthly median solar zenith angle daily means. Because Park Falls and Lauder are the only TCCON sites that had started taking measurements over this time period, they are the only sites used to generate smoothed columns for the comparisons to the experimental simulations.

Emissions in the aseasonal simulation were derived by running a two-dimensional regression on the annual emissions to determine the scale factors that would produce the smallest residual of total emissions and the interhemispheric gradient. Figure 13 illustrates the difference in total emissions between the base and aseasonal simulations for each zonal band.

The updated OH simulation used OH output from a 2012 GEOS-Chem standard chemistry simulation with extensive updates to the photochemical oxidation mechanisms of biogenic volatile organic compounds (VOCs), described in Bates et al. (2016) and references therein. These were converted to 3D monthly mean OH concentrations to conform to the infrastructure of the

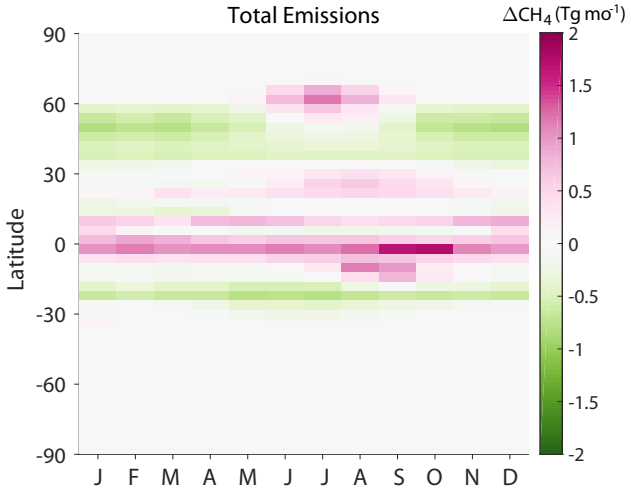

Figure 13. Monthly averages of the difference in total CH_4 emissions between the base and aseasonal GEOS-Chem simulations, summed over each zonal band, in $Tg{\cdot}mo^{-1}$.

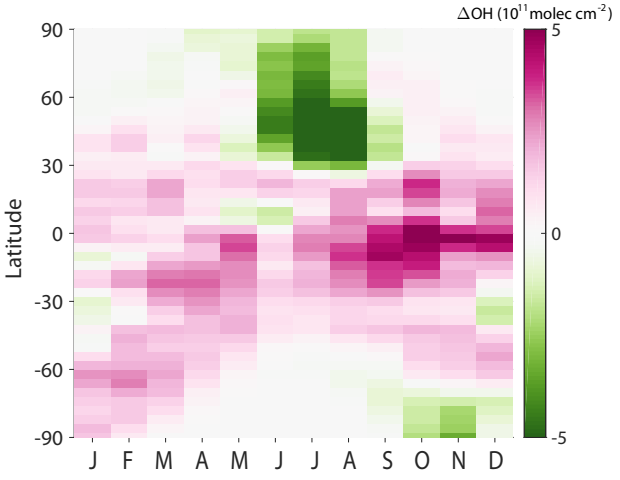

Figure 14. Zonal averages of the difference in total column OH (molec·cm^{-2}) between the base and updated monthly OH fields.

GEOS-Chem offline CH_4 tropospheric loss mechanism. The OH was then scaled by 90% to keep the lifetime above 8 years, and emissions were scaled by 112% to maintain the same balance between sources and sinks in the base simulation. Figure 14 provides zonal averages of the difference between the base and updated OH columns.

The full list of simulations run is provided in Table 3, with descriptions and the CH_4 emissions, tropospheric OH, and total chemical loss lifetimes. Figure 15 shows each simulation's seasonality of $X^t_{CH_4}$ at Park Falls, with TCCON seasonality plotted as reference, as well as the seasonality of the difference between the base and each simulation.

B2 Derivation of Dry Gas Values

Versions of GEOS-Chem prior to v.10 have inconsistencies in wet versus dry definitions of pressure, temperature, and air mass, which propagate into model diagnostics and conversions calculated using these terms. As a consequence, CH_4 concentrations are output assuming air masses that include water vapor but calculated with the molar mass of dry air. For all comparisons in this analysis CH_4 DMFs are calculated taking into account the GEOS-5 specific humidity, SPHU (in units of $g_{H2O} \cdot kg^{-1}_{air}$), such that

$$\chi x_{\mathrm{CH_4},dry} = \frac{\chi_{\mathrm{CH_4}}}{1 - SPHU \times 10^{-3}} \frac{x_{\mathrm{CH_4}}}{1 - SPHU \times 10^{-3}} \tag{B1}$$

where ~~χ_{CH_4}~~ x_{CH_4} is the model profile in mole fractions. Dry air profiles were derived by subtracting the water vapor mole fraction, also calculated from the GEOS-5 specific humidity, from the total air mass at each pressure level, as in Wunch et al. (2010); Geibel et al. (2012).

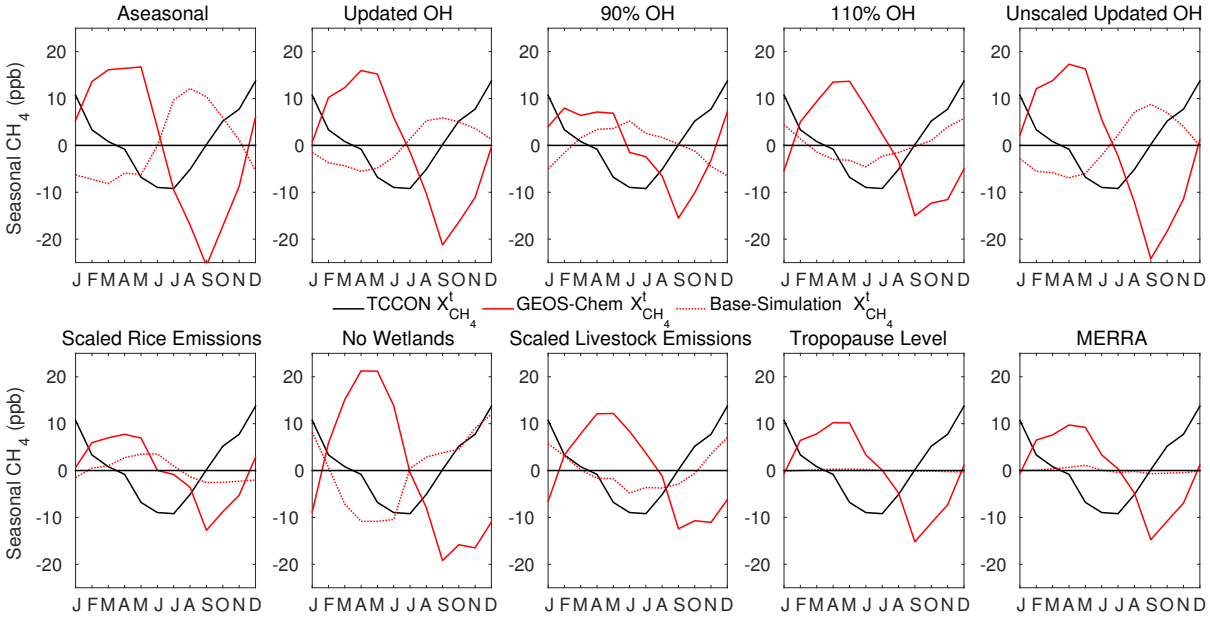

Figure 15. Seasonality of tropospheric methane ($X^t_{CH_4}$) at Park Falls for TCCON (black solid line), GEOS-Chem (red solid line), and the difference from the base simulation (dotted red line) for each of the sensitivity experiments, in ppb.

B3 Model Smoothing for Measurement Comparisons

Base and aseasonal daily runs were initialized using CH_4 fields from their respective 34th equilibrium cycles. Daily CH_4 mole fractions averaged over both 24-hour and 10-14 local time were output to test whether TCCON's daytime-only observations would introduce a bias in the comparisons. Measurement-model differences were not sensitive to averaging times. Comparison of measurements to model columns produced using the 24-hour and 10-14 local time averages produce equivalent slopes and only slightly different intercepts and correlation coefficients. The seasonality of 10-14 local time column-averaged DMFs does not differ, except that the fall seasonal maximum of the adjusted troposphere and stratospheric contribution at Park Falls in October, one month later than the 24-hour column-averaged DMF seasonality.

CH_4 dry vertical profiles for each grid box associated with a TCCON site, $\boldsymbol{x^m_{CH_4}}$, were smoothed with corresponding FTS column averaging kernels, $\boldsymbol{a_{CH_4}}$, and scaled priors for each day and vertically integrated using pressure-weighted levels:

$$\underline{\chi} X^s_{\mathrm{CH_4}} = \gamma_{\mathrm{CH_4}} \cdot \underline{\chi} X^a_{\mathrm{CH_4}} + \boldsymbol{a^{\S}_{CH_4}}(\boldsymbol{x^m_{CH_4}} - \gamma_{\mathrm{CH_4}} \boldsymbol{x^a_{CH_4}}) \quad \text{(B2)}$$

where ~~$\chi^s_{\mathrm{CH_4}}$~~ $X^s_{\mathrm{CH_4}}$ is the smoothed GEOS-Chem column-averaged DMF, $\gamma_{\mathrm{CH_4}}$ is the TCCON daily median retrieved profile scaling factor, and $\boldsymbol{x^a_{CH_4}}$ and ~~$\chi^a_{\mathrm{CH_4}}$~~ $X^a_{\mathrm{CH_4}}$ are respectively the a priori profile and column-integrated CH_4 DMFs (Rodgers and Connor, 2003). The pressure weighting function, $\boldsymbol{h}$, was applied such that ~~$\chi = \boldsymbol{h}^T \boldsymbol{x}$~~ $X = \boldsymbol{h}^T \boldsymbol{x}$. TCCON priors were interpolated to the GEOS-Chem pressure grid, and GEOS-Chem pressure and corresponding gas profiles were adjusted using daily mean surface pressures local to each site (Wunch et al., 2010; Messerschmidt et al., 2011). The averaging kernels were

interpolated for the local daily mean solar zenith angle and the GEOS-Chem pressure grid so that it could be applied to the difference between the GEOS-Chem and TCCON profiles as $\boldsymbol{a}^{\S}\boldsymbol{x} = \sum_{i=1}^{N} a_i h_i x_i$ from the surface to the highest level, N, at i pressure levels (Connor et al., 2008; Wunch et al., 2011b). Figure 16 shows how the smoothed column compares to the column that only uses the dry gas correction.

Appendix C: Derivation of Stratospheric Contribution

Considering the CH_4 profile integration as in Equation A4, and substituting the profile of CH_4 in the stratosphere, $x_{CH_4}(P) = x_{CH_4}(P^t) + \delta \cdot P$ described in Appendix A, the total column is calculated as:

$$\int_0^{P^s} x_{CH_4} \frac{dP}{gm} = \int_{P^t}^{P^s} x_{CH_4} \frac{dP}{gm} + \int_0^{P^t} [x_{CH_4}(P^t) + \delta \cdot P] \frac{dP}{gm} \tag{C1}$$

$$X_{CH_4} \cdot P^s = X^t_{CH_4}[P^s - P^t] + x_{CH_4}(P^t) \cdot P^t + c^{\delta}_{CH_4} \tag{C2}$$

where $c^{\delta}_{CH_4}$, is the pressure-weighted column average of CH_4 loss in the stratosphere. Rearranging terms, Equation C2 becomes:

$$[X_{CH_4} - X^t_{CH_4}]P^s = [x_{CH_4}(P^t) - X^t_{CH_4}]P^t + c^{\delta}_{CH_4} \tag{C3}$$

$$X^t_{CH_4} - X_{CH_4} = [X^t_{CH_4} - x_{CH_4}(P^t)]\frac{P^t}{P^s} - \frac{c^{\delta}_{CH_4}}{P^s} \tag{C4}$$

such that the difference between the tropospheric and total column-averaged DMFs is a function of the two terms governing the stratospheric contribution to the total column: the gradient across the tropopause, $x_{CH_4}(P^t) - X^t_{CH_4}$, and stratospheric CH_4 loss, $c^{\delta}_{CH_4}$. The stratospheric contribution is thus a proxy for the impact of stratospheric variability on the total column of CH_4; given a constant tropospheric column, as the stratospheric contribution becomes larger the total column-averaged DMF becomes smaller.

Acknowledgements. ~~Support for this research is provided by~~ This work was supported by NASA Headquarters under the NASA Earth and Space Science Fellowship Program grant NNX14AL30H and NASA's Carbon Cycle Science program. Park Falls, Lamont, and JPL are funded by NASA grants NNX14AI60G, NNX11AG01G, NAG5-12247, NNG05-GD07G, and NASA Orbiting Carbon Observatory Program; we are grateful to the DOE ARM program and Jeff Ayers for their technical support in Lamont and Park Falls, respectively. Darwin and Wollongong are funded by NASA grants NAG5-12247 and NNG05-GD07G and the Australian Research Council grants DP140101552, DP110103118, DP0879468 and LP0562346, and Nicholas Deutscher is supported by an Australian Research Council Fellowship, DE140100178; we are grateful to the DOE ARM program for technical support in Darwin. Bremen, Bialystok, and Orleans are funded by the EU projects InGOS and ICOS-INWIRE and by the Senate of Bremen. Réunion Island is funded by the EU FP7 project ICOS-INWIRE, the national Belgian support to ICOS and the AGACC-II project (Science for Sustainable Development Program), the Université de

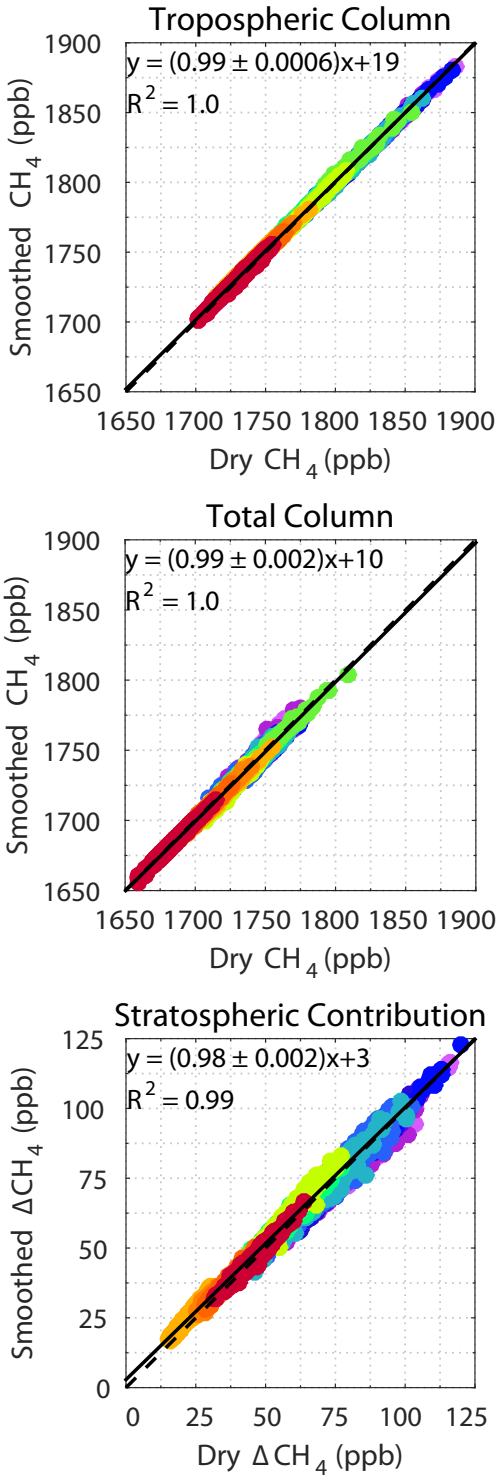

Figure 16. ~~Smoothed~~ GEOS-Chem smoothed versus dry integrated ~~GEOS-Chem~~ CH_4 DMFs for base simulation tropospheric columns, total columns, and stratospheric contribution. Site colors are as in Fig. 1. Dashed lines mark the one-to-one lines.

la Réunion, and the French regional and national organizations (INSU, CNRS). From 2004 to 2011 the Lauder TCCON program was funded by the New Zealand Foundation of Research Science and Technology contracts CO1X0204, CO1X0703 and CO1X0406. We thank Shuji Kawakami for his technical support in Saga. We thank Peter Bernath, Kaley Walker, and Chris Boone for their guidance using the ACE-FTS data, which were obtained through the Atmospheric Chemistry Experiment (ACE) mission, primarily funded by the Canadian Space Agency. We are grateful to Geoff Toon for his continuous efforts developing the GGG software, ~~as well as~~ for providing the MkIV data, and his input on the manuscript. We thank Arlyn Andrews for providing the LEF surface flask data, which were generated by NOAA-ESRL, Carbon Cycle Greenhouse Gases Group. Baring Head NIWA surface data were provided courtesy of Gordon Brailsford, Dave Lowe and Ross Martin. ~~We~~ We would also acknowledge the contributions of in situ vertical profiles from the AirCore, HIPPO, IMECC, INTEX, Learjet, and START08 campaigns. We are grateful to Kelvin Bates for providing monthly OH fields for the GEOS-Chem Updated OH sensitivity experiments.

References

Allen, D., Pickering, K., Duncan, B., and Damon, M.: Impact of lightning NO emissions on North American photochemistry as determined using the Global Modeling Initiative (GMI) model, Journal of Geophysical Research: Atmospheres, 115, 2010.

Baker, D., Law, R., Gurney, K., Rayner, P., Peylin, P., Denning, A., Bousquet, P., Bruhwiler, L., Chen, Y., Ciais, P., Fung, I., Heimann, M., John, J., Maki, T., Maksyutov, S., Masarie, K., Prather, M., Pak, B., Taguchi, S., and Zhu, Z.: TransCom 3 inversion intercomparison: Impact of transport model errors on the interannual variability of regional CO2 fluxes, 1988-2003, Global Biogeochemical Cycles, 20, doi:10.1029/2004GB002439, 2006.

Bates, K. H., Nguyen, T. B., Teng, A. P., Crounse, J. D., Kjaergaard, H. G., Stoltz, B. M., Seinfeld, J. H., and Wennberg, P. O.: Production and Fate of C4 Dihydroxycarbonyl Compounds from Isoprene Oxidation, The Journal of Physical Chemistry A, 120, 106–117, doi:10.1021/acs.jpca.5b10335, http://dx.doi.org/10.1021/acs.jpca.5b10335, 2016.

Bergamaschi, P., Frankenberg, C., Meirink, J. F., Krol, M., Dentener, F., Wagner, T., Platt, U., Kaplan, J. O., Körner, S., Heimann, M., Dlugokencky, E. J., and Goede, A.: Satellite chartography of atmospheric methane from SCIAMACHY on board ENVISAT: 2. Evaluation based on inverse model simulations, Journal of Geophysical Research: Atmospheres, 112, n/a–n/a, doi:10.1029/2006JD007268, http://dx.doi.org/10.1029/2006JD007268, d02304, 2007.

Bergamaschi, P., Houweling, S., Segers, A., Krol, M., Frankenberg, C., Scheepmaker, R. A., Dlugokencky, E., Wofsy, S. C., Kort, E. A., Sweeney, C., Schuck, T., Brenninkmeijer, C., Chen, H., Beck, V., and Gerbig, C.: Atmospheric CH4 in the first decade of the 21st century: Inverse modeling analysis using SCIAMACHY satellite retrievals and NOAA surface measurements, Journal of Geophysical Research: Atmospheres, 118, 7350–7369, doi:10.1002/jgrd.50480, http://dx.doi.org/10.1002/jgrd.50480, 2013.

Bernath, P. F.: Atmospheric Chemistry Experiment (ACE): Mission overview, Geophysical Research Letters, 32, L15S01, doi:10.1029/2005GL022386, http://doi.wiley.com/10.1029/2005GL022386, 2005.

Bey, I., Jacob, D., Yantosca, R., Logan, J., Field, B., Fiore, A., Li, Q., Liu, H., Mickley, L., and Schultz, M.: Global modeling of tropospheric chemistry with assimilated meteorology: Model description and evaluation, Journal of Geophysical Research-Atmospheres, 106, 23 073–23 095, doi:10.1029/2001JD000807, 2001.

Blumenstock, T., Hase, F., Schneider, M., Garcia, O., and Sepulveda, E.: TCCON data from Izana, Tenerife, Spain, Release GGG2014R0, http://dx.doi.org/10.14291/tccon.ggg2014.izana01.R0/1149295, doi:10.14291/tccon.ggg2014.izana01.R0/1149295, TCCON data archive, hosted by the Carbon Dioxide Information Analysis Center, Oak Ridge National Laboratory, Oak Ridge, Tennessee, U.S.A., 2014.

Boering, K., Wofsy, S., Daube, B., Schneider, H., Loewenstein, M., Podolske, J., and Conway, T.: Stratospheric Mean Ages and Transport Rates from Observations of Carbon Dioxide and Nitrous Oxide, Science, 274, 1340–1343, doi:10.1126/science.274.5291.1340, 1996.

Boering, K. A., Hintsa, E. J., Wofsy, S. C., Anderson, J. G., Daube, B. C., Dessler, A. E., Loewenstein, M., McCormick, M. P., Podolske, J. R., Weinstock, E. M., and Yue, G. K.: Measurements of stratospheric carbon dioxide and water vapor at northern midlatitudes: Implications for troposphere-to-stratosphere transport, Geophysical Research Letters, 22, 2737–2740, doi:10.1029/95GL02337, http://dx.doi.org/10.1029/95GL02337, 1995.

Boone, C. D., Walker, K. A., and Bernath, P. F.: Version 3 Retrievals for the Atmospheric Chemistry Experiment Fourier Transform Spectrometer (ACE-FTS), in: The Atmospheric Chemistry Experiment ACE at 10: A Solar Occultation Anthology, edited by Bernath, P. F., pp. 103–127, A. Deepak Publishing, Hampton, Virginia, U.S.A., 2013.

Brewer, A.: Evidence for a world circulation provided by the measurements of helium and water vapour distribution in the stratosphere, Quarterly Journal of the Royal Meteorological Society, 75, 351–363, 1949.

Buchwitz, M., Reuter, M., Schneising, O., Boesch, H., Guerlet, S., Dils, B., Aben, I., Armante, R., Bergamaschi, P., Blumenstock, T., Bovensmann, H., Brunner, D., Buchmann, B., Burrows, J. P., Butz, A., Chédin, A., Chevallier, F., Crevoisier, C. D., Deutscher, N. M., Frankenberg, C., Hase, F., Hasekamp, O. P., Heymann, J., Kaminski, T., Laeng, A., Lichtenberg, G., De Mazière, M., Noël, S., Notholt, J., Orphal, J., Popp, C., Parker, R., Scholze, M., Sussmann, R., Stiller, G. P., Warneke, T., Zehner, C., Bril, A., Crisp, D., Griffith, D. W. T., Kuze, A., O'Dell, C., Oshchepkov, S., Sherlock, V., Suto, H., Wennberg, P., Wunch, D., Yokota, T., and Yoshida, Y.: The Greenhouse Gas Climate Change Initiative (GHG-CCI): Comparison and quality assessment of near-surface-sensitive satellite-derived CO_2 and CH_4 global data sets, Remote Sensing of Environment, 162, 344–362, 2015.

Butz, A., Galli, A., Hasekamp, O., Landgraf, J., Tol, P., and Aben, I.: TROPOMI aboard Sentinel-5 Precursor: Prospective performance of {CH4} retrievals for aerosol and cirrus loaded atmospheres, Remote Sensing of Environment, 120, 267–276, doi:http://dx.doi.org/10.1016/j.rse.2011.05.030, http://www.sciencedirect.com/science/article/pii/S003442571200082X, the Sentinel Missions - New Opportunities for Science, 2012.

Connor, B. J., Boesch, H., Toon, G., Sen, B., Miller, C., and Crisp, D.: Orbiting Carbon Observatory: Inverse method and prospective error analysis, Journal of Geophysical Research, 113, 1–14, doi:10.1029/2006JD008336, 2008.

Considine, D. B., Logan, J. A., and Olsen, M. A.: Evaluation of near-tropopause ozone distributions in the Global Modeling Initiative combined stratosphere/troposphere model with ozonesonde data, Atmospheric Chemistry and Physics, 8, 2365–2385, 2008.

De Mazière, M., Vigouroux, C., Bernath, P. F., Baron, P., Blumenstock, T., Boone, C., Brogniez, C., Catoire, V., Coffey, M., Duchatelet, P., Griffith, D., Hannigan, J., Kasai, Y., Kramer, I., Jones, N., Mahieu, E., Manney, G. L., Piccolo, C., Randall, C., Robert, C., Senten, C., Strong, K., Taylor, J., Tétard, C., Walker, K. A., and Wood, S.: Validation of ACE-FTS v2.2 methane profiles from the upper troposphere to the lower mesosphere, Atmospheric Chemistry and Physics, 8, 2421–2435, doi:10.5194/acp-8-2421-2008, http://www.atmos-chem-phys.net/8/2421/2008/, 2008.

De Maziere, M., Sha, M. K., Desmet, F., Hermans, C., Scolas, F., Kumps, N., Metzger, J.-M., Duflot, V., and Cammas, J.-P.: TCCON data from Reunion Island (La Reunion), France, Release GGG2014R0, http://dx.doi.org/10.14291/tccon.ggg2014.reunion01.R0/1149288, doi:10.14291/tccon.ggg2014.reunion01.R0/1149288, TCCON data archive, hosted by the Carbon Dioxide Information Analysis Center, Oak Ridge National Laboratory, Oak Ridge, Tennessee, U.S.A., 2014.

Deutscher, N., Notholt, J., Messerschmidt, J., Weinzierl, C., Warneke, T., Petri, C., Grupe, P., and Katrynski, K.: TCCON data from Bialystok, Poland, Release GGG2014R1, http://dx.doi.org/10.14291/tccon.ggg2014.bialystok01.R1/1183984, doi:10.14291/tccon.ggg2014.bialystok01.R1/1183984, TCCON data archive, hosted by the Carbon Dioxide Information Analysis Center, Oak Ridge National Laboratory, Oak Ridge, Tennessee, U.S.A., 2014.

Dlugokencky, E., Lang, P., Crotwell, A., Mund, J., Crotwell, M., and Thoning, K.: Atmospheric Methane Dry Air Mole Fractions from the NOAA ESRL Carbon Cycle Cooperative Global Air Sampling Network, 1983-2015, ftp://aftp.cmdl.noaa.gov/data/trace_gases/ch4/flask/surface/, 2016.

Dlugokencky, E. J., Nisbet, E. G., Fisher, R., and Lowry, D.: Global atmospheric methane: budget, changes and dangers, Philosophical Transactions of the Royal Society of London A: Mathematical, Physical and Engineering Sciences, 369, 2058–2072, doi:10.1098/rsta.2010.0341, http://rsta.royalsocietypublishing.org/content/369/1943/2058, 2011.

Dobson, G.: Origin and distribution of the polyatomic molecules in the atmosphere, Proceedings of the Royal Society of London. Series A, Mathematical and Physical Sciences, 236, 187–193, 1956.

Eastham, S. D., Weisenstein, D. K., and Barrett, S. R.: Development and evaluation of the unified tropospheric–stratospheric chemistry extension (UCX) for the global chemistry-transport model GEOS-Chem, Atmospheric Environment, 89, 52–63, doi:http://dx.doi.org/10.1016/j.atmosenv.2014.02.001, http://www.sciencedirect.com/science/article/pii/S1352231014000971, 2014.

European Commission Joint Research Centre, Netherlands Environmental Assessment Agency: Emission Database for Global Atmospheric Research (EDGAR), http://edgar.jrc.ec.europa.eu, available at http://edgar.jrc.ec.europa.eu, 2011.

Fraser, A., Chan Miller, C., Palmer, P. I., Deutscher, N. M., Jones, N. B., and Griffith, D. W. T.: The Australian methane budget: Interpreting surface and train-borne measurements using a chemistry transport model, Journal of Geophysical Research: Atmospheres, 116, n/a–n/a, doi:10.1029/2011JD015964, http://dx.doi.org/10.1029/2011JD015964, d20306, 2011.

Fraser, A., Palmer, P. I., Feng, L., Boesch, H., Cogan, A., Parker, R., Dlugokencky, E. J., Fraser, P. J., Krummel, P. B., Langenfelds, R. L., O'Doherty, S., Prinn, R. G., Steele, L. P., van der Schoot, M., and Weiss, R. F.: Estimating regional methane surface fluxes: the relative importance of surface and GOSAT mole fraction measurements, Atmospheric Chemistry and Physics, 13, 5697–5713, doi:10.5194/acp-13-5697-2013, http://www.atmos-chem-phys.net/13/5697/2013/, 2013.

Fung, I., John, J., Lerner, J., Matthews, E., Prather, M., Steele, L., and Fraser, P.: Three-dimensional model synthesis of the global methane cycle, Journal of Geophysical Research: Atmospheres, 96, 13 033–13 065, 1991.

Geibel, M. C., Messerschmidt, J., Gerbig, C., Blumenstock, T., Chen, H., Hase, F., Kolle, O., Lavrič, J. V., Notholt, J., Palm, M., Rettinger, M., Schmidt, M., Sussmann, R., Warneke, T., and Feist, D. G.: Calibration of column-averaged CH_4 over European TCCON FTS sites with airborne in-situ measurements, Atmospheric Chemistry and Physics, 12, 8763–8775, doi:10.5194/acp-12-8763-2012, http://www.atmos-chem-phys.net/12/8763/2012/, 2012.

Gentner, D. R., Ford, T. B., Guha, A., Boulanger, K., Brioude, J., Angevine, W. M., de Gouw, J. A., Warneke, C., Gilman, J. B., Ryerson, T. B., Peischl, J., Meinardi, S., Blake, D. R., Atlas, E., Lonneman, W. A., Kleindienst, T. E., Beaver, M. R., St Clair, J. M., Wennberg, P. O., VandenBoer, T. C., Markovic, M. Z., Murphy, J. G., Harley, R. A., and Goldstein, A. H.: Emissions of organic carbon and methane from petroleum and dairy operations in California's San Joaquin Valley, Atmospheric Chemistry and Physics, 14, 4955–4978, doi:10.5194/acp-14-4955-2014, 2014.

Griffith, D. W. T., Deutscher, N., Velazco, V. A., Wennberg, P. O., Yavin, Y., Aleks, G. K., Washenfelder, R., Toon, G. C., Blavier, J.-F., Murphy, C., Jones, N., Kettlewell, G., Connor, B., Macatangay, R., Roehl, C., Ryczek, M., Glowacki, J., Culgan, T., and Bryant, G.: TCCON data from Darwin, Australia, Release GGG2014R0, http://dx.doi.org/10.14291/tccon.ggg2014.darwin01.R0/1149290, doi:10.14291/tccon.ggg2014.darwin01.R0/1149290, TCCON data archive, hosted by the Carbon Dioxide Information Analysis Center, Oak Ridge National Laboratory, Oak Ridge, Tennessee, U.S.A., 2014a.

Griffith, D. W. T., Velazco, V. A., Deutscher, N., Murphy, C., Jones, N., Wilson, S., Macatangay, R., Kettlewell, G., Buchholz, R. R., and Riggenbach, M.: TCCON data from Wollongong, Australia, Release GGG2014R0, http://dx.doi.org/10.14291/tccon.ggg2014.wollongong01.R0/1149291, doi:10.14291/tccon.ggg2014.wollongong01.R0/1149291, TCCON data archive, hosted by the Carbon Dioxide Information Analysis Center, Oak Ridge National Laboratory, Oak Ridge, Tennessee, U.S.A., 2014b.

Hase, F., Blumenstock, T., Dohe, S., Gross, J., and Kiel, M.: TCCON data from Karlsruhe, Germany, Release GGG2014R1, http://dx.doi.org/10.14291/tccon.ggg2014.karlsruhe01.R1/1182416, doi:10.14291/tccon.ggg2014.karlsruhe01.R1/1182416, TCCON data archive, hosted by the Carbon Dioxide Information Analysis Center, Oak Ridge National Laboratory, Oak Ridge, Tennessee, U.S.A., 2014.

Jones, A., Walker, K. A., Jin, J. J., Taylor, J. R., Boone, C. D., Bernath, P. F., Brohede, S., Manney, G. L., McLeod, S., Hughes, R., and Daffer, W. H.: Technical Note: A trace gas climatology derived from the Atmospheric Chemistry Experiment Fourier Transform Spectrometer

(ACE-FTS) data set, Atmospheric Chemistry and Physics, 12, 5207–5220, doi:10.5194/acp-12-5207-2012, http://www.atmos-chem-phys.net/12/5207/2012/, 2012.

Kalnay, E., Kanamitsu, M., Kistler, R., Collins, W., Deaven, D., Gandin, L., Iredell, M., Saha, S., White, G., Woollen, J., and Zhu, Y.: The NCEP/NCAR 40-year reanalysis project, Bulletin of the American Meteorological Society, 77, 437–471, 1996.

Kawakami, S., Ohyama, H., Arai, K., Okumura, H., Taura, C., Fukamachi, T., and Sakashita, M.: TCCON data from Saga, Japan, Release GGG2014R0, http://dx.doi.org/10.14291/tccon.ggg2014.saga01.R0/1149283, doi:10.14291/tccon.ggg2014.saga01.R0/1149283, TCCON data archive, hosted by the Carbon Dioxide Information Analysis Center, Oak Ridge National Laboratory, Oak Ridge, Tennessee, U.S.A., 2014.

Keller, C. A., Long, M. S., Yantosca, R. M., Da Silva, A. M., Pawson, S., and Jacob, D. J.: HEMCO v1.0: a versatile, ESMF-compliant component for calculating emissions in atmospheric models, Geoscientific Model Development, 7, 1409–1417, doi:10.5194/gmd-7-1409-2014, http://www.geosci-model-dev.net/7/1409/2014/, 2014.

Kirschke, S., Bousquet, P., Ciais, P., Saunois, M., Canadell, J. G., Dlugokencky, E. J., Bergamaschi, P., Bergmann, D., Blake, D. R., Bruhwiler, L., et al.: Three decades of global methane sources and sinks, Nature Geoscience, 6, 813–823, 2013.

Mahieu, E., Duchatelet, P., Demoulin, P., Walker, K. A., Dupuy, E., Froidevaux, L., Randall, C., Catoire, V., Strong, K., Boone, C. D., Bernath, P. F., Blavier, J.-F., Blumenstock, T., Coffey, M., De Mazière, M., Griffith, D., Hannigan, J., Hase, F., Jones, N., Jucks, K. W., Kagawa, A., Kasai, Y., Mebarki, Y., Mikuteit, S., Nassar, R., Notholt, J., Rinsland, C. P., Robert, C., Schrems, O., Senten, C., Smale, D., Taylor, J., Tétard, C., Toon, G. C., Warneke, T., Wood, S. W., Zander, R., and Servais, C.: Validation of ACE-FTS v2.2 measurements of HCl, HF, CCl_3F and CCl_2F_2 using space-, balloon- and ground-based instrument observations, Atmospheric Chemistry and Physics, 8, 6199–6221, doi:10.5194/acp-8-6199-2008, http://www.atmos-chem-phys.net/8/6199/2008/, 2008.

Messerschmidt, J., Geibel, M. C., Blumenstock, T., Chen, H., Deutscher, N. M., Engel, A., Feist, D. G., Gerbig, C., Gisi, M., Hase, F., Katrynski, K., Kolle, O., Lavrič, J. V., Notholt, J., Palm, M., Ramonet, M., Rettinger, M., Schmidt, M., Sussmann, R., Toon, G. C., Truong, F., Warneke, T., Wennberg, P. O., Wunch, D., and Xueref-Remy, I.: Calibration of TCCON column-averaged CO_2: the first aircraft campaign over European TCCON sites, Atmospheric Chemistry and Physics, 11, 10 765–10 777, doi:10.5194/acp-11-10765-2011, http://www.atmos-chem-phys.net/11/10765/2011/, 2011.

Mote, P. W., Rosenlof, K. H., McIntyre, M. E., Carr, E. S., Gille, J. C., Holton, J. R., Kinnersley, J. S., Pumphrey, H. C., Russell, J. M., and Waters, J. W.: An atmospheric tape recorder: The imprint of tropical tropopause temperatures on stratospheric water vapor, Journal of Geophysical Research: Atmospheres, 101, 3989–4006, doi:10.1029/95JD03422, http://dx.doi.org/10.1029/95JD03422, 1996.

Mu, M., Randerson, J. T., van der Werf, G. R., Giglio, L., Kasibhatla, P., Morton, D., Collatz, G. J., DeFries, R. S., Hyer, E. J., Prins, E. M., Griffith, D. W. T., Wunch, D., Toon, G. C., Sherlock, V., and Wennberg, P. O.: Daily and 3-hourly variability in global fire emissions and consequences for atmospheric model predictions of carbon monoxide, Journal of Geophysical Research: Atmospheres, 116, doi:10.1029/2011JD016245, http://dx.doi.org/10.1029/2011JD016245, d24303, 2011.

Murray, L. T., Jacob, D. J., Logan, J. A., Hudman, R. C., and Koshak, W. J.: Optimized regional and interannual variability of lightning in a global chemical transport model constrained by LIS/OTD satellite data, Journal of Geophysical Research: Atmospheres, 117, 2012.

Notholt, J., Petri, C., Warneke, T., Deutscher, N., Buschmann, M., Weinzierl, C., Macatangay, R., and Grupe, P.: TCCON data from Bremen, Germany, Release GGG2014R0, http://dx.doi.org/10.14291/tccon.ggg2014.bremen01.R0/1149275, doi:10.14291/tccon.ggg2014.bremen01.R0/1149275, TCCON data archive, hosted by the Carbon Dioxide Information Analysis Center, Oak Ridge National Laboratory, Oak Ridge, Tennessee, U.S.A., 2014.

Ostler, A., Sussmann, R., Rettinger, M., Deutscher, N. M., Dohe, S., Hase, F., Jones, N., Palm, M., and Sinnhuber, B.-M.: Multistation intercomparison of column-averaged methane from NDACC and TCCON: impact of dynamical variability, Atmospheric Measurement Techniques, 7, 4081–4101, doi:10.5194/amt-7-4081-2014, http://www.atmos-meas-tech.net/7/4081/2014/, 2014.

Ostler, A., Sussmann, R., Patra, P. K., Wennberg, P. O., Deutscher, N. M., Griffith, D. W. T., Blumenstock, T., Hase, F., Kivi, R., Warneke, T., Wang, Z., De Mazière, M., Robinson, J., and Ohyama, H.: The imprint of stratospheric transport on column-averaged methane, doi:10.5194/acpd-15-20395-2015, http://www.atmos-chem-phys-discuss.net/15/20395/2015/, 2015.

Park, R. J., Jacob, D. J., Field, B. D., Yantosca, R. M., and Chin, M.: Natural and transboundary pollution influences on sulfate-nitrate-ammonium aerosols in the United States: Implications for policy, Journal of Geophysical Research: Atmospheres, 109, 2004.

Parker, R., Boesch, H., Cogan, A., Fraser, A., Feng, L., Palmer, P. I., Messerschmidt, J., Deutscher, N., Griffith, D. W. T., Notholt, J., Wennberg, P. O., and Wunch, D.: Methane observations from the Greenhouse Gases Observing SATellite: Comparison to ground-based TCCON data and model calculations, Geophysical Research Letters, 38, n/a–n/a, doi:10.1029/2011GL047871, http://dx.doi.org/10.1029/2011GL047871, l15807, 2011.

Patra, P. K., Houweling, S., Krol, M., Bousquet, P., Belikov, D., Bergmann, D., Bian, H., Cameron-Smith, P., Chipperfield, M. P., Corbin, K., Fortems-Cheiney, A., Fraser, A., Gloor, E., Hess, P., Ito, A., Kawa, S. R., Law, R. M., Loh, Z., Maksyutov, S., Meng, L., Palmer, P. I., Prinn, R. G., Rigby, M., Saito, R., and Wilson, C.: TransCom model simulations of CH_4 and related species: linking transport, surface flux and chemical loss with CH_4 variability in the troposphere and lower stratosphere, Atmospheric Chemistry and Physics, 11, 12 813–12 837, doi:10.5194/acp-11-12813-2011, http://www.atmos-chem-phys.net/11/12813/2011/, 2011.

Pickett-Heaps, C. A., Jacob, D. J., Wecht, K. J., Kort, E. A., Wofsy, S. C., Diskin, G. S., Worthy, D. E. J., Kaplan, J. O., Bey, I., and Drevet, J.: Magnitude and seasonality of wetland methane emissions from the Hudson Bay Lowlands (Canada), Atmospheric Chemistry and Physics, 11, 3773–3779, doi:10.5194/acp-11-3773-2011, http://www.atmos-chem-phys.net/11/3773/2011/, 2011.

Rodgers, C. D. and Connor, B. J.: Intercomparison of remote sounding instruments, Journal of Geophysical Research, 108, 4116, doi:10.1029/2002JD002299, 2003.

Saad, K. M., Wunch, D., Toon, G. C., Bernath, P., Boone, C., Connor, B., Deutscher, N. M., Griffith, D. W. T., Kivi, R., Notholt, J., Roehl, C., Schneider, M., Sherlock, V., and Wennberg, P. O.: Derivation of tropospheric methane from TCCON CH_4 and HF total column observations, Atmospheric Measurement Techniques, 7, 2907–2918, doi:10.5194/amt-7-2907-2014, http://www.atmos-meas-tech.net/7/2907/2014/, 2014.

Santoni, G. W., Daube, B. C., Kort, E. A., Jimenez, R., Park, S., Pittman, J. V., Gottlieb, E., Xiang, B., Zahniser, M. S., Nelson, D. D., McManus, J. B., Peischl, J., Ryerson, T. B., Holloway, J. S., Andrews, A. E., Sweeney, C., Hall, B., Hintsa, E. J., Moore, F. L., Elkins, J. W., Hurst, D. F., Stephens, B. B., Bent, J., and Wofsy, S. C.: Evaluation of the airborne quantum cascade laser spectrometer (QCLS) measurements of the carbon and greenhouse gas suite - CO2, CH4, N2O, and CO - during the CalNex and HIPPO campaigns, Atmospheric Measurement Techniques, 7, 1509–1526, doi:10.5194/amt-7-1509-2014, 2014.

Sepúlveda, E., Schneider, M., Hase, F., Barthlott, S., Dubravica, D., García, O. E., Gomez-Pelaez, A., González, Y., Guerra, J. C., Gisi, M., Kohlhepp, R., Dohe, S., Blumenstock, T., Strong, K., Weaver, D., Palm, M., Sadeghi, A., Deutscher, N. M., Warneke, T., Notholt, J., Jones, N., Griffith, D. W. T., Smale, D., Brailsford, G. W., Robinson, J., Meinhardt, F., Steinbacher, M., Aalto, T., and Worthy, D.: Tropospheric CH_4 signals as observed by NDACC FTIR at globally distributed sites and comparison to GAW surface in situ measurements, Atmospheric Measurement Techniques, 7, 2337–2360, doi:10.5194/amt-7-2337-2014, http://www.atmos-meas-tech.net/7/2337/2014/, 2014.

Sheese, P. E., Boone, C. D., and Walker, K. A.: Detecting physically unrealistic outliers in ACE-FTS atmospheric measurements, Atmospheric Measurement Techniques, 8, 741–750, doi:10.5194/amt-8-741-2015, http://www.atmos-meas-tech.net/8/741/2015/, 2015.

Sherlock, V., Connor, B., Robinson, J., Shiona, H., Smale, D., and Pollard, D.: TCCON data from Lauder, New Zealand, 120HR, Release GGG2014R0, http://dx.doi.org/10.14291/tccon.ggg2014.lauder01.R0/1149293, doi:10.14291/tccon.ggg2014.lauder01.R0/1149293, TCCON data archive, hosted by the Carbon Dioxide Information Analysis Center, Oak Ridge National Laboratory, Oak Ridge, Tennessee, U.S.A., 2014a.

Sherlock, V., Connor, B., Robinson, J., Shiona, H., Smale, D., and Pollard, D.: TCCON data from Lauder, New Zealand, 125HR, Release GGG2014R0, http://dx.doi.org/10.14291/tccon.ggg2014.lauder02.R0/1149298, doi:10.14291/tccon.ggg2014.lauder02.R0/1149298, TCCON data archive, hosted by the Carbon Dioxide Information Analysis Center, Oak Ridge National Laboratory, Oak Ridge, Tennessee, U.S.A., 2014b.

Stephens, B. B., Gurney, K. R., Tans, P. P., Sweeney, C., Peters, W., Bruhwiler, L., Ciais, P., Ramonet, M., Bousquet, P., Nakazawa, T., Aoki, S., Machida, T., Inoue, G., Vinnichenko, N., Lloyd, J., Jordan, A., Heimann, M., Shibistova, O., Langenfelds, R. L., Steele, L. P., Francey, R. J., and Denning, A. S.: Weak Northern and Strong Tropical Land Carbon Uptake from Vertical Profiles of Atmospheric CO2, Science, 316, 1732–1735, doi:10.1126/science.1137004, http://science.sciencemag.org/content/316/5832/1732, 2007.

Sussmann, R. and Rettinger, M.: TCCON data from Garmisch, Germany, Release GGG2014R0, http://dx.doi.org/10.14291/tccon.ggg2014.garmisch01.R0/1149299, doi:10.14291/tccon.ggg2014.garmisch01.R0/1149299, TCCON data archive, hosted by the Carbon Dioxide Information Analysis Center, Oak Ridge National Laboratory, Oak Ridge, Tennessee, U.S.A., 2014.

Toon, G. C. and Wunch, D.: A stand-alone a priori profile generation tool for GGG2014, http://dx.doi.org/10.14291/tccon.ggg2014.priors.R0/1221661, doi:10.14291/tccon.ggg2014.priors.R0/1221661, 2014.

Turner, A. J., Jacob, D. J., Wecht, K. J., Maasakkers, J. D., Lundgren, E., Andrews, A. E., Biraud, S. C., Boesch, H., Bowman, K. W., Deutscher, N. M., Dubey, M. K., Griffith, D. W. T., Hase, F., Kuze, A., Notholt, J., Ohyama, H., Parker, R., Payne, V. H., Sussmann, R., Sweeney, C., Velazco, V. A., Warneke, T., Wennberg, P. O., and Wunch, D.: Estimating global and North American methane emissions with high spatial resolution using GOSAT satellite data, Atmospheric Chemistry and Physics, 15, 7049–7069, doi:10.5194/acp-15-7049-2015, http://www.atmos-chem-phys.net/15/7049/2015/, 2015.

van der Werf, G. R., Randerson, J. T., Giglio, L., Collatz, G. J., Mu, M., Kasibhatla, P. S., Morton, D. C., DeFries, R. S., Jin, Y., and van Leeuwen, T. T.: Global fire emissions and the contribution of deforestation, savanna, forest, agricultural, and peat fires (1997â€“2009), Atmospheric Chemistry and Physics, 10, 11 707–11 735, doi:10.5194/acp-10-11707-2010, http://www.atmos-chem-phys.net/10/11707/2010/, 2010.

von Clarmann, T., Höpfner, M., Kellmann, S., Linden, A., Chauhan, S., Funke, B., Grabowski, U., Glatthor, N., Kiefer, M., Schieferdecker, T., Stiller, G. P., and Versick, S.: Retrieval of temperature, H₂O, O₃, HNO₃, CH₄, N₂O, ClONO₂ and ClO from MIPAS reduced resolution nominal mode limb emission measurements, Atmospheric Measurement Techniques, 2, 159–175, doi:10.5194/amt-2-159-2009, http://www.atmos-meas-tech.net/2/159/2009/, 2009.

Wang, J., Logan, J., McElroy, M., Duncan, B., Megretskaia, I., and Yantosca, R.: A 3-D model analysis of the slowdown and interannual variability in the methane growth rate from 1988 to 1997, GLOBAL BIOGEOCHEMICAL CYCLES, 18, doi:10.1029/2003GB002180, 2004.

Wang, Z., Deutscher, N. M., Warneke, T., Notholt, J., Dils, B., Griffith, D. W. T., Schmidt, M., Ramonet, M., and Gerbig, C.: Retrieval of tropospheric column-averaged CH_4 mole fraction by solar absorption FTIR-spectrometry using N_2O as a proxy, Atmospheric Measurement Techniques, 7, 3295–3305, doi:10.5194/amt-7-3295-2014, http://www.atmos-meas-tech.net/7/3295/2014/, 2014.

Warneke, T., Messerschmidt, J., Notholt, J., Weinzierl, C., Deutscher, N., Petri, C., Grupe, P., Vuillemin, C., Truong, F., Schmidt, M., Ramonet, M., and Parmentier, E.: TCCON data from Orleans, France, Release GGG2014R0, http://dx.doi.org/10.14291/tccon.ggg2014.orleans01.R0/1149276, doi:10.14291/tccon.ggg2014.orleans01.R0/1149276, TCCON data archive, hosted by the Carbon Dioxide Information Analysis Center, Oak Ridge National Laboratory, Oak Ridge, Tennessee, U.S.A., 2014.

Washenfelder, R. A., Wennberg, P. O., and Toon, G. C.: Tropospheric methane retrieved from ground-based near-IR solar absorption spectra, Geophysical Research Letters, 30, 2226, doi:10.1029/2003GL017969, http://doi.wiley.com/10.1029/2003GL017969http://dx.doi.org/10.1029/2003GL017969, 2003.

Washenfelder, R. A., Toon, G. C., Blavier, J.-F., Yang, Z., Allen, N. T., Wennberg, P. O., Vay, S. A., Matross, D. M., and Daube, B. C.: Carbon dioxide column abundances at the Wisconsin Tall Tower site, Journal of Geophysical Research: Atmospheres, 111, D22 305, doi:10.1029/2006JD007154, http://dx.doi.org/10.1029/2006JD007154, 2006.

Waugh, D. and Hall, T.: Age of Stratospheric Air: Theory, Observations, and Models, Reviews of Geophysics, 40, 1–1–1–26, doi:10.1029/2000RG000101, http://dx.doi.org/10.1029/2000RG000101, 1010, 2002.

Waymark, C., Walker, K., Boone, C., and Bernath, P.: ACE-FTS version 3.0 data set: validation and data processing update, Annals of Geophysics, 56, http://www.annalsofgeophysics.eu/index.php/annals/article/view/6339, 2014.

Wecht, K. J., Jacob, D. J., Frankenberg, C., Jiang, Z., and Blake, D. R.: Mapping of North American methane emissions with high spatial resolution by inversion of SCIAMACHY satellite data, Journal of Geophysical Research: Atmospheres, 119, 7741–7756, doi:10.1002/2014JD021551, http://dx.doi.org/10.1002/2014JD021551, 2014JD021551, 2014a.

Wecht, K. J., Jacob, D. J., Sulprizio, M. P., Santoni, G. W., Wofsy, S. C., Parker, R., Bösch, H., and Worden, J.: Spatially resolving methane emissions in California: constraints from the CalNex aircraft campaign and from present (GOSAT, TES) and future (TROPOMI, geostationary) satellite observations, Atmospheric Chemistry and Physics, 14, 8173–8184, doi:10.5194/acp-14-8173-2014, http://www.atmos-chem-phys.net/14/8173/2014/, 2014b.

Wennberg, P. O., Roehl, C., Blavier, J.-F., Wunch, D., Landeros, J., and Allen, N.: TCCON data from Jet Propulsion Laboratory, Pasadena, California, USA, Release GGG2014R0, http://dx.doi.org/10.14291/tccon.ggg2014.jpl02.R0/1149297, doi:10.14291/tccon.ggg2014.jpl02.R0/1149297, TCCON data archive, hosted by the Carbon Dioxide Information Analysis Center, Oak Ridge National Laboratory, Oak Ridge, Tennessee, U.S.A., 2014a.

Wennberg, P. O., Roehl, C., Wunch, D., Toon, G. C., Blavier, J.-F., Washenfelder, R., Keppel-Aleks, G., Allen, N., and Ayers, J.: TCCON data from Park Falls, Wisconsin, USA, Release GGG2014R0, http://dx.doi.org/10.14291/tccon.ggg2014.parkfalls01.R0/1149161, doi:10.14291/tccon.ggg2014.parkfalls01.R0/1149161, TCCON data archive, hosted by the Carbon Dioxide Information Analysis Center, Oak Ridge National Laboratory, Oak Ridge, Tennessee, U.S.A., 2014b.

Wennberg, P. O., Wunch, D., Roehl, C., Blavier, J.-F., Toon, G. C., Allen, N., Dowell, P., Teske, K., Martin, C., and Martin, J.: TCCON data from Lamont, Oklahoma, USA, Release GGG2014R0, http://dx.doi.org/10.14291/tccon.ggg2014.lamont01.R0/1149159, doi:10.14291/tccon.ggg2014.lamont01.R0/1149159, TCCON data archive, hosted by the Carbon Dioxide Information Analysis Center, Oak Ridge National Laboratory, Oak Ridge, Tennessee, U.S.A., 2014c.

Wennberg, P. O., Wunch, D., Yavin, Y., Toon, G. C., Blavier, J.-F., Allen, N., and Keppel-Aleks, G.: TCCON data from Jet Propulsion Laboratory, Pasadena, California, USA, Release GGG2014R0, http://dx.doi.org/10.14291/tccon.ggg2014.jpl01.R0/1149163, doi:10.14291/tccon.ggg2014.jpl01.R0/1149163, TCCON data archive, hosted by the Carbon Dioxide Information Analysis Center, Oak Ridge National Laboratory, Oak Ridge, Tennessee, U.S.A., 2014d.

Wunch, D., Toon, G. C., Wennberg, P. O., Wofsy, S. C., Stephens, B. B., Fischer, M. L., Uchino, O., Abshire, J. B., Bernath, P., Biraud, S. C., Blavier, J.-F. L., Boone, C., Bowman, K. P., Browell, E. V., Campos, T., Connor, B. J., Daube, B. C., Deutscher, N. M., Diao, M., Elkins, J. W., Gerbig, C., Gottlieb, E., Griffith, D. W. T., Hurst, D. F., Jiménez, R., Keppel-Aleks, G., Kort, E. a., Macatangay, R., Machida, T., Matsueda, H., Moore, F., Morino, I., Park, S., Robinson, J., Roehl, C. M., Sawa, Y., Sherlock, V., Sweeney, C., Tanaka, T., and Zondlo, M. a.: Calibration of the Total Carbon Column Observing Network using aircraft profile data, Atmospheric Measurement Techniques, 3, 1351–1362, doi:10.5194/amt-3-1351-2010, http://www.atmos-meas-tech.net/3/1351/2010/, 2010.

Wunch, D., Toon, G. C., Blavier, J.-F. L., Washenfelder, R. a., Notholt, J., Connor, B. J., Griffith, D. W. T., Sherlock, V., and Wennberg, P. O.: The Total Carbon Column Observing Network, Philosophical transactions. Series A, Mathematical, physical, and engineering sciences, 369, 2087–2112, doi:10.1098/rsta.2010.0240, http://www.ncbi.nlm.nih.gov/pubmed/21502178, 2011a.

Wunch, D., Wennberg, P. O., Toon, G. C., Connor, B. J., Fisher, B., Osterman, G. B., Frankenberg, C., Mandrake, L., O'Dell, C., Ahonen, P., Biraud, S. C., Castano, R., Cressie, N., Crisp, D., Deutscher, N. M., Eldering, a., Fisher, M. L., Griffith, D. W. T., Gunson, M., Heikkinen, P., Keppel-Aleks, G., Kyrö, E., Lindenmaier, R., Macatangay, R., Mendonca, J., Messerschmidt, J., Miller, C. E., Morino, I., Notholt, J., Oyafuso, F. a., Rettinger, M., Robinson, J., Roehl, C. M., Salawitch, R. J., Sherlock, V., Strong, K., Sussmann, R., Tanaka, T., Thompson, D. R., Uchino, O., Warneke, T., and Wofsy, S. C.: A method for evaluating bias in global measurements of CO2 total columns from space, Atmospheric Chemistry and Physics, 11, 12 317–12 337, doi:10.5194/acp-11-12317-2011, http://www.atmos-chem-phys.net/11/12317/2011/acp-11-12317-2011.htmlhttp://www.atmos-chem-phys.net/11/12317/2011/, 2011b.

Wunch, D., Toon, G. C., Sherlock, V., Deutscher, N. M., Liu, C., Feist, D. G., and Wennberg, P. O.: The Total Carbon Column Observing Network's GGG2014 Data Version, Tech. rep., Carbon Dioxide Information Analysis Center, Oak Ridge National Laboratory, Oak Ridge, Tennessee, U.S.A. doi: 10.14291/tccon.ggg2014.documentation.R0/1221662, doi:10.14291/tccon.ggg2014.documentation.R0/1221662, http://dx.doi.org/10.14291/tccon.ggg2014.documentation.R0/1221662, 2015.

Yang, Z., Washenfelder, R. a., Keppel-Aleks, G., Krakauer, N. Y., Randerson, J. T., Tans, P. P., Sweeney, C., and Wennberg, P. O.: New constraints on Northern Hemisphere growing season net flux, Geophysical Research Letters, 34, L12 807, doi:10.1029/2007GL029742, http://doi.wiley.com/10.1029/2007GL029742, 2007.

Table 3. List of Sensitivity Experiments

Run Name	Description	CH_4 Lifetime (years) with respect to			Final CH_4
		Emissions	Tropospheric OH	Total Loss	Burden (Tg)
Base	Default OH and Emissions	9.6	10.7	9.7	4825
Aseasonal	Constant Monthly Emission Rates	9.6	10.7	9.7	4872
Updated OH	Monthly OH fields from Standard Chemistry + Biogenic VOCs, scaled down by 10%	8.5	9.4	8.6	4828
Unscaled Updated OH	Monthly OH fields from Standard Chemistry + Biogenic VOCs	7.7	8.4	7.8	4917
90% OH	Default OH scaled down by 10%	10.5	11.9	10.7	5296
110% OH	Default OH scaled up by 10%	8.8	9.7	8.8	4425
Scaled Rice Emissions	Rice Emissions Increased by 20%	9.6	10.7	9.6	4780
No Wetlands	Wetland Emissions Turned Off	10.7	10.6	9.5	3768
Scaled Livestock Emissions	Scale livestock emissions by 50%	9.6	10.7	9.6	4359
MERRA	MERRA meteorology fields	9.6	10.7	9.6	4849
Tropopause Level	Set top of troposphere 2 vertical levels higher	9.6	10.6	9.6	4855